

UNIVERSITY OF THESSALY

Taylor Spatial Frame and Ilizarov Apparatus:
A Biomechanical Analysis using the Finite Element Method (FEM)

by

THEMIS P. TOUMANIDOU

*Submitted to the Department of Mechanical Engineering
in Partial Fulfillment of the Requirements for the Degree of*

Master of Science

March 2011

© Copyright 2011
by Themis P. Toumanidou

To my beloved sister

Thesis Committee

Professor Nikolaos Aravas (adviser)

Department of Mechanical Engineering, University of Thessaly

Professor Antonios Giannakopoulos (examiner)

Department of Civil Engineering, University of Thessaly

Lecturer Alexios Kermanidis (examiner)

Department of Mechanical Engineering, University of Thessaly

Acknowledgments

First of all, I would like to express my gratitude to my thesis adviser, Professor Nikos Aravas, for his guidance and support throughout my studies. I would have never been in this position, if he had not believed in our good cooperation and in my willingness to meet his expectations.

I would like to express my special thanks to Dr. Leonidas Spyrou, whose contribution to this thesis is invaluable. His research work, together with Professor Aravas, inspired me to follow the extremely interesting field of biomechanics. I would like to thank him for his unconditioned help during the difficult moments of this research and for his patience to reach to the end.

I would also like to thank the surgeons from the Orthopaedic Department of the University Hospital of Larisa, and especially Professor Konstantinos Malizos and Dr. Nikos Karamanis, for providing us with prototype models of the fixators and for their clinical experience that contributed a lot to this work.

At the end of a wonderful era, I would like to thank Kiki, Leonis and Alkmini, for their optimism, their remarkable patience and support to my choices and to every difficulty that occurred in this way. Special thanks to Dimitris and Marina, for making the last two years of my life unique.

Last but not least, I would like to express my deepest gratitude to my family, for unsparingly supporting my studies and encouraging me over all these years.

ABSTRACT

Taylor Spatial Frame and Ilizarov Apparatus : A Biomechanical Analysis using the Finite Element Method (FEM)

Themis P. Toumanidou

Advisor : Professor Nikolaos Aravas

External fixation devices are widely used for treating unstable bone fractures. The Taylor Spatial Frame (TSF) and the Ilizarov apparatus are typical examples of circular external fixators used to stabilize reconstruction of large segmental tibia defects. These external fixation devices have successful clinical use because of their minimal invasiveness and extreme versatility. The wide range of fracture types treated led to a variety of configurations of the Ilizarov and TSF frames which have substantial differences in stiffness and stability of fixation.

The stiffness of the fixation systems under axial compression loading is an important factor of their mechanical behavior and is influenced by the individual components involved, such as the wires, half-pins, connecting rods, telescopic struts and the fracture zone itself.

The main objective of this work is the study of the mechanical characteristics of the TSF and Ilizarov fixators. Detailed three-dimensional finite element calculations are carried out and the axial stiffness of the systems is studied for various load cycles. The effects of wire-diameter, wire-crossing angles, and pretension level on the stiffness of the systems are studied in detail. Different stages of callus consolidation in the tibia bones are simulated and the system behavior is studied in terms of load transmission and frame rigidity.

Contents

1 Introduction and review

	1
1.1 Introduction	1
1.2 Thesis overview	3

2 Literature Review

	6
2.1 Bones	6
2.1.1 Composition and structure	6
2.1.2 Biomechanical behavior	11
2.1.3 Mechanical properties	11
2.1.4 Skeletal Processes	15
2.2 Human Lower Extremity	18
2.2.1 Skeletal Anatomy	18
2.2.2 Tibia : Structure and properties	19
2.3 Bone failure: Fractures	21
2.3.1 Causes	21
2.3.2 Types	21
2.3.3 Treatment	24
2.3.4 Complications	27
2.3.5 Rehabilitation	27
2.4 External Skeletal Fixators	28
2.4.1 History and types	28
2.4.2 Classification	32
2.4.3 Comparison of Internal and External Fixators	34
2.4.4 Comparison of Unilateral and Circular Fixators	35
2.4.5 Complications	37
2.4.6 The Ilizarov apparatus	38
2.4.7 The Taylor Spatial Frame	45

3	Computational modeling	53
3.1	Introduction	
	53
3.2	Materials and method	54
3.2.1	Model geometry	54
3.2.2	Material assignment	61
3.2.3	Assembly and constraints	62
3.2.4	Load and Boundary Conditions	
	65
3.3	FE Models	
	66
3.4	Results	
	70
3.5	Discussion	
	90
4	Closure	92
	References	96

List of figures

1	Human Skeleton from Vesalius' book <i>De Humani Corporis Fabrica Libri Septem</i>	4
2	Tropocollagen is the basic structural unit of all forms of collagen	6
3	Structure of the osteon	7
4	Microscopic anatomy of a bone	8
5	Photomicrographs of cortical bone (40x) and of cancellous bone (30x) from a human tibia	9
6	Front view of an adult human skeleton	10
7	Mechanical behavior of bone showing its anisotropy and its viscoelasticity . .	12
8	Example of stress–strain curves of cortical and trabecular bone tested in compression	13
9	Stress–strain curves for metal, glass and bone	13
10	Magnitude of ultimate stress for cortical and trabecular bone	14
11	Endochondrial ossification	16
12	Formation of Internal callus consisting of fibrous tissue and cartilage	16
13	Human lower extremity anatomy	18
14	Tibia structure	19
15	Tibia articulates with the femur through the patella (X-Ray image)	20
16	Types of fractures according to the pattern in which bone breaks	22
17	Types of tibia fractures (X-Ray image)	24
18	Immobilization using casts and splints, internal fixation with IM rod, external fixation and ankle fusion	26
19	Malgaigne's pin in a leather strap and patella	28
20	Roux's and Ollier's devices	28
21	Parkhill's bone clamp and Lambotte's external fixator	29
22	Roger Anderson's reduction apparatus and fixator frame	30
23	Stader's fixator and Hoffmann's device	30
24	Charnley's compression clamp, Vidra-Adrey quadrilateral device and Ilizarov ring fixator	31
25	Kronner ring fixator, Fischer half-ring fixator and Taylor Spatial Frame	32
26	Wagner apparatus, ASIF fixator and Kronner four bar fixator	33
27	Ilizarov apparatus, a CEF system used to correct tibial deformity	38
28	Relationship between wire pretension and axial stiffness of the frame (1.8-mm wires, 150mm rings)	40
29	The effect of varying wire-crossing angles on the stiffness of external fixation .	41

30	(A.) Safe zone of wire insertion in tibia, (B.) Smooth and olive wires	41
31	Relationship between wire positioning within the bone and stiffness parameters in different loading configurations	42
32	Opposing olive beads can prevent bone sliding despite narrow crossing angles	43
33	Four ring Ilizarov construct used to stabilize a comminuted fracture	44
34	Stewart-Gough platform (SGP) and Taylor Spatial Frame	45
35	Radiograph of tibia fracture treated with TSF using 3 half-pins, 3 smooth and 1 olive wire	46
36	A short strut and a medium strut both set to 120 mm and close-up of the mid-position of a short strut	47
37	Types of rings used in TSF fixators	47
38	The three parameters that fully describe a configuration are proximal and distal internal diameter and neutral strut length or frame height	48
39	In anatomical reduction, the O and CP are coincident and there is no angulation or rotation between the fragments	49
40	Half-pins are placed with 90° divergence at the mid tibia (left), Three-hole Rancho cube (right)	50
41	HA coated pins	50
42	Final segmentation step in Avvizo. The tibia set is noted in red and the marrow in green	54
43	Solid model of tibia (left) and marrow (right) in *.stl form	54
44	Three-dimensional FE model of tibia from CT images (left) and bone simulation with solid FE cylinder model (right)	55
45	Tetrahedral mesh of bone and half-pins in a hybrid TSF configuration using 2HP at the proximal ring and 3HP at the distal ring	56
46	The rings consisting the Ilizarov fixators have internal diameter 180 mm . . .	57
47	Single-ring block configuration with one ring at each bone fragment	58
48	Double-ring block with two levels of fixation at each bone fragment; Prototype configuration (left) and numerical model (right)	58
49	Half-pins are clamped with one or two-hole rancho cubes (left) The TSF ring geometry (right)	59
50	The divergence angle between ring and strut was 60°	60
51	TSF Configuration with 2W per bone segment (left), hybrid fixator with 2W and 5HP (right)	60
52	Local CSYS (left), Universal Joints (right)	62
53	Multi-point constraints between wire and tibia nodes at the tibia cross-section	63
54	Tie constraints imposed at ring-cube surfaces	64

55	Coupling constraints imposed between rings and rods	64
56	Compressive load is applied on the upper bound of the tibia	65
57	Boundary conditions	65
58	Hybrid TSF treating transversely fractured tibia using 2W and 5HP	67
59	Hybrid TSF supporting a tibia with callus (red region) formed at the fracture site	68
60	The relationship between load and axial displacement for single and double-ring Ilizarov frames (180-mm rings, 1.5mm wires, 70kg pretension)	70
61	The non-linear effect of load on axial stiffness for single and double-ring Ilizarov frames (tangent modulus) (180-mm rings, 1.5-mm wires, 70kg pretension)	71
62	The effect of wire pretension on axial stiffness (Ilizarov config. 2 , 180-mm rings, 1.5mm wires)	72
63	Deformed (contour plot) and undeformed (green) shapes of Configuration 2 (Ilizarov config. 2, 180-mm rings, 490.5 N pretension, load 500 N)	73
64	Bone resorption on the tibia cross-section in the areas where wires are bended (wire - bone interface) (Ilizarov config. 2, 180-mm rings, 883 N pretension, load 500 N)	73
65	The effect of wire diameter on load-displacement profile (Ilizarov config. 1, 180-mm rings, 981 N pretension)	74
66	The effect of wire diameter on axial stiffness (Ilizarov Config. 1, 180-mm rings, 981 N pretension)	74
67	Load-displacement curves of single-ring Ilizarov and TSF (180-mm rings, 1.5-mm wires with 883 N pretension)	75
68	The effect of wire pretension on axial stiffness (TSF Config. 3 , 180-mm rings, 1.5mm wires)	77
69	Deformed (green) and undeformed (grey) shapes (left), Free Body Diagram (right) (180-mm rings, 1.5-mm wires with 883 N pretension, 300 N)	77
70	Load-displacement curves of TSF and hybrid TSF Configurations (180-mm rings, 1.5-mm wires with 883 N pretension)	78
71	Von-Mises stress distribution on half-pins (Hybrid TSF, load 500 N)	79
72	Wire-crossing angle effect on axial stiffness of hybrid TSF Configurations (180-mm rings, 1.5-mm wires, 883 N pretension, load 500 N)	80
73	Stress distribution on rings for 45° (left) and 29° (right) wire-angle (Hybrid TSF, 180-mm rings, 1.5-mm wires, 883 N pretension, load 500 N)	81

74	Stress distribution on tibiae with (A) fracture gap, (B) Callus Type I, (C) II and (D) III (Hybrid TSF, 180-mm rings, 1.5-mm wires, 883 N pretension, 500N)	82
75	Effect of callus elastic characteristics on axial stability (Hybrid TSF, 180-mm rings, 1.5-mm wires, 883 N pretension, 500N)	83
76	Load-displacement curves for different stages of fracture healing (Hybrid TSF, 180-mm rings, 1.5-mm wires, 883 N pretension, 500N)	83
77	Hybrid TSF configuration with 3 wires and 3 half-pins (Case from the Orthopaedics Department of UHL)	84
78	Anterior and medial view of proximal tibia fracture (X-ray image) – 31-year-old male (Case from the Orthopaedics Department of UHL, 2011)	85
79	Front and lateral view of the fracture – Immediate and 1 Month after Post. Op. (X-ray image) (Case from the Orthopaedics Department of UHL, 2011)	85
80	Front and lateral view of the tibia – 3 and 5 Months Post. Op. (X-ray image) (Case from the Orthopaedics Department of UHL, 2011)	86
81	Open bipolar tibia fractures (X-ray image) – 25-year-old male (Case from the Orthopaedics Department of UHL, 2006)	87
82	Open bipolar tibia fracture (X-ray image) – Immediate Post. Op. (Case from the Orthopaedics Department of UHL, 2006)	87
83	Open bipolar tibia fracture (X-ray image) – 1 Month Post. Op. (Case from the Orthopaedics Department of UHL, 2006)	88
84	Open bipolar tibia fracture (X-ray image) – 9 Month Post. Op. (Case from the Orthopaedics Department of UHL, 2006)	89
85	X-ray image of healed tibia – 23 Months & 4,5 Years Post. Op. (Case from the Orthopaedics Department of UHL, 2006)	89

1 Introduction and review

1.1 Introduction

Research in biomechanics is aimed at improving our knowledge of a very complex structure—the human body. In general, biomechanical research quantifies :

- Movement of different body segments and factors that influence movement
- Deformation of biological structures and factors that influence their deformity, and
- Biological effects of locally acting forces on living tissues (effects such as growth and development or overload and injuries)

Research activities can be divided into three areas: experimental studies, model analyses and applied research. Experimental techniques are fundamental to the study of soft tissues and are conducted to determine the mechanical properties of biological materials, including bones, cartilage, muscles, tendons, ligaments, skin and blood. All the studies involving experimental results are based on tests performed on animal tissues or human cadavers. The experimental procedure is highly demanding, therefore its sensitivity to many parameters turns it to a great challenge for the researcher. Theoretical studies, on the other hand, involve mathematical model analyses. The latter are a very important component of research in biomechanics since any produced model based on experimental findings can be used to predict the effect of environmental and operational factors without resorting to laboratory experiments.

Computational modeling enables the researcher to experiment with the model by changing the parameters of a system performing sensitivity studies and comparing with the corresponding experimental results. Recent and ongoing advances in computational mechanics (finite-element methods and boundary-element methods) provide a means for more comprehensive and more accurate modeling of biological materials than has previously been possible. The application of scientific knowledge in conjunction with the increasing development of computing softwares can help scientists to better answer questions in health and disease.

There is a wide variety of professions that can benefit from the results of the biomechanical research to the prevention, reduction or treatment of human injuries concerning the disabled and the non-disabled, athletes and non-athletes. Orthopaedic surgery, kinesiology, orthotics, automotive safety, sports and rehabilitation engineering are some of the professions that are using the research findings to improve performance in sports or activities,

design sport equipment for champions, affect an athlete's technique to reach success or simply improve human performance and give people a better living. However, despite the efforts of injury prevention, many injuries occur day by day and are confronted with difficulties. Biomechanical research in this field is very important as it helps the development of medical devices, prosthetics and fixators, improve the surgery procedure and post-surgical treatment. Consequently, the development of a realistic computational model demands interdisciplinary knowledge of anatomy, physiology, mechanics and materials and the minimum assumptions. Y.C. Fung, a pioneer of Modern Biomechanics, stated the four basic prerequisites to the solution of any problem in biomechanics :

1. The geometry of the system, that leads to anatomical, morphological and histological studies,
2. The materials of the system and their mechanical properties, that leads to the study of chemistry and constitutive equations,
3. The basic laws governing the system (the ideal approach is to minimize the number of assumptions), and
4. The boundary conditions, that depend on the specific problem at hand.

1.2 Thesis overview

In this thesis, special emphasis is given to the mechanical behavior of different configurations of the Ilizarov apparatus and Taylor Spatial Frame (TSF). The fixator stiffness is an important factor, since it is a criterion for successful fracture healing. Parameters affecting the frame's rigidity and stability are being assessed using numerical modeling.

In Chapter 2, a literature review of the anatomy and material characteristics of human bones is presented. Their biomechanical behavior and the fundamental skeletal processes occurring in human bones are reported in terms of defining the ossification process and the mechanical properties of the tissue in different stages of consolidation. Special informations are documented for the tibia bone, with respect to its structure and mechanical characteristics.

In Section 2.3, the mechanics of bone failure is analyzed. Main causes, different categorization of types of fractures and, in particular, categories of tibia fractures are reported in detail, accompanied by X-ray images of real cases of breakage. The techniques of fracture treatment, including surgical and non-surgical methods, are reported with respect to literature and clinical references. In the end of the chapter, possible complications and the rehabilitation procedure are mentioned.

In Section 2.4 are presented the typical fixation systems and the various classifications. An interesting comparison between internal and external fixators reveals advantages and disadvantages of each method. In paragraph 2.4.4, the mechanics of unilateral frames is compared to that of circular frames and interesting conclusions come for the cases that each fixator is recommended. The most important parts of this section, are 2.4.6 and 2.4.7, where a detailed analysis of the frame components of Ilizarov and TSF fixators and their mechanics is documented. The impact of each element on axial stiffness is suggested, accompanied by literature reviews and references of other theoretical and experimental studies performed on the subject.

Chapter 3 is the core chapter in the thesis. The development of the numerical models is presented in steps. At first, the design of the non-linear geometry of the problem, the materials assigned and next, all the constraints and boundary conditions defined give information about the final FE models produced for different configurations. In Section 3.4, the results of the simulation analysis are presented in graphs, charts, free body diagrams and stress distribution plots. The numerical data obtained are correlated to corresponding literature findings of other researches.

Finally, Chapter 4 provides a brief summary of the contribution of this work together with some prospects for future investigation.

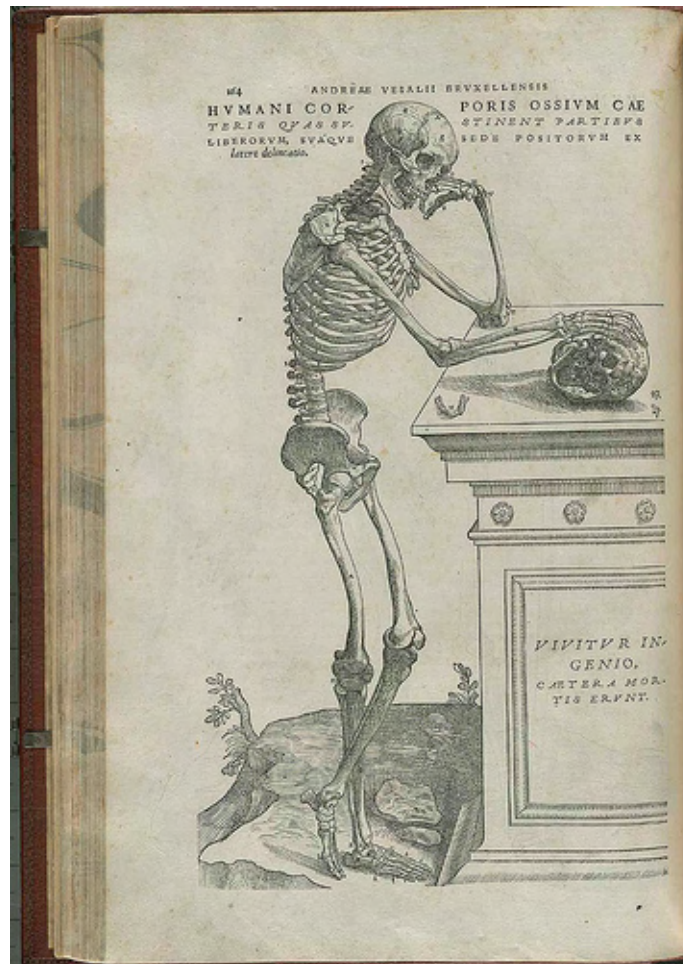


Figure 1: Human Skeleton from Vesalius' book *De Humani Corporis Fabrica Libri Septem*
(http://farm5.static.flickr.com/4034/4266575511_c94130bbd8.jpg)

2 Literature Review

2.1 Bones

Bones are rigid organs that form part of the endoskeleton of vertebrates. Bone tissue is a specialized type of dense connective tissue whose solid composition suits it for its supportive and protective roles. Like other connective tissues, it consists of cells and an extracellular matrix of fibers and ground substance produced by the cells. The distinguishing feature of bone is its high content of inorganic materials (in the form of mineral salts) that combine intimately with the organic matrix (Buckwalter et al., 1995). The composition of bone differs depending on a large number of factors, such as the species, animal age, sex, type of bone, site and presence of diseases.

2.1.1 Composition and structure

In a typical human bone, the inorganic (mineral) portion of bone consists primarily of calcium and phosphate, mainly in the form of small crystals resembling synthetic hydroxyapatite crystals with the composition $\text{Ca}_{10}(\text{PO}_4)_6(\text{OH})_2$ and account for 60-70% of its dry weight. The mineral component gives the tissue its hardness and rigidity, while the organic component makes it flexible and resilient. The fibrous portion of the extracellular matrix consists of variously oriented fibers of the protein named collagen (Figure 2), which, despite being tough and pliable, resist stretching and have little extensibility.



Figure 2: Tropocollagen is the basic structural unit of all forms of collagen
(<http://www.pt.ntu.edu.tw/hmchai/biomechanics/BMmaterial/Collagen.files/Tropocollagen.jpg>)

Collagen composes approximately 90% of the inorganic matrix and accounts approximately 25-30% of the dry weight of bone. The mineralized collagen fibers are surrounded by a gelatinous ground substance that consists mainly of protein polysaccharides or glycosaminoglycans (GAGs), primarily in the form of complex macromolecules called proteoglycans (PGs) and constitute approximately 5% of the extracellular matrix. Water accounts for 5-8%, approximately 85% of which is found in the organic matrix (around the collagen fibers and ground substance) that makes up the remainder of the tissue. The other 15% of

water is located in the canals and cavities that house bone cells and carry nutrients to the bone tissue.

The mineralized osseous tissue is one of the types that makes up bone and provides it rigidity and a honeycomb-like three-dimensional internal structure. Other types of tissue found in bone include marrow, periosteum and endosteum, nerves, blood vessels and cartilage. The periosteum is a dense fibrous membrane whose outer layer is permeated by blood vessels and covers the entire bone except for the joint surfaces, which are covered with articular cartilage. In the long bones, the endosteum is a thinner largely cellular connective tissue membrane that lines the central cavity filled with yellow fatty marrow. The endosteum contains osteoblasts, cells that are active in bone formation, growth and healing (bone modeling), and giant multinucleated bone cells called osteoclasts, that perform bone and mineral absorption or resorption (bone remodeling).

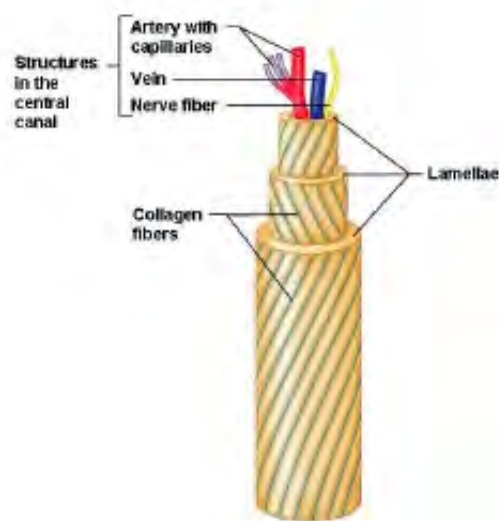


Figure 3: Structure of the osteon (From Marieb and Hoehn, 2007)

Bones have a complex internal and external structure that can be approached in two levels: a microscopic and a macroscopic one. From the microscopic view, the fundamental structural unit of bone is the osteon (Fig. 3), or Haversian System at the center of which exists the harvesian canal, a small channel that contains blood vessels and nerve fibers. The osteon itself consists of a concentric series of layers (lamellae) of mineralized matrix that surround the central canal. Along the boundaries of each lamella, are the lacunae, small cavities containing one bone cell, known as osteocyte.

Numerous small channels, called canaliculi, radiate from each lacuna, connecting the lacunae of adjacent lamellae and ultimately reaching the harvesian canal (Fig. 4). Various cell processes extend from the osteocytes into the canaliculi, allowing nutrients from the blood vessels in the harvesian canal to pass through the red marrow (a hemopoietic tissue that produces red and white blood cells and platelets) and reach the osteocytes. Like the

canaliculi, the collagen fibers in the bone matrix interconnect from one lamella to another within an osteon but do not cross the cement line, a narrow area of cement-like ground substance at the periphery of each osteon. This characteristic of collagen fibers undoubtedly increases the bone's resistance to mechanical stress and probably explains why the cement line is the weakest portion of the bone's microstructure.

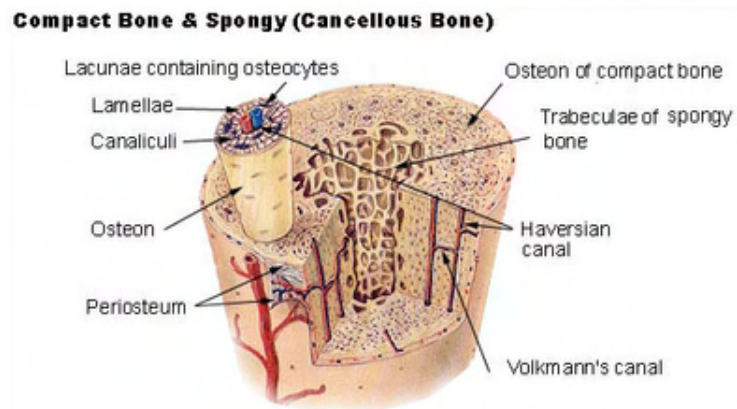


Figure 4: Microscopic anatomy of a bone (<http://www.ask.com/wiki/Osteon>)

On microscopic level, bone consists of woven and lamellar bone. The first one is found in the embryo, in the newborn, in the fracture callus and in the metaphysial region of growing bone as well as in tumors, osteogenesis imperfecta and pagetic bone. These are the reasons why woven bone is often called immature bone. Lamellar bone begins to form 1 month after birth and actively replaces woven bone, therefore is a mature bone.

At the macroscopic level, all bones are consisted of two types of osseous tissue: cortical (or compact) and cancellous (or trabecular) bone. Cortical bone forms the outer shell (hard surface), or cortex, of the bone and has a dense structure similar to that of ivory (Fig. 5A). It always surrounds cancellous bone, but the relative quantity of each type varies among bones and within individual bones according to functional requirements. The hardness of bone is due to the presence of mineral salts (calcium and phosphorus), which are held together by the matrix of collagen. The salt/collagen compound forms a composite structure analogous to concrete with metal reinforcing rods. It is resistant to bending and its thickness varies between and within bones as a function of the mechanical requirements of the bone. Cancellous bone is called the soft, spongy interior of the bone and is composed of rods and plates with the trabeculae (little beams) generally oriented in the direction of bone loading (Fig. 5B). It is arranged in concentric lacunae – containing lamellae but does not contain harvesian canals. Trabecular bones are highly resistant to compressive loads and in their areas exists the red marrow.

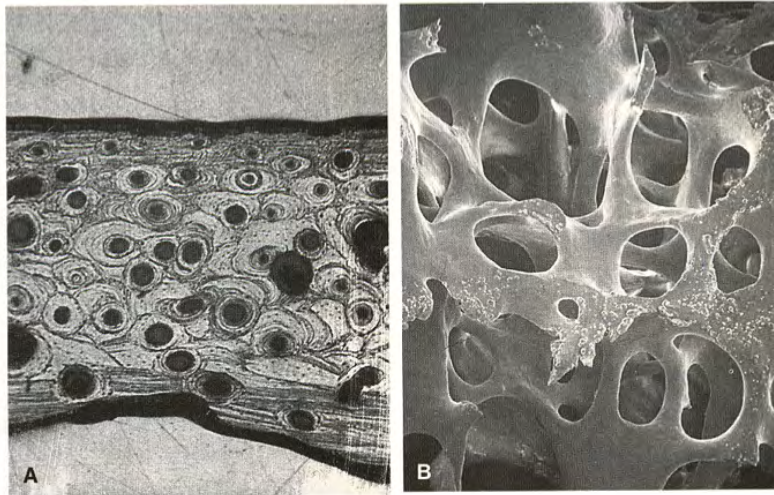


Figure 5: **A.** Reflected-light photomicrograph of cortical bone from a human tibia (40x)
B. Scanning electron photomicrograph of cancellous bone from a human tibia (30x)

In an infant human body there are 270 bones while in the adult body there are 206 bones of which, 64 are in the upper extremities and 62 in the lower extremities. The bones are held together by ligaments, cartilage, and muscle/tendon groups. Bones come in a variety of shapes and sizes. Their size vary from the large leg, arm, and trunk bones (femur, humerus, and pelvis) to the small ear bones (incus, malleus, and stapes) while their shape ranges from long, beam-like bones (as in the arms, legs and extremities), to concentrated annular structures (vertebrae) to relatively flat plates and shells (scapula and skull bones). Despite the considerable varieties in size and shape, all bones are lightweight, yet strong and hard, in addition to fulfilling their many other functions.

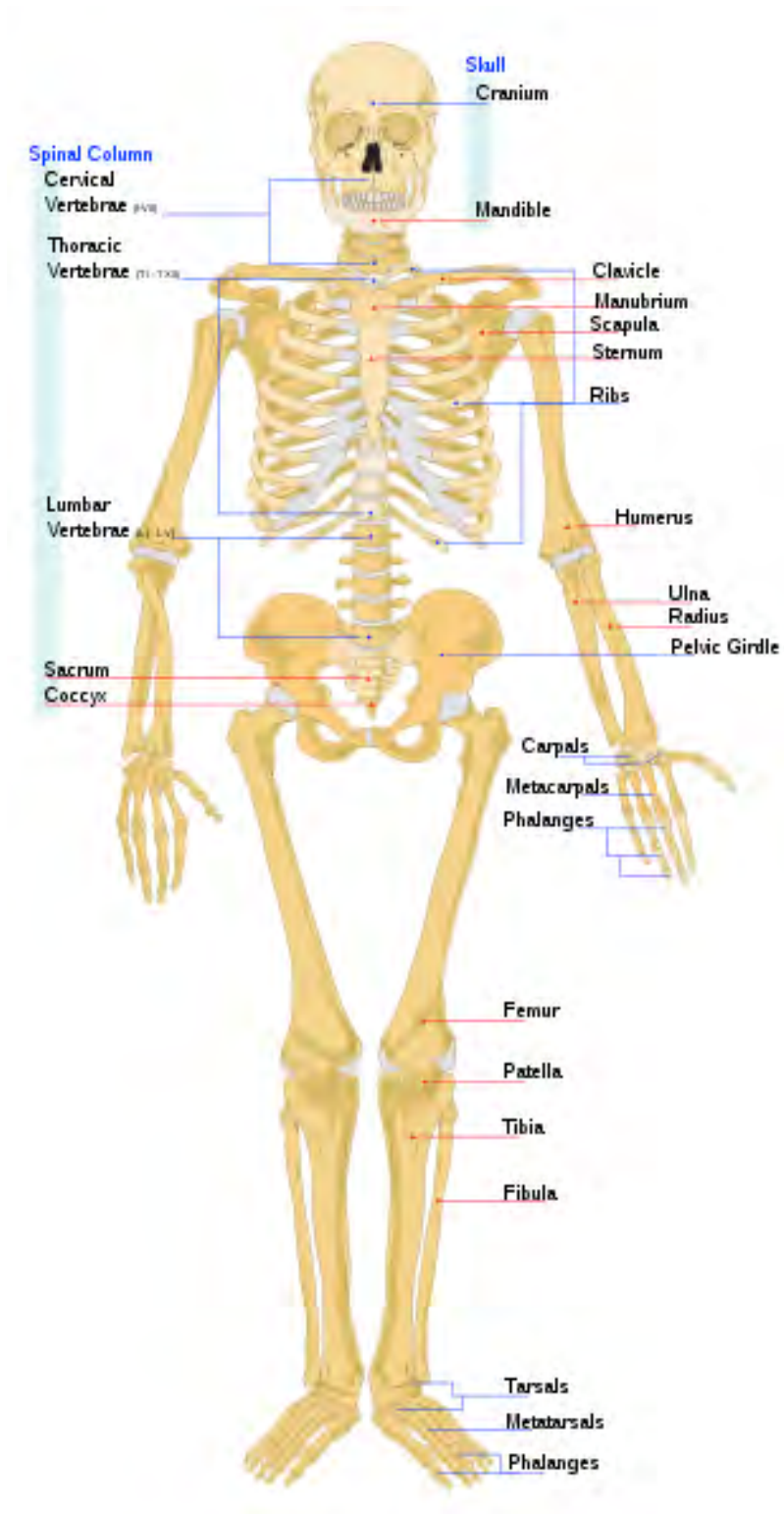


Figure 6: Front view of an adult human skeleton

Bones perform mechanical and physiological functions, by providing the mechanical integrity for static posture, locomotion and protection of internal organs and by contributing to the functioning of the metabolic pathway associated with mineral homeostasis (Einhorn, 1996) :

Mechanical functions :

- Provide *support* for the body against external forces (e.g. gravity),
- Act as a *lever* system to transfer forces (e.g. muscular forces), and
- Supply *protection* for vital internal organs (e.g. the brain)

Physiological functions :

- Form blood cells (*hematopoiesis*)
- Store calcium (*mineral homeostasis*)

2.1.2 Biomechanical behavior

Bone tissue, as with all biological tissue, is neither homogeneous nor isotropic. Since the structure of bone is dissimilar in the transverse and longitudinal directions, it exhibits different mechanical properties when loaded along different axes; a typical characteristic of composite materials known as anisotropy. Therefore, biomechanically, bone can be considered as a two-phase (biphasic) composite material, with the mineral as one phase and the collagen and ground substance as the other. In general, when a strong, brittle material (like collagen) is embedded in a weaker, more flexible one (like mineral), the resulted material has considerably improved mechanical properties. Its viscoelasticity (Fig. 7) makes bone stiffer when loads are applied at higher -within the physiological range- rates (sustains a higher load to failure) and stores more energy before failure.

2.1.3 Mechanical properties

Practically, the most important mechanical properties of bone are its stiffness and strength and can be examined by the load-deformation curve derived under the influence of externally applied loads in known direction. The knowledge of the mechanical properties of a whole bone, an entire ligament, a tendon or a metal implant is significantly helpful in the study of fracture behavior and repair or the effect of various treatment programs.

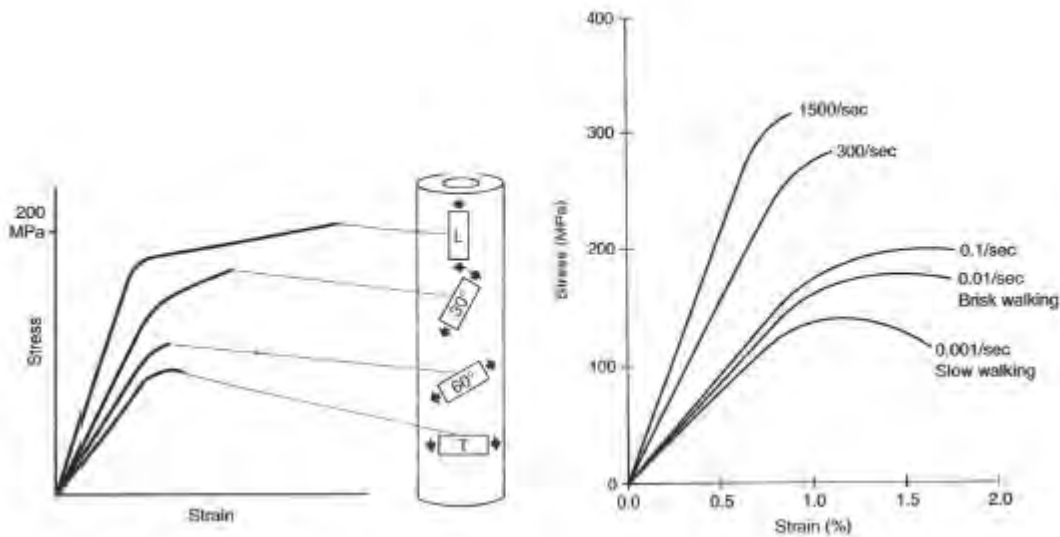


Figure 7: Mechanical behavior of bone showing its anisotropy (left). Mechanical behavior of bone showing its viscoelasticity (right). (From Nordin and Frankel, 2001)

However, characterizing a bone or other structure in terms of the material of which it is composed, independent of its geometry, requires standardization of the testing conditions and the size and shape of the test specimens. Such standardized testing is useful in cases of comparison of the mechanical properties of two or more materials, such as the relative strength or stiffness of bone and tendon tissue.

Since bone is anisotropic and non-homogeneous material, its physical properties vary both in location and in direction. Hence, they can be described with only approximate values for the associated density, strength and elastic moduli. Mechanical properties differ in the two bone types. Cortical bone is stiffer than cancellous bone, resisting greater stress but less strain before failure. The mass density for cortical bone is approximately $1800\text{--}1900\text{ kg/m}^3$. Cancellous bone in vitro may sustain up to 50% of strains before yielding, while cortical bone yields and fractures when the strain exceeds 1.5–2%. In addition, because of its porous structure, cancellous bone has a large capacity for energy storage (Keaveny & Hayes, 1993). The density of trabecular bone varies significantly depending upon its porosity ranging from 5% to 70% of that of cortical bone. (Nigg & Herzog, 1994 – Hayes & Bouxsein, 1997).

Figure 8 shows the typical stress–strain curves of cortical and trabecular bone with different bone densities tested under similar conditions. The apparent density is defined as the mass of bone tissue present in a unit of bone volume [g/cc].

Figure 9 better depicts the relationship of cortical bone to metal and glass and the differences in mechanical behavior among the three materials.

It is obvious that the steeper the slope, the stiffer the material is. The linear elastic behavior of glass and metal is indicated with the straight line, without yielding before the yielding point is reached. In comparison to these two, bone testing shows that the elastic portion of the curve is not straight but instead slightly curved, indicating its non-linear

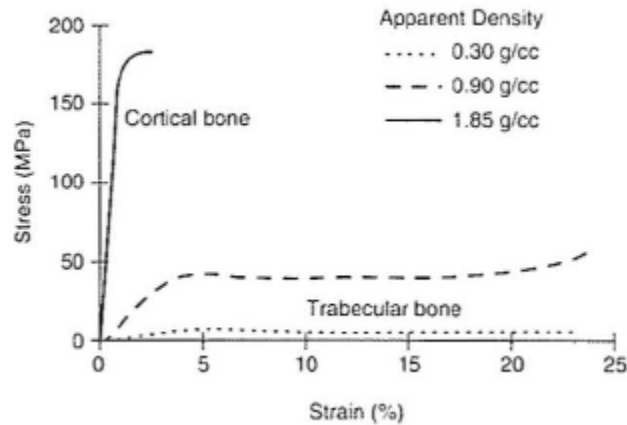


Figure 8: Example of stress-strain curves of cortical and trabecular bone tested in compression (From Nordin and Frankel, 2001)

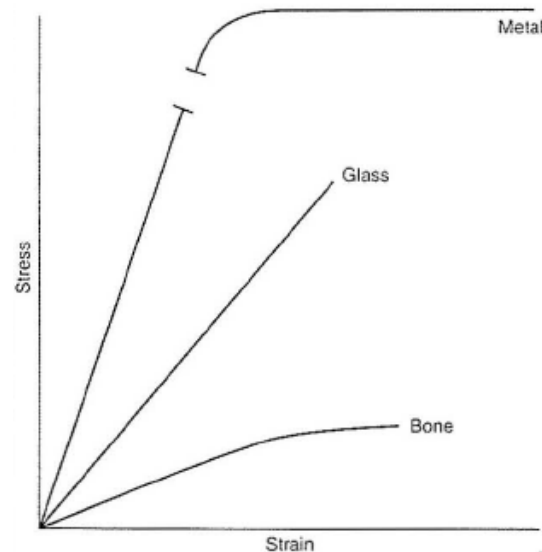


Figure 9: Stress-strain curves for metal, glass and bone (From Nordin and Frankel, 2001)

behavior. Bone, in general, exhibits more brittle or more ductile behavior depending on its age and its loading rate. Younger bone is more ductile whereas it becomes more brittle at higher loading speeds. Bone deforms before failing but to a much lesser extent than metal. When tested in tension, yielding in bone is caused by debonding of the osteons at the cement lines and microfracture while when tested in compression, yielding is indicated by osteons' cracking. Cortical and cancellous bone exhibit different values for ultimate stress under compression, tensile and shear loading. As shown in Figure 10, cortical bone can withstand greater stress in compression (approximately 190MPa) than in tension (nearly 130MPa) and far greater than in shear (70MPa). Young's modulus is approximately 17–20GPa in longitudinal or axial loading and approximately 11GPa in transverse loading. The corresponding values for the trabecular bone vary among papers. Yamanda (1970),

Steindler (1977), Reilly & Burstein (1975) and Martin & Burr (1989) give nearly 8MPa ultimate stress when loaded both in tension and compression.

Nordin and Frankel (2001) mention that trabecular bone can withstand 50MPa in compression loading and almost 8MPa if loaded in tension. The modulus of elasticity is very low (typical value 1GPa) and dependent on the apparent density of the cancellous bone and direction of loading.

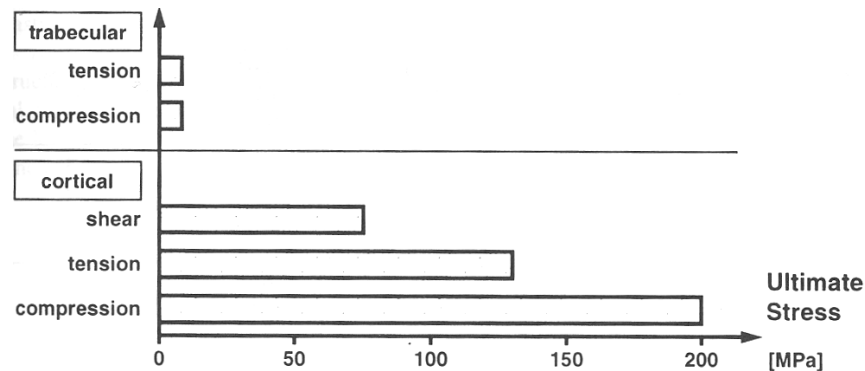


Figure 10: Magnitude of ultimate stress for cortical and trabecular bone (From Nigg and Herzog, 2005))

Hayes and Bouxsein (1997) model the dependence of the strength upon density as being quadratic and the Young's modulus dependence as being cubic :

$$\sigma = 60\rho^2 MPa \quad \text{and} \quad E = 2915\rho^3 MPa$$

where ρ is the mass density (g/cm^3).

Typical values for the elastic modulus E are :

- 1 GPa for trabecular (spongy) bone
- 20 GPa for cortical (compact) bone
- 200 GPa for metals

Concerning Poisson's ratio of cortical and cancellous bone, quite different data are presented in the literature. The cited values are between 0.2 and 0.5 (average: 0.3) for cortical bone and between 0.01 and 0.35 (average: 0.12) for trabecular bone density. (Knaub, 1981b; Reilly & Burstein, 1974; Ashman et al., 1984/88). No details have been given about any correlation to bone density (Wirtz, 2000).

2.1.4 Skeletal Processes

During human life, there are essentially four fundamental and distinct skeletal processes that occur at different ages in human bones: growth (intramembranous and endochondral), modeling, remodeling and repair. Even if the same types of bone cells are involved in all four processes, they are operating under different controls, in different locations and at various stages of human life.

Bone growth

The formation of bone during the fetal stage of development occurs by two processes:

- Intramembranous ossification mainly occurs during formation of the flat bones of the skull but also the mandible, maxilla and clavicles. The bone is formed from connective tissue such as mesenchyme tissue rather than from cartilage. The four steps in this type of ossification are :
 1. Development of ossification center
 2. Calcification
 3. Formation of trabeculae
 4. Development of periosteum

- Endochondral ossification is the process through which the majority of bones in the skeleton grow, including long bones. In this type of growth, bone is preceded by cartilage, which initially is a hyaline cartilage that continues to grow. The steps in endochondral ossification shown in Figure 11, are:
 1. Development of cartilage model
 2. Growth of cartilage model
 3. Development of the primary ossification center, responsible for the formation of the diaphyses of long bones, short bones and certain parts of irregular bones
 4. Development of the secondary ossification center that form the epiphyses of long bones and the extremities of irregular and flat bones
 5. Formation of articular cartilage and epiphyseal plate, a growing zone which separates the diaphysis and epiphysis in a growing bone

Ossification and growth of the bone come to a halt when cells at the growth plate stop dividing and the epiphysis fuses with the metaphysis of the shaft (skeletal maturity – 18 to 25

years of age). The growth of bone in a maturing skeleton is the only process that continually creates new trabeculae. Interesting changes in the size and shape of adult bones are noticed through the process of modeling.

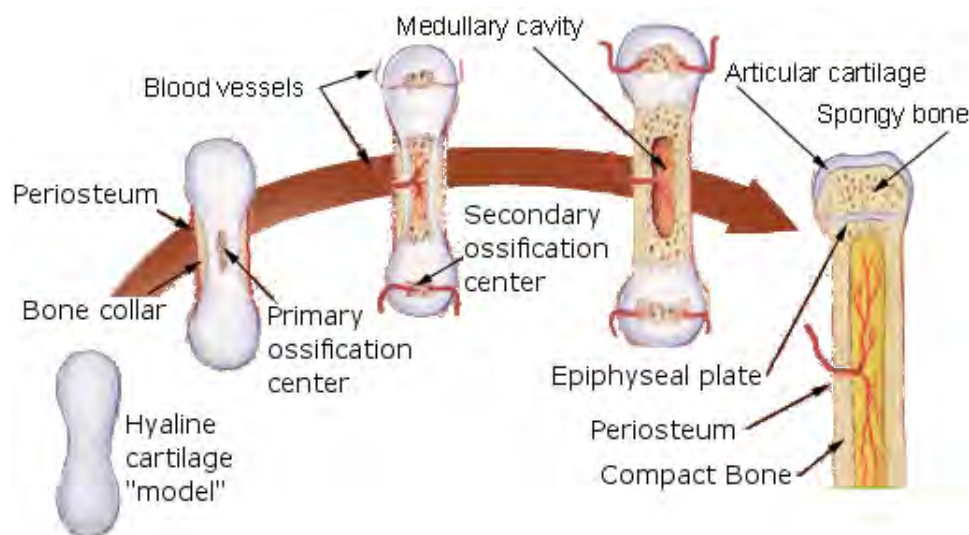


Figure 11: Endochondral ossification
(http://training.seer.cancer.gov/module_anatomy/unit3.3_bone_growth.html)

Bone modeling

Modeling is defined as the process by which bone mass is increased. It can occur through modeling drifts, which thicken cortices and trabeculae in children, or through mini-modeling drifts, which can thicken trabeculae in children and adults. Bone modeling, however, becomes inefficient in cortical bone of adults.

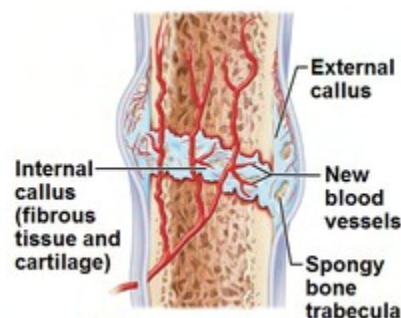


Figure 12: Formation of Internal callus consisting of fibrous tissue and cartilage

Bone remodeling

Remodeling in both cortical and trabecular bone occurs at Basic Multicellular Units (BMU) on all bone surfaces throughout life, at rates that vary. It is the phenomenon in which, bone gains or loses cancellous and/or cortical bone in response to the level of stress sustained,

summarized as Wolff's law. This fundamental law states that "*The shape of bone is determined only by static stressing.*" (Wolff, 1870). Hence, a positive correlation exists between bone mass and body weight. Specifically, a greater body weight has been associated with a larger bone mass (Exner et al., 1979). On the contrary, a long period of weightlessness, for example during space traveling, has been found to result in decreased bone mass in weight-bearing bones. In partial or total immobilization, bone is not subjected to the usual mechanical stresses, which results to resorption of the periosteal and subperiosteal bone as well as a decrease in the mechanical properties of bone, like stiffness.

Bone repair

This process is initiated with blood flow into the fracture region that normally coagulates to form a hematoma. Then, the fracture ruptures the periosteum, stimulating the rapid formation of the callus or woven bone and provides temporary strength and support for the fractured bone. Mineralization of the final callus may take nearly six weeks in an adult body and it is followed by a gradual remodeling to produce lamellar bone.

Age, nutrition, loading conditions, fracture position and type, patient disease, immobilization are some typical factors affecting the process of bone formation and modeling. In general, the factors influencing osteoblast function and bone formation include physical, chemical, hormonal, growth factors and antimineralization agents. (Wallach et al., 1989)

2.2 Human Lower Extremity

2.2.1 Skeletal Anatomy

The human lower limb consists of the hip, thigh, knee, leg, ankle and foot. There are 32 bones found in the lower limb, as shown in Figure 13: hip bone, femur, patella, tibia, fibula, tarsals (8), metatarsals (5), proximal (5), intermediate (5) and distal (5) phalanges. The major long bones of the human leg are the *femur* in the thigh and in the crus the *tibia* and the *fibula*. The femur (thigh bone) is the largest bone and the tibia (lower leg) and humerus (upper arm) are the next larger in the human body.

On its proximal end, the femur is connected to the pelvis with the hip joint, one of the biggest joints in the human body while distally, the shaft expands into a broad, double condyle which articulates with the crus to the knee joint, through the patella. In the normal case, the large joints of the lower limb are aligned on a straight line which represents the mechanical longitudinal axis of the leg, the Mikulicz line and stretches from the hip joint, through the knee joint and down to the center of the ankle. The eight bones of the tarsus make up the posterior section of the foot, with the calcaneus forming the heel. Articulation with the tibia is through the trochlear surface of the talus. Human legs are used for standing, walking, jumping running, kicking and similar activities and constitute a significant portion of a person's mass.

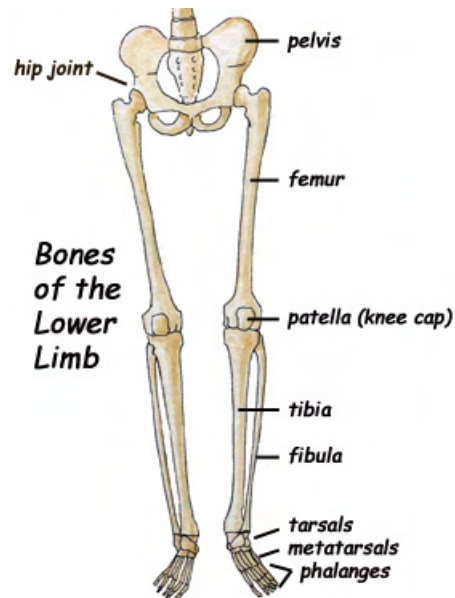


Figure 13: Human lower extremity anatomy (<http://www.exploringnature.org>)

2.2.2 Tibia : Structure and properties

The tibia (Fig. 14), shinbone or shankbone is the medial and strongest bone of the lower part of the leg and connects the knee with the ankle bones. It is named for the Greek *aulos* flute, also known as a tibia. Proximally, the tibia has a broad articular surface which articulates with the femur, entering into the knee-joint. The shaft (*diaphysis*) is prismoid in section and hollow, with a sharp crest running down much of the anterior border. On its distal end, the shaft is also expanded with a prominent process, the medial malleolus, and articulates laterally with the fibula and with the talus inferiorly.

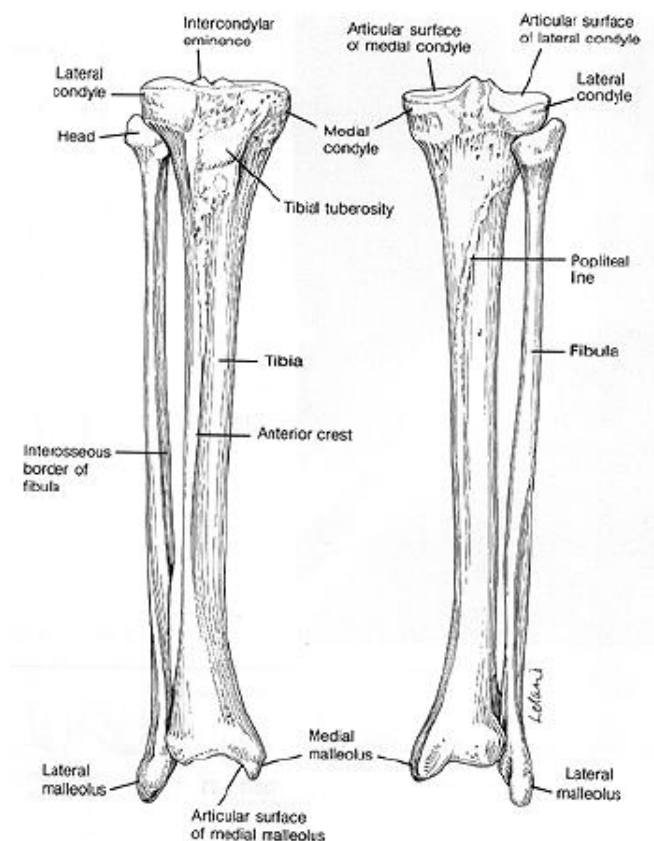


Figure 14: Tibia structure (From Spence, 1990)

The superior tibiofibular articulation is an arthrodial joint between the lateral condyle of the tibia and the head of the fibula. The inferior tibiofibular articulation (tibiofibular syndesmosis) is formed by the rough, convex surface of the medial side of the lower end of the fibula, and a rough concave surface on the lateral side of the tibia. The tibia is connected to the fibula by an interosseous membrane, forming a type of joint called a syndesmoses. The forward flat part of the tibia is called the fibia. The tibia derives its arterial blood supply from two sources : mainly, the nutrient artery and periosteal vessels entering from

the periphery which supply the epiphyseal–metaphyseal regions (Kelly et al., 1960)

In the male, its direction is vertical, and parallel with the bone of the opposite side. In the female, it has a slightly oblique direction downward and laterally, to compensate for the greater obliqueness of the femur.



Figure 15: Tibia articulates with the femur through the patella (X-Ray image)
(<http://www.fighttimes.com/magazine>)

For what concerns its strength, during walking, the tibia is taking an axial force that is up to 4.7 bodyweight while its bending moment in the sagittal plane in the late stance phase is up to 71.6 bodyweight times millimeter. When subjected to torsional loading, the proximal cross-sections of the tibia have a much higher moment of inertia from the distal ones, since much of the bone tissue is distributed at a distance from the neutral axis at the first ones but consequently the distal sections are subjected to much higher shear stress. Therefore, clinically, torsional fractures of the tibia commonly occur distally.

Selected mechanical properties of cortical tibia bone (From Nigg and Herzog, 2005) :

- Tensile strength : 95–140 MPa
- Compressive strength : 106–200 MPa

2.3 Bone failure: Fractures

Bones usually fail by fracturing under trauma. A bone fracture is a medical condition in which there is a break in the continuity of the bone. There are many reasons that produce bone fractures and a variety of types ranging from simple microcracks to comminuted fractures (multiple, fragmented disintegration).

2.3.1 Causes

Bone fractures occur due to reasons that can be sorted in two general categories: excessive load and weakened material.

Fracture due to excessive load occurs when the load is applied in any direction different from the direction of maximum strength of the bone. However, even in cases when the actual forces acting on the bone do not extent the physiological range for the bone but the structure has small dimensions then the stresses produced are beyond the limits. During impact, e.g. in contact sports or accidents, the forces and thus the bone loading can be very large, but they usually occur only for a few milliseconds.

Fatigue fracture occurs from repeated loadings when the combination of their frequency and amplitude exceed the ability of bone to remodel. That is, few repetitions of a high load or many repetitions of a relative normal load cause a fatigue fracture. In this case, fracture occurs when the rate of damage is higher than the rate of remodeling. Grimston and Zernicke (1993) examined the factors affecting the development of stress fracture in their model and concluded to a series of factors including biomechanical ones, muscle fatigue and hormone perturbations.

A bone fracture can also be a result of certain medical conditions that weaken the bones, such as osteoporosis, bone cancer or osteogenesis imperfecta (pathologic fracture). Osteoporosis (or porous bones) occurs when the mineral content of the bones decreases and makes bones more brittle and frequently changes their geometry.

2.3.2 Types

Clinically, bone fractures are divided into three general categories based on the amount of energy released at fracture: low-energy (e.g. simple torsional ski fracture), high-energy (e.g. automobile accidents) and very high energy fracture (e.g. very high-muzzle velocity gunshot).

In orthopaedics, fractures are classified in various ways. However, a more systematic classification of fractures is given below and depicted in Figure 16:

- *Closed (simple) fractures*, in which the skin is intact

- *Open (compound) fractures*, involving wounds that communicate with the fracture or cases where fracture hematoma is exposed

Different types of bone fractures according to the pattern in which bone breaks are:

- *Transverse fracture*, in which the break is across the bone at a right angle to the long axis of the bone
- *Oblique fracture*, in which the break goes in oblique direction to the long axis of the bone and the fracture is confined to one plane
- *Spiral fracture*, in which the break traverses both the planes
- *Comminuted fracture*, an injury with multiple breaks that are visible as different fragments
- *Greenstick fracture*, an incomplete fracture in which the bone is bent and occurs most often in children
- *Compacted (or Impacted) fracture*, which is caused when bone fragments are driven into each other
- *Avulsion fracture*, which is a closed fracture where a piece of bone is broken off by a sudden, forceful contraction of a muscle.

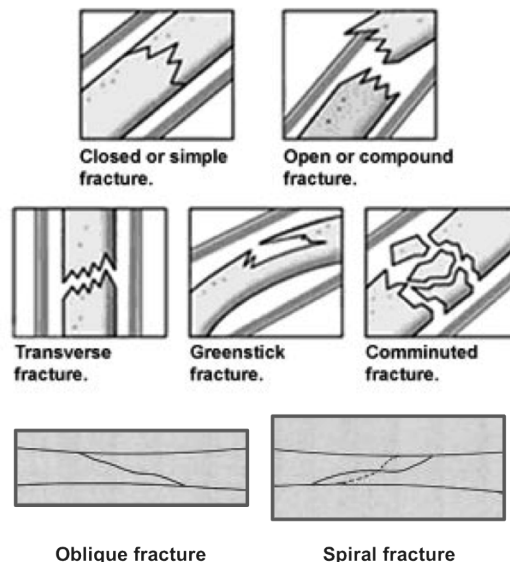


Figure 16: Types of fractures according to the pattern in which bone breaks
(<http://socalboneandjoint.com/fracture-care>)

- *Complete fracture*, when bone fragments separate completely
- *Incomplete fracture*, when bone fragments are still partially joined

Another categorization of fracture is *displacement (fracture gap)* and *angulation*. In case displacement or angulation is large, there is maybe the need for reduction and care by the surgeon.

TIBIA FRACTURES

Fractures to the tibia can occur from many types of injuries and in many different positions on the bone. They come in different shapes and sizes, and each of them must be treated dependent on a number of factors into account, such as location, displacement, alignment of the fracture, associated injuries, soft-tissue condition around it and of course the general health of the patient.

In general, tibia fractures can be separated into three categories based on the location of the fracture:

1. Tibial shaft fractures, which are the most common and occur at a point between the knee and ankle joints. Such type is exemplified by *Segond fracture*, an avulsion fracture of the lateral tibial condyle (Fig. 17 left)
2. Tibial plafond fractures, which are found near the bottom of the shin where the bone meets the ankle. This type requires attention due to the likelihood of soft tissue damage and the propensity for injuring the ankle cartilage surface. Examples of this category are *Gosselin fracture*, a break of the tibial plafond into anterior and posterior fragments, and *Toddler fracture*, an undisplaced and spiral fracture of the distal third to distal half of the tibia. (Fig. 17 top)
3. Tibial plateau fractures, which occur just below the knee joint and must be taken seriously into account since they can lead to developing knee arthritis. These fractures are the most injurious to the knee and possibly affecting both the bone and cartilage surface. *Bumper fracture* is an example of this category with a bone break of the lateral tibial plateau caused by a forced valgus applied to the knee. (Fig. 17 bottom)

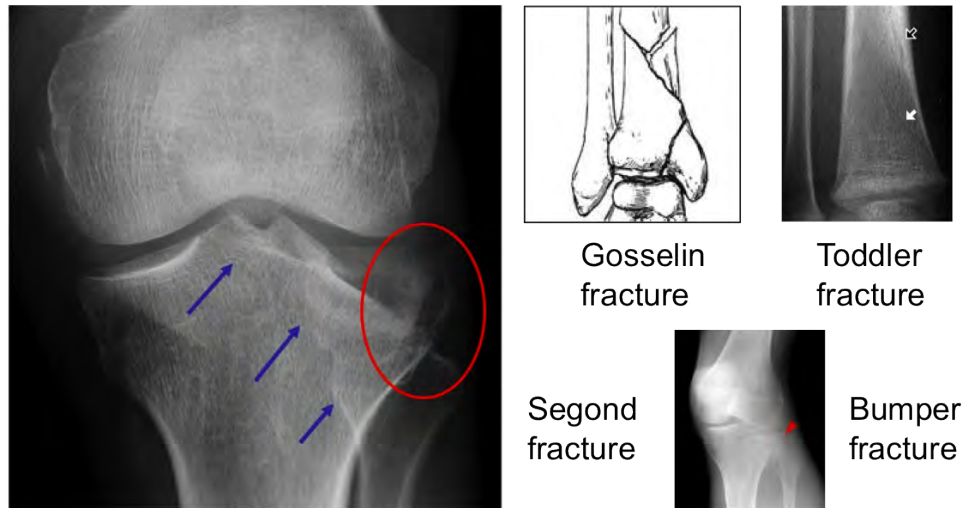


Figure 17: Types of tibia fractures (X-Ray image)
<http://www.e-radiography.net/radpath/t/toddlersfrx.html>

2.3.3 Treatment

Treatment of bone fractures are broadly classified as surgical and non-surgical (or conservative) procedures. The second category includes techniques such as pain management and immobilization while the surgical methods are done only in case the non-surgical treatment has failed or is possible to fail.

- **PAIN MANAGEMENT:**

In cases of arm fracture in children, non-steroidal anti-inflammatory drugs (NSAID) and opiates like ibuprofen and acetaminophen in combination with codeine are given to patients as pain reliever.

- **IMMOBILIZATION:**

Bone fractures are typically treated by restoring, under anesthesia, the fractured pieces of bone to their natural positions, when it is needed, and must maintain those positions during the whole healing procedure. An X-ray image shows the condition after the reduction and in case of any complication to this point, immobilization follows. The fractured limb is commonly immobilized with a plaster or fiberglass cast or splint (Fig. 1.16) which holds the bones in the corrected positions and immobilizes the joints above and below the break. In small bones, like phalanges of the toes and fingers, instead of fiberglass cast, buddy wrapping serves the similar function. When the initial post-fracture edema or swelling leaves, the fracture may then be placed in a removable brace or orthosis. Since movement is limited, fixation helps preserve anatomical alignment while enabling callus formation (bone growth).

When the conservative techniques fail or there is likelihood of failure, open treatment is chosen during surgical operations. There is a variety of internal and external fixation methods using surgical nails, screws, plates and wires to hold the fractured pieces together more directly (Fig. 18).

TIBIA FRACTURES

Tibial shaft fractures can be treated by several methods depending on the type of fracture and alignment of the bone. Occasionally, minor tibial shaft fractures are treated with long leg casts, from above the knee to below the ankle zone, to ensure successful healing as well as to avoid infections. In more serious shaft fractures, with too much displacement or angulation, conservative methods are not enough. Intramedullary (IM) metal rods are fitted along the middle of the tibia, under general anesthesia, to hold bone alignment and are secured within the tibia by screws.

Displaced tibia plateau fractures often require surgery to realign the fractured bones and alignment of the knee joint. There are several surgical options in their treatment depending on the fracture pattern. Surgical treatment usually involve the placement of screws, plates or combination of them (Fig. 18 middle) into the fractured bone and maybe followed by small or larger incisions using X-ray. Most tibial plateau fractures result in a period of non-walking for at least 3 months.

For what concerns the tibia plafond fractures, the treatment methods are similar with those described above for the plateau fractures. One major factor that should be considered with these injuries is the soft-tissue around the ankle joint. In case the soft-tissues are too swollen or damaged, any surgery is delayed. During the healing of soft-tissues, the fractured bone and ankle joint is immobilized using a cast, splint or external fixators (avoiding internal placement of plates and rods). The latter is chosen in cases requiring more precise fixation than a cast and the available systems will be discussed in the following sections. For the most severe fractures, the treatment is done through ankle fusion (Fig. 18 bottom) so as to provide a stable walking platform that has minimal pain.

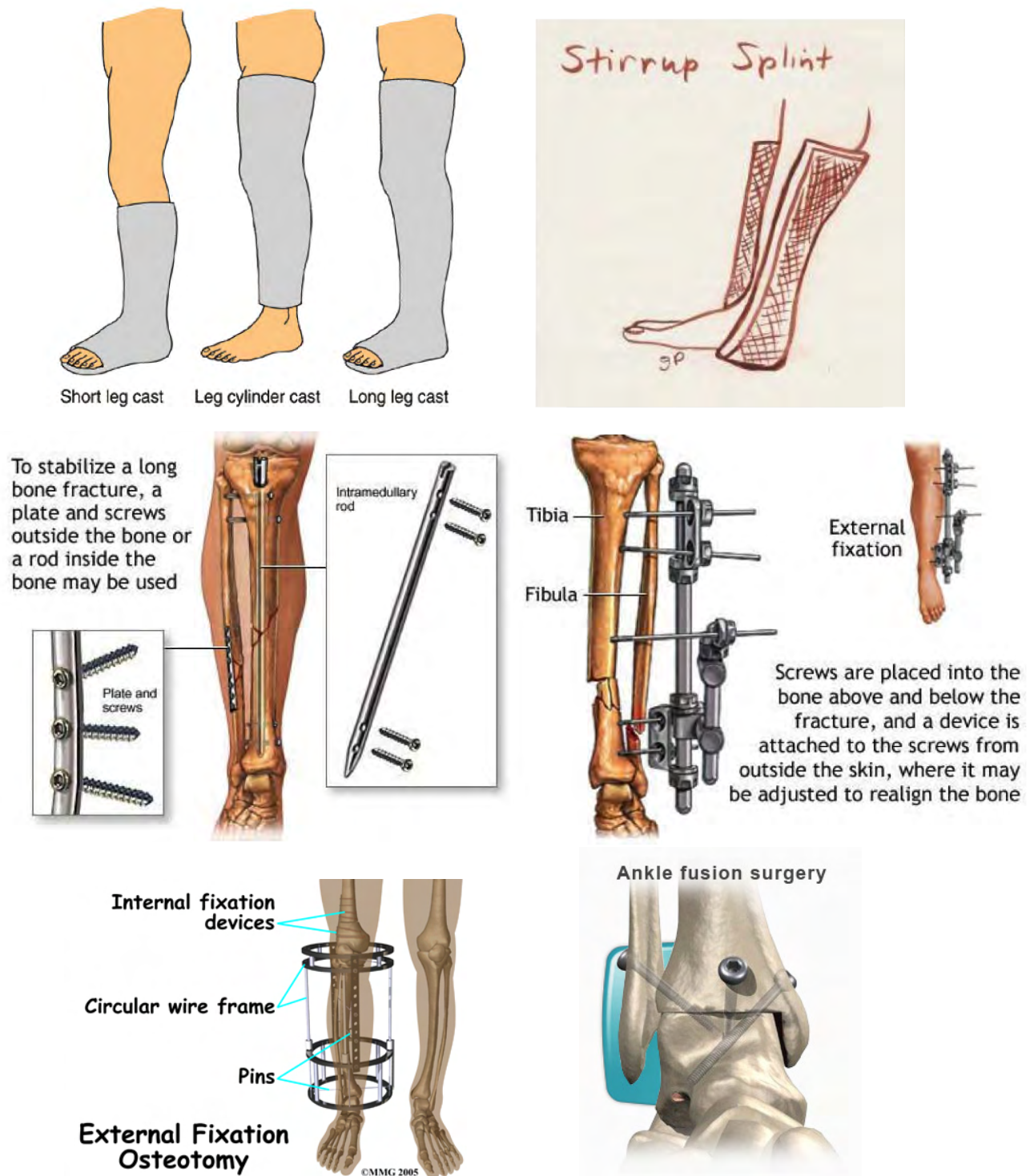


Figure 18: Immobilization using casts and splints (top). Internal fixation with IM rod and external fixation (middle) with screws, pins and plates lateral or circular (bottom). Ankle fusion (bottom) (<http://test.teachengineering.org/>, <http://www.orthopediatrics.com/docs/Guides/blounts.html>)

2.3.4 Complications

The severity of a fracture depends upon its location and the damage done to the bone and tissue near it. Serious fractures can have dangerous complications if they are not treated promptly.

One serious complication is the compression of nerves, blood vessels and muscle which is known as compartment syndrome, which if not treated can result in amputation of the affected limb. Other possible complications include the infection of the bone (osteomyelitis) or surrounding tissue, pseudarthrosis (non-union) or mal-union. Pseudarthrosis is the movement of the bone at the location of the fracture resulting from inadequate healing of the fracture whereas mal-union describes the case when the fractured bone heals in a deformed manner. A more detailed documentation for complications due to external fixators, which has been reported by surgeons and orthopaedists, is presented in the Section [2.4.5](#).

2.3.5 Rehabilitation

Bone healing after fracture may need weeks or months to be completed, depending on the type and the position of the fracture as well as the age of the patient. Teenagers tend to take longer to heal than children but still the period ranges between one and two months. Once the cast or splint is off, the patient should gently start exercising and follow a program planned by a doctor or physiotherapist.

In specific, recovery from a tibial plateau fracture can take several months. Because the cartilage surface of the joint is involved, the knee must be protected from weight until the fracture has healed. Most commonly patients will be allowed to move the knee joint, but not put weight on the leg for about three months. The amount of weight bearing, hence the healing period, depends on the fracture type and the portion and quality of callus formation.

In general, a minor fracture in a child may heal within a few weeks while a serious fracture in an older person may take months to heal.

2.4 External Skeletal Fixators

2.4.1 History and types

The development of external fixation systems dates back to ancient time and Greeks. Hippocrates in about 400 BC wrote about a simple external fixation to splint a fracture of the tibia. The device consisted of closely fitting proximal and distal Egyptian leather rings connected by four wooden rods from a cornel tree. The first use of “pins” is credited to the French Jean-Francois Malgaigne who, in 1840, created a simple metal pin in a leather strap for the percutaneous pin treatment of tibial fractures (Fig. 19 left). In 1843 he used a claw-like device, a new external fixator, to percutaneously hold the fragments of a fractured patella that he called “griffe” or “claw” (Fig. 19 right).

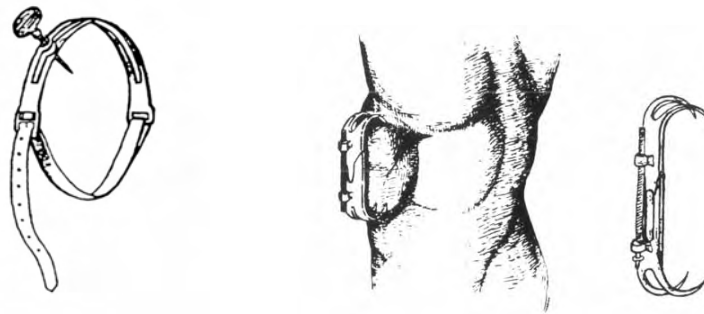


Figure 19: Malgaigne's pin in a leather strap (left) and patella (“griffe”) fixator (right) (From Nelson, 2001)

Since then, many external skeletal fixation systems employing percutaneously applied pins incorporated into plaster, methacrylate, epoxy-filed tubing, or mechanical exoskeletons have been developed. According to Burny (1965), Malgaigne's pin became popular and was improved by others, including Bonnet, Deltheil, Roux (Fig. 20 left) and Ollier (Fig. 20 right).

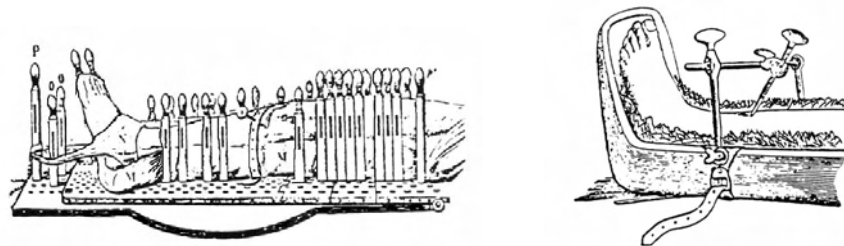


Figure 20: Roux's (left) and Ollier's devices (right) (From Nelson, 2001)

In the US, Clayton Parkhill, in 1894, devised a system utilizing percutaneous threaded pins connected to rigid external plates to treat fractures, non-unions, and mal-unions (Fig. 21 left). Coincidentally, Albin Lambotte from Belgium created, a system quite similar in design to Parkhill's. He was the first to develop a device specially designed for external

fixation, in 1902 (Fig. 21 right). For the first time, the device allowed the placement of pins in any needed direction and the pins were connected to the rod by adjustment clamps, which meant manipulation of the fracture in all three planes! The fracture had to be reduced prior to application of the external fixator. Lambotte was, furthermore, credited with developing the first self-tapping threaded pins. His device was a precursor to many of the modern devices in use today.

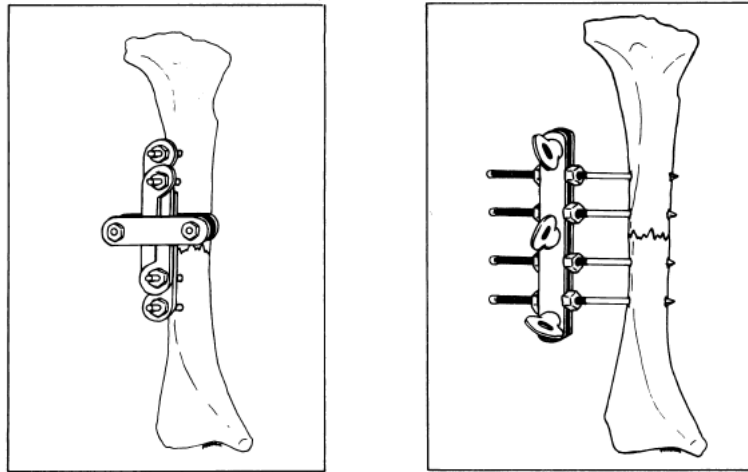


Figure 21: Parkhill's bone clamp (left) and Lambotte's external fixator (right) (From Pontarelli, 1982)

Shanz, Reidel and Anderson used nails, and screws in conjunction with casts and developed the idea of non-parallel pins for firmer control of bone fragments. Roger Anderson, from Switzerland in 1934, invented a fracture reduction apparatus utilizing, for the first time, transfixing pins that penetrated bone in a through-in through fashion. The pins were connected to movable horseshoe-shaped clamps that encircled the leg posteriorly and permitted multiplanar adjustments of the fracture (Fig. 22 left). The use of this device included reduction of the fracture and stability of alignment under compression until the surgeon applied a plaster cast, which permitted frame and clamps' removal when hardened. Later, Anderson developed a frame connecting the transfixing pins. The frame included bars which were attached to the pins by articulating clamps that, again, permitted multiplanar adjustments of fracture fragments. This frame, shown in Figure 22 (right), was the one that eliminated plaster casts.

Concurrently, the veterinarian Otto Stader, fabricated a system to treat long bone fractures in dogs. His adjustable external fixator provided stability of the fracture fragments and reduction in three planes independently (Fig. 23 left). His contribution was of a great interest for Veterinary Surgery because he improved fracture treatment in dogs who, until that time, destroyed casts by tearing and biting.

In addition, Dr Stader's work was more successful because he encouraged surgeons to

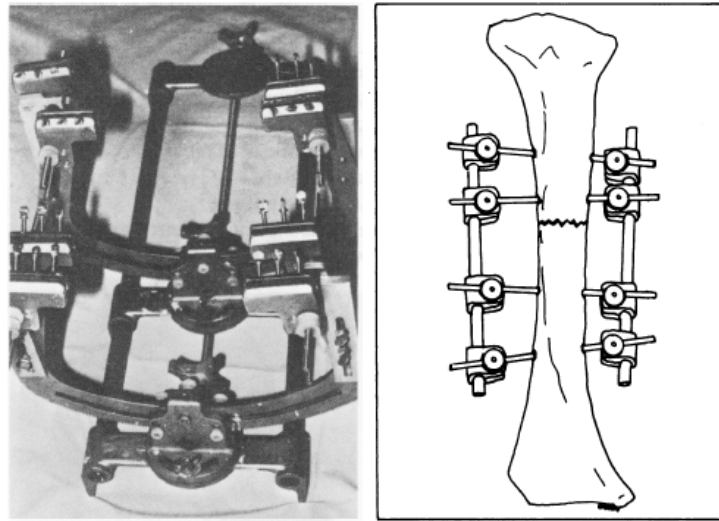


Figure 22: Roger Anderson's reduction apparatus (left) and fixator frame (right) (From Pontarelli, 1982)

apply his system to long bone fractures.

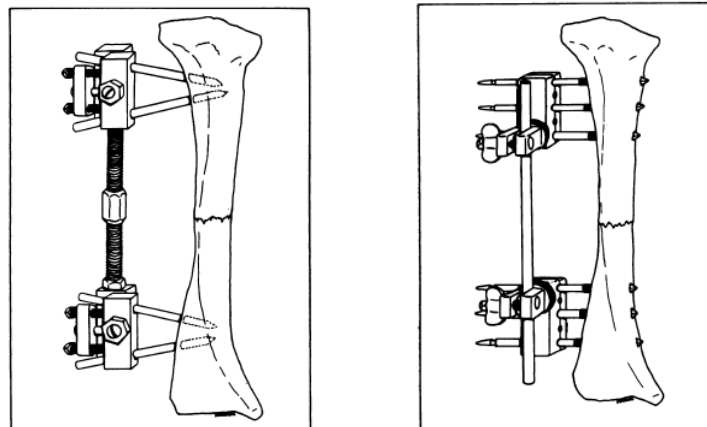


Figure 23: Stader's fixator (left) and Hoffmann's device (right) (From Pontarelli, 1982)

In Europe, in 1938, Raoul Hoffmann was the second, after Anderson, who expanded Lambotte's original concept of external skeletal fixation. He created a device that incorporated a universal ball joint pin holder that gripped a connecting rod (Pontarelli, 1982). The universal joint permitted fracture alignment in three planes with the fixator assembled, similar to Stadler's. In addition, Hoffmann substituted a sliding compression-distraction bar for a rigid bar which connected to the pin clamps. His device could achieve interfragmentary compression or limb length restoration (Fig. 23 right).

However, during the Second World War (1939–1945), external fixation developed a bad reputation and many papers described the complications of the technique, including pin infections, metacarpal fractures from pin holes, pin breakage or loosening, nerve or tendon damage from pin insertion and loss of reduction (Nelson, 2001). Allied forces used external

fixation only to encounter countless nonunions, giving the technique the nickname “ the nonunion machine”. Consequently, external fixators quickly fell out of favor since American military surgeons banned the device (in 1940) and hence their development was retarded in the United States. Between, 1950-1970, although American orthopaedists generally did not favor mechanical skeletal fixation to treat difficult fractures, they did employ pins-in-plaster for special problems like high-energy fractures of the tibia and fibula in the Vietnam War (1955–1975).

Unlike America, in Europe, surgeons continued to improve external skeletal fixation techniques after the end of World War II. Charnley impressed the orthopedic community by introducing (around 1950) an external fixator for knee arthrodesis, using a simple clamp that applied compression across cut cancellous surfaces of a joint (Fig. 24 left). During the 1960’s, Jacques Vidal and Jose Adrey recognized the need for rigid fixation and modified the original Hoffmann frame. They created a device (Fig. 24 middle) to treat septic non-union of long bones and after performing biomechanical testing, they showed that a quadrilateral design provided the optimum amount of rigidity (Pontarelli, 1982). In 1952, in Siberia, Professor Gavril Ilizarov developed circular external fixators that employed rings connected to bone by transfixion wires, known as Kirschner wires (Fig. 24 right).

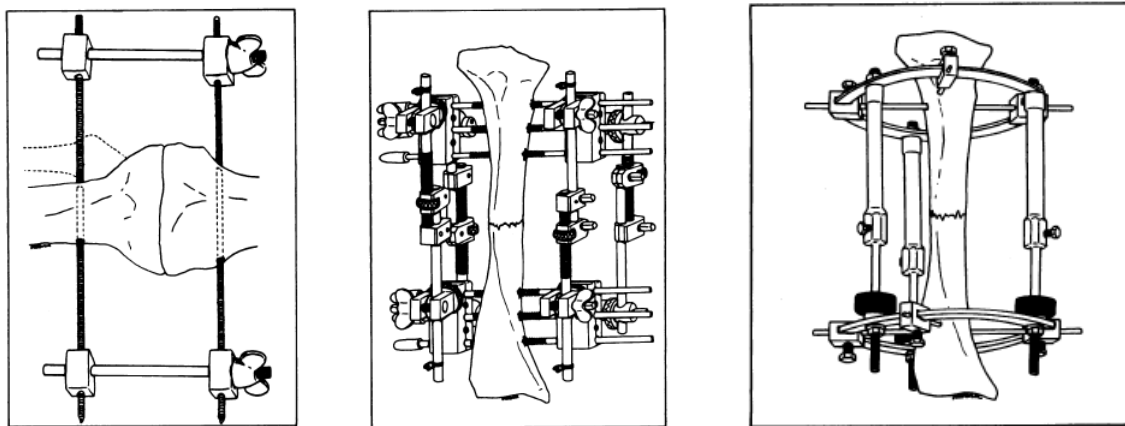


Figure 24: Charnley’s compression clamp (left), Vidra-Adrey quadrilateral device (middle) and Ilizarov ring fixator (right) (From Pontarelli, 1982)

The Western reply came by Kronner, an American orthopaedic surgeon, who modified the Russian design by using plaster components and transfixing pins instead of wires, as shown in Figure 25 left. The Ace-Fischer apparatus followed with a titanium half-ring frame, which allowed for simpler multiplanar fracture adjustment than that of the Vidley-Adrey frame. In addition, the half-ring configuration permits multiplanar insertion of half-pins that provides adequate stability while minimizing complications of transfixing pins (Fig. 25 middle). Many years later, Dr. Charles Taylor, in 1994, introduced in Houston the Taylor Spatial Frame (TSF), a second-generation circular external fixator expanding

the Ilizarov apparatus. The device was a three-dimensional spatial frame (Fig) consisting of two rings, wires and/or half-pins and six telescopic struts that enabled six degrees of freedom manipulation and therefore could correct displacements of angulation, translation and rotation simultaneously (Figure 25 right).

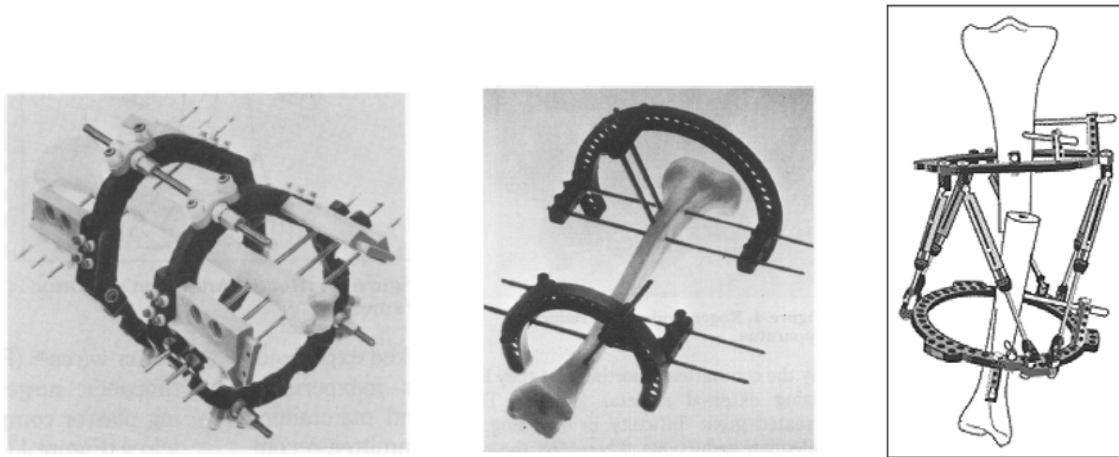


Figure 25: Kronner ring fixator (left), Fischer half-ring fixator (middle) and Taylor Spatial Frame (right)
(From Pontarelli, 1982)

2.4.2 Classification

It is obvious that the development of improved external fixators or the creation of new devices made possible a variety of applications and gave surgeons many different choices on dealing with bone fractures. Therefore, different classifications could be presented according to the *type of components* used (Simple pin, Clamp and Ring Fixators), the *mounting position* (Unilateral single-planar and Multiplanar Circular Fixators) or *frame configuration* (Unilateral, Bilateral, Quadrilateral, Biplanar, Ring and Half-Ring).

According to Chao and co-workers at the Mayo Clinic (USA), external fixators configurations have a terminology that includes the following categories (Green, 1981) :

- UNILATERAL : The unilateral frame employs one bar or rod connecting two or more pin clamps attached to half-pins. Examples of this category are Hoffman and Wagner apparatus (Fig. 23, 26)
- BILATERAL : A bilateral frame uses bars on both sides of a limb connected to pin clamps attached to through-in-through transfixing pins. The Anderson and ASIF tubular fixator exemplifies this type (Fig. 22, 26)

- **QUADRILATERAL:** This type employs four bars within the system, two on each side of the limb. The Vida-Adrey and 4-Bar Kronner serve as examples for this group (Fig. 24, 26)
- **BIPLANAR:** A biplanar frame uses pins placed in two or more planes for added stability. The ASIF tubular is often used in this configuration
- **RING:** This group utilize complete circular rings or hoops attached to bone by transfixing pins. The hoop surrounds the leg transverse to its long axis. This provides numerous possible pin insertion sites and also many connecting rods can be applied, which gives extremely rigid frames. The Ilizarov apparatus (Fig. 24), the Kronner ring or even the TSF device (Fig. 25) typify this group, and
- **HALF-RING:** It encircles the leg in the same way with the Ring Fixators and employs transfixing pins and half-pins, alone or in combination. The fracture pattern and associated soft-tissue injury determines the geometric placement of pin groups and the number and type of pin within a group. Examples for this type are the Ace-Fischer Fixator and the TSF apparatus for foot or femur fractures.

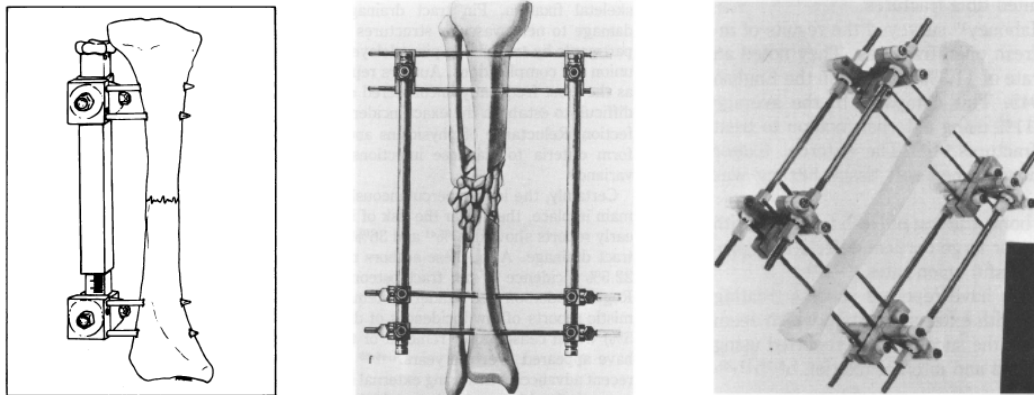


Figure 26: Wagner apparatus (left), ASIF fixator (middle) and Kronner four bar fixator (right) (From Pontarelli, 1982)

2.4.3 Comparison of Internal and External Fixators

Each type of fixation described above, no matter its configuration or its mounting position, gathers a number of advantages and disadvantages that makes it appropriate or not for the treatment of a bone fracture. However, research has shown that in certain fractures, external fixation is more beneficial compared to other means of fixation, such as open reduction and internal fixation (ORIF) and Intramedullary(IM) nailing, since they share the following advantages:

- *They cause less disruption of the soft tissues, osseous blood supply and periosteum :*
This property makes external fixators ideal for soft tissue management in the setting of acute trauma with skin contusions and open wounds, in chronic trauma where the extremity is covered in thin skin grafts and muscle flaps and in patients with poor skin whose healing potential is compromised as in cases of rheumatoid disease, peripheral vascular disease, diabetes mellitus and Charcot disease. Hence, wounds and soft tissues around the fracture are easily accessible for examination and care.
- *Bony stability :* The temporary nature of the pins and wires makes external frames ideal for stabilizing the bone in the setting of osteomyelitis, where the presence of internal implants make eradication of infection more challenging
- *Position:* The ability to avoid putting fixation into the infected area is an important benefit
- *Solid fusions:* External fixators have been particularly helpful in obtaining solid fusions of large joints with recurrent osteomyelitis
- *Application procedure:* Their mounting involves relatively low risk of failure and minimal blood loss
- *Quality of fixation:* External fixators are fixed-angle devices and as such they provide superior fixation in compromised bone (e.g. 82-year-old patient suffering from diabetes mellitus with an aseptic tibial nonunion healed in 4 months (Fragomen et al., 2006))
- *Multiplanar adjustment:* The ability to use these fixed-angle pins in multiple planes offers the versatility needed to reach the optimum stability while minimizing tissue damage. That is, external frames offer the great ability to choose ideal points on the fractured extremity to place wires and half-pins, especially in case with severe trauma where “good skin” is scarce
- *Adjustability:* Unlike internal plates and IM nails, external fixators provide postoperative adjustability. The adjustable frame allows for fracture alignment and realignment, which means surgical manipulation to gain exposures to fracture fragments for a wash out. In limb lengthening or deformity correction operations particularly, gradual manipulation is possible with frame adjustment

- *Use in pediatrics:* External fixators have been used in pediatric fracture care where open physes preclude IM nailing.
- Leg length discrepancy can be reliably treated with circular and monolateral design fixators. Many fixators provide excellent stability making early weight bearing and joint motion exercises well tolerated

2.4.4 Comparison of Unilateral and Circular Fixators

THE MECHANICS OF UNILATERAL FRAMES :

Unilateral frames are distinguished from circular frames in that they are positioned on one side of the limb. These frames allow the limb to remain functional, avoid complications, provide bony stability and are versatile enough to allow pins to be placed both near to the fracture and far from the fracture providing excellent control of the bone segment. However, when they are loaded out of plane, with varus - valgus and torsional forces, they have poor control of the bone fragments with significant motion at the fracture site. When subjected to axial loading, the unilateral frames show cantilever bending with asymmetric loading at the fracture site.

THE MECHANICS OF CIRCULAR FRAMES :

The classical circular frame is the Ilizarov apparatus that has been integrated with the newer Taylor Spatial Frame, described above. The basic components of both are rings, connecting rods, struts, wires and/or half-pins. Different Ilizarov configurations include full or partial rings or arches, with the last being helpful in areas like joints. Frame stability is greatly affected by ring properties, such as ring diameter, width, height, the type of ring connectors, the position of the bone in the ring, the distance between the rings, the wires pretension and the angle between them.

Many studies have been performed that compare the mechanical stability of unilateral and circular fixators in different modes of loading. But, since frame stability directly impacts osteogenesis, the comparison should include clinical aspects. The optimal design for an external fixator is the one that is rigid in torsion, bending, and shear but allows for axial movement.

Mechanically, Paley et al. (1990) found that specific monobody frames showed higher rigidity than the Ilizarov tibial frame, preventing axial motion at the osteotomy site, a fact that concerned scientists that the first are far too stiff and delay healing due to stress shielding. Gasser et al. (1990) and Podolsky and Chao (1993) noticed that the Ilizarov frame showed a non-linear load deformation curve in response to axial loading that was not exhibited in the monolateral fixators. Also, with weight bearing, monolateral frames

showed asymmetric compression to the fracture site whereas the circular frame led to uniform compression. The Ilizarov fixator demonstrated a load dependence of axial stiffness; at higher loads the stiffness of the wires and frame increased significantly and is thought to protect the healing fracture tissues from excessive motion preventing pain and fibrous nonunion. This property may explain how the Ilizarov frame has been able to promote osteogenesis while other fixators, like monolateral, failed to. According to Fragomen et al. (2006), there are studies which have shown that hybrid fixators, Ilizarov ringed frames with extra half-pins, show similar mechanical behavior with all-wired fixators while others reported increased stiffness of the hybrid in bending and torsional loading.

Clinically, the monobody fixators have offered several advantages over circular fixation in cases of lengthenings and deformity correction particularly of the humerus and femur. For example, because the arm is close to the torso, the use of full rings is impractical, as is for the thigh, since they disable the patient on sitting and lying down easily. When compared with ringed fixators, the monolateral designs are less awkward and practically, their reduced bulk facilitates hygiene maintenance and accommodates the use of greater clothing options. On the other hand, the rings in circular fixators provide circumferential access to the limb for placement of wires and half-pins making multiplanar fixation simple. Unlike monolateral frames, the circular nature prevents cantilever bending and in addition, gradual corrections of deformity and shortening can be simultaneously addressed. For large bone defects, multilevel osteotomies can be made to reduce bone transport time. When a bone defect is accompanied by overlying soft tissue loss, simultaneous transport of bone and soft tissue has been successfully performed using the Ilizarov method (Fragomen et al., 2006).

2.4.5 Complications

Although many authors have documented the success of treating serious bone fractures of the tibia by external fixations, there are still complications reported to be taken into account. Pin site infection, malunions, materials/component failure, fracture through pin site, damage to neurovascular structures and musculotendinous impalement are some of their usual complications.

According to Pontarelli (1982), the longer percutaneously applied pins remain in place, the higher the risk of infection. The usual treatment in these infections is aggressive local pin care and empiric oral antibiotics. If the infection does not resolve quickly, then culture-specific antibiotics are used and then, if needed, pins or wire are removed, to avoid operative intervention. In the same paper Pontarelli (1982) reports that, regardless of the incidence of infection, abscess formation surrounding the pin, necrotic skin, muscle and bone in the pin tract and excessive motion lead to infection. To avoid this, he details the procedure to be followed by a surgeon in order to minimize pin tract infection, including the application of fixators under sterile conditions in the operating room, reduction of the fracture prior to pin insertion, generous skin incisions at least 1cm long preferably transverse to the long axis of the tibial shaft and pin placement in the posterior $\frac{2}{3}$ of the shaft of the tibia.

Historically, malunions have been a commonly reported complication for fracture treatment with external fixators. Definite treatment with an external frame typically involves the use of the newer generation reconstruction fixators including the Ilizarov/TSF or a solid,adjustable monobody design. These frames have the versatility to provide postoperative adjustability, apart from the stability they offer. An impending malunion can be realigned postoperatively by using the fixator to correct deformity, which does not usually require additional surgery. Therefore, by correcting any deformity before the bone heals, a malunion is avoided.

Another complication is deep vein thrombosis that accompanies any lower extremity surgery and typically is treated with anticoagulation postoperatively. Furthermore, although the fixator protects the bone that it spans, it creates a stress riser in the adjacent bone that is not within the frame. This situation can lead to frame fracture, often through the most proximal or the more distal screw hole.

Other reports document the presence of significant neurovascular injuries. Pontarelli (1982) documented that during the development of a circular frame the transfixing pins tend to push vessels aside thereby making it impossible to penetrate a major vessel. However, as pin pushes a vessel aside without transecting it, the vessel rubs against the pin and the latter will erode the vessel causing arterial bleeding. Raimbeau (1979) also reported anterior compartment syndromes developed in patients who followed the insertion of transfixing pins. Similarly, sparse reports have noted nerve injuries by the use of transfixing pins.

Stiffness of adjacent joints occurs if the joint has been spanned for some time and during lengthening procedures. When fixators are used to treat tibia fractures, strong consideration should be given to the prevention of development of an early equinus contracture. Since the transfixing pins can seriously restrict joint mobility by impaling muscle and tendons, they should be inserted into the medial subcutaneous border of the tibia, even if the design of a stabilized configuration with this restriction is difficult.

2.4.6 The Ilizarov apparatus

The Ilizarov apparatus (Fig. 27) is a circular external fixator (CEF) system named and developed by Professor G. Ilizarov in 1952 to correct deformity through distraction osteogenesis. The method relies on the basic biomechanical principle of axial compressive loads and micro movement in the osteogenic zone stimulating biological bone bridging of the fracture gap (Davidson et al., 2003). The basic components of this frame are rings, connecting rods, and Kirschner wires (K-wires or simply referred to as wires).

The rings are connected to each other with the threaded rods attached through bolts or clamps consisting the metal frame. A hinge can be added to the rods to enable deformity correction. The rings are fixed to the bone fragments through the K-wires, which are pre-tensioned before being affixed to the rings while the frame is mounted to the patient. The K-wires, the rods as well as the rings are made of stainless steel and sometimes the rings may be made of titanium, or more recently carbon fiber.

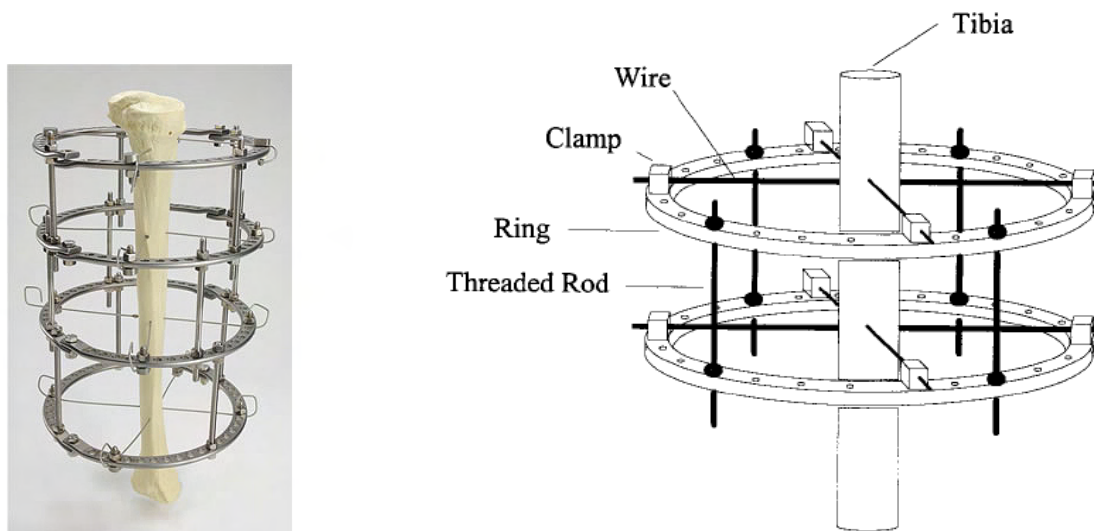


Figure 27: Ilizarov apparatus, a CEF system used to correct tibial deformity (<http://mistngo.org/category/gallery/medical>)

The ideal Ilizarov fixator is the configuration with the highest stability that is rigid in torsion, bending and shear but allows for axial movement, which stimulates callus formation in the fracture site. *Biomechanical studies have shown that frame stability is greatly impacted by ring properties, wire diameter and pretension and wire orientation. Hence, each parameter needs to be studied carefully and to be taken into account separately.*

WIRES : The wires number, diameter, orientation, type and pretension level varies affecting the fixator's stability; In general, increasing the number of fixation wires, increases the stability of the frame. Olive wires change the rigidity of the frame when they are replacing simple wires and typically wire strength and stiffness increases proportional to the diameter of the wire squared. Due to their small dimensions (thin wires), wire pretension is necessary in order to remain stiff under all possible loadings, to surpass the resistance of the intermediate soft tissue and avoid wire slipping at the fixation elements.

- WIRE NUMBER: Lewis et al. (1998) documented that increasing the number of fixation wires increases the stability of the fixation. Nikonovas and Harrison (2005), modeled the wires used in ring fixators and tested the effect of wire number and pretension on overall fixator stiffness. They concluded that if more wires are used to secure the bone segments on to the ring, the stiffness of the wire ring system linearly increases, for both axially and torsionally loaded wire systems.
- WIRE DIAMETER: Wires must be of the minimum and sufficient diameter to prevent plastic deformation or breakage. Wire diameter is reported to have the major impact in torsional stability. In human patients, the commonly used wire diameter is 1.5 , 1.8 and 2.0 mm. Podolsky and Chao (1992) tested four double-ring block constructs (two rings per bone segment) of 150mm ring diameter in axial compression and concluded that the use of 1.8-mm wires gives a 10–23% higher stiffness compared to 1.5-mm wires.
- WIRE PRETENSION: The relationship between wire tension and frame stiffness is non-linear because of self-tensioning effect of the wire (Aronson et al., 1992). When an untensioned wire is subjected to axial loading initially, at low loads, has a substantial deformation and the wire stiffness increases in a non linear exponential manner while loading is increasing, proving the necessity of pretensioning the Kirschner wires . Pretension loading is usually reported to bibliography between 50kg to 70kg for adolescents, 100–110 kg for adult patients and 120–130 kg in cases of weighty patients but varies depending on the wire diameter chosen. Lewis et al. (1998) have reported that the yield stress for the wires commonly used in human patients is 120 kg/mm², that is 210kg for 1.5-mm diameter wires and 305kg for 1.8-mm diameter wires. Wire tension should not exceed 50% of the yield strength in order to minimize the possibility of wire plastic deformation and breakage, which means 105kg for 1.5-mm diameter wires and 150kg

for 1.8-mm diameter wires.

Kummer (1992) noted that the effect of wire tension on stiffness reached a plateau once wire tension exceeded 90kg for 1.5-mm diameter wires and 130kg for 1.8-mm diameter wires (Figure 28). Since increasing the wire tension improves stability, the question is which is the limit to pretensioning in order not to decrease the transverse displacement of the wires and the axial displacement of bone segments during weight bearing. Practically, Gasser et al. (1990) reported that for a frame using 1.8-mm wires, doubling wire tension from 60kg to 120kg produced only a 10% increase in the axial stiffness. Similarly, Bronson et al. (1995) concluded that raising wire tensions of 90kg to 130kg in a single-ring construct was not a major factor affecting frame's stability.

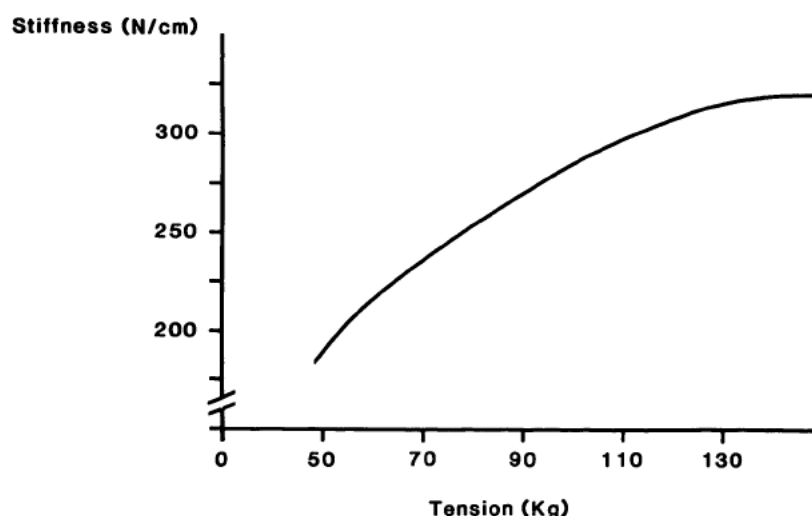


Figure 28: Relationship between wire pretension and axial stiffness of the frame (1.8-mm wires, 150-mm rings) (Kummer, 1992)

Sequential tensioning, also, during fixation application is not recommended because it can result in a decreased final tension in the wire and consequently a lower frame rigidity. According to all the above, the maximum recommended limits for wire tension are 90kg for 1.5-mm wires and 130kg for 1.8-mm wires.

- **WIRE ORIENTATION:** The angle of intersection between wires attached to the same ring affects the biomechanical profile of the fixator. Ilizarov (1992) taught that increasing the crossing angles of wires approaching the 90° provided maximal stability. Clinically, however, this is unattainable since there is a safe zone in which there are particular “safe corridors” where wires can be placed in order to avoid causing neurovascular and tendon injuries (Figure 30). Further testing verifies the 90°-rule only in cases of axial loading, whereas in medial bending forces, a 30° crossing angle for medial-to-lateral wires is preferred (Figure 29) (Roberts et al., 2005). Two wires that cross at an angle

of less than 60° permit unwanted sliding of the bone segment along the wires. When this orientation is inevitable, olive wires (Figure 28) can be used to buttress the bone, since they are inserted from opposite direction, and if needed, the addition of half pins can greatly reduce any bone sliding.

Wire-crossover angle (°)	Central (N/mm)	Medial (N/mm)	Posterior (N/mm)	Postero-medial (N/mm)	Torque (N m/°)
30	88.2 ± 2.34	57.4 ± 1.55	19.1 ± 1.6	22.5 ± 2.71	1 ± 0.17
40	95.3 ± 0.54	55.6 ± 1.33	26.7 ± 0.25	23.2 ± 1.66	1.3 ± 0.07
50	96.4 ± 1.49	56.5 ± 2.16	32 ± 1.36	25.7 ± 1.08	1.3 ± 0.08
60	99.8 ± 0.39	51.9 ± 2.65	45.4 ± 1.12	32.6 ± 0.75	1.4 ± 0.02
70	103.5 ± 0.61	50.8 ± 1.68	46.1 ± 0.74	34 ± 0.5	1.6 ± 0.001
80	106.8 ± 2.38	49.8 ± 1.2	50.5 ± 0.38	37.5 ± 0.83	1.8 ± 0.11
90	117.5 ± 4.41	48.5 ± 0.23	54.4 ± 1.23	40.1 ± 1.59	1.9 ± 0.16

Figure 29: The effect of varying wire-crossing angles on the stiffness of external fixation. The increasing wire crossing angle from 30° to 90° increased by 75% the overall fixation stiffness and decreased by 16% the medial bending stiffness (Roberts et al., 2005)

Podolsky and Chao (1992) found that in double-ring block fixators (150mm ring diameter), the configuration with wires crossing at 45° had less axial and greater torsional stiffness when compared with wires crossing at 90°. Sirkin et al. (2000), mentioned that the greater divergence of the wires would increase the strength of the frame, while Kummer (1992), under clinical considerations, proposed setting the wire angles of at least 60°.

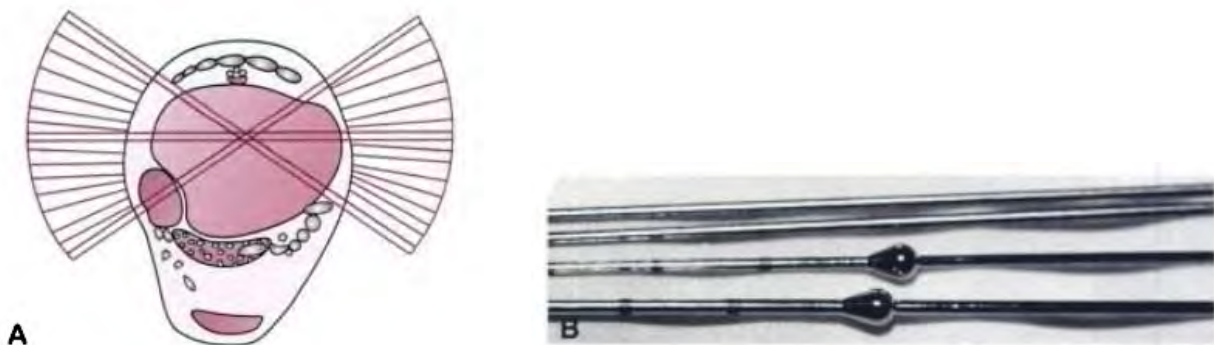


Figure 30: **A.** Safe zone of wire insertion in tibia **B.** Smooth and olive wires
(Banks, Downey, D.Martin, S.Miller, *McGlamry's comprehensive textbook of foot and ankle surgery*, 2001),
(GS Kulkarni, *Textbook of Orthopedics and Trauma*, 2008)

Another significant consideration relative to wire orientation is the positioning of the bone relative to the center of the ring. Antoci et al. (2006), tested different wire positioning of two and three 1.8-mm wires within a fiberglass tibia. The wires were crossed subsequently in the center (C) of the tibia, 1cm anteriorly (A) from the center, 1cm

laterally (L) from the center, 1cm medially (M) from the center and 1cm posteriorly (P) from the center, as shown in Figure 31, keeping them always in these zones that did not increase the crossing angle more than 60°. The samples with the wires crossed in the center of the tibia (Figure 31 point C) were significantly stiffer than all other samples in central axial loading configuration.

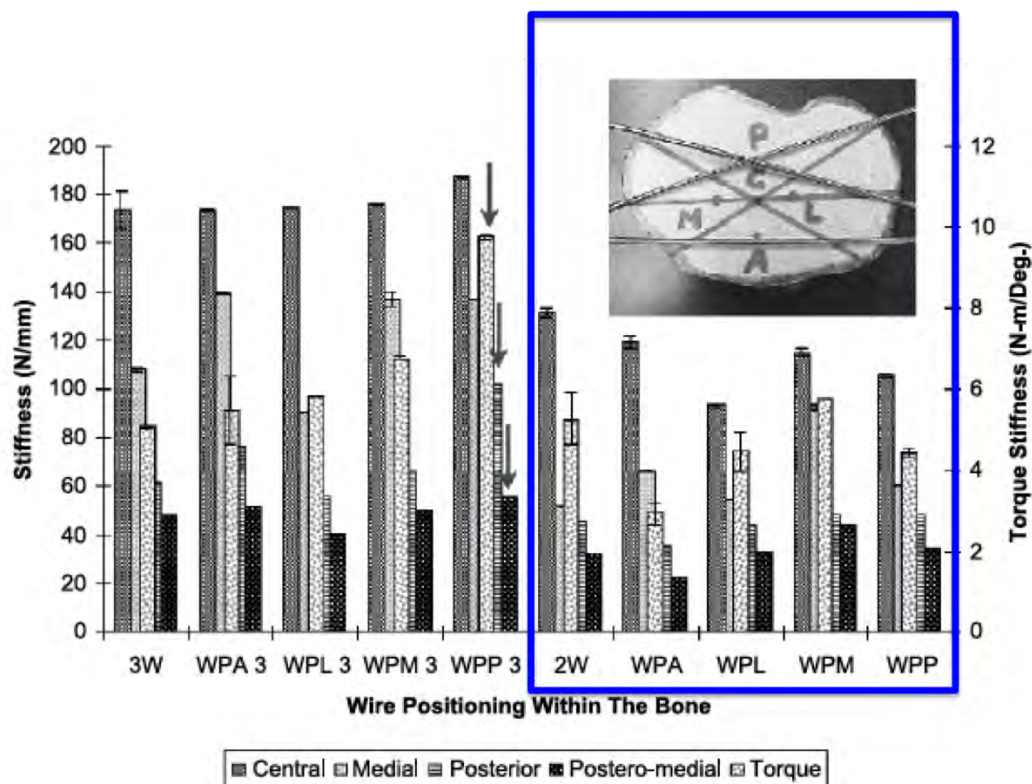


Figure 31: Relationship between wire positioning within the bone and stiffness parameters in different loading configurations (Antoci et al., 2006)

The results demonstrated that, in eccentric loading at points M and P, the samples with two wires crossed 1 cm medially (M) from the center of the tibia, were obviously stiffer than all other samples with two wires. In particular, when compared with the configurations with two wires crossed at the center (C), they are by 78% and 3% stiffer, when loaded at point M and P, respectively. The samples with 3 wires were overall significantly stiffer than the samples with 2 wires. Antoci et al. concluded that the configuration with 2 wires crossed 1 cm posteriorly (P) from the center of the tibia and a third placed in coronal plane 1 cm anteriorly (A) from the tibial center, increased overall stiffness of the fixator and predominantly in sagittal plane.

- **WIRE TYPE:** Smooth wires penetrate the bone and are affixed to the rings with bolts after being pretensioned. Olive or stopper wires, on the other hand, have a small bead that lies along the midportion of the wire, in direct contact with the cortical part of the bone (Figure 32). The use of olive wires improves bending stiffness and stability by minimizing translation of the bone along the wire. As it can be seen in the figure, when olive wires are inserted on opposite sides of the fracture, they greatly increase stability of fixation. Lewis et al. (1998) noted that parallel, opposing olive wires placed across an oblique osteotomy improved distractive stiffness from two to five times compared to smooth wires placed across, in distraction osteogenesis processes (limb lengthening).



Figure 32: Opposing olive beads can prevent bone sliding despite narrow crossing angles
(http://www.wheelsonline.com/ortho/tibia_fractures.ilizarov.circular.wire.fixators)

RINGS : Ring diameter has an important influence on the mechanical properties of the fixator because it dictates wire length. Ilizarov recommended to choose the smallest diameter ring possible, leaving a minimum of 2cm distance between the skin and the inner circumference of the ring, in order to enable soft tissue swelling and wire tract care. Increasing the diameter means increasing the length of wire spanning the ring, thereby decreases stability. Although the ring diameter impacts stability in all modes of loading, the significant effect is on axial stability, which is the most important factor in fracture healing, callus maturation and bone remodeling. It must be noted that stiffness is an inverse nonlinear function

of wire length. Increasing the diameter from 120mm to 160mm leads to a 30% reduction of axial stiffness and only a 10% decrease of torsional and bending stiffness (Bronson, 1995). Gasser et al. (1990), reported that the influence of ring diameter is more evident at lower axial loads. This load-related response was attributed to a self-tensioning effect of the wires during loading, resulting in a progressive increase in stiffness. In general, ring diameter selection in clinical practice is dictated by anatomic constraints. Typical values of internal ring diameters are 150mm and 180mm.

The appropriate configuration for each case varies depending on the intended application of the apparatus. Generally, configurations that secure individual bone segments at a minimum of two levels (two rings per segment - Figure 33) profoundly increase the fixation's stability compared to configurations at one level (one ring per segment - Figure 27 right). A one level configuration is often adequate for limb lengthening and angular corrections, but for fracture stabilization a two level configuration is preferred. It is important to widely separate the fixation levels; Gasser et al (1990) showed that if a four ring frame is used to stabilize a fracture, then its stability is maximized if the middle two rings are placed in close proximity to the fracture site.

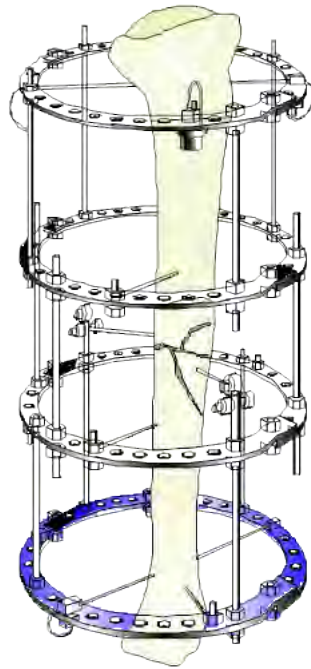


Figure 33: Four-ring Ilizarov construct used to stabilize a comminuted fracture (Department of Orthopaedic Surgery - University Stellenbosch's website)

2.4.7 The Taylor Spatial Frame

The Taylor Spatial Frame (TSF; Smith&Nephew, Memphis, TN,USA) is a second generation circular external fixator that can treat a variety of fractures, nonunions and malunions in both adults and children. Angular, translational, rotational, and length deformities can all be corrected simultaneously with the TSF on behalf of the six degrees of freedom (DOFs) of its struts. The TSF is a hexapod device based on the Stewart-Gough platform (Figure 34) (publicised in 1965 by D. Stewart, a six-jack layout first used by E.Gough in 1954, both in UK) that shares a number of components and features of the previously described Ilizarov apparatus.

It was developed by Dr. Charles Taylor in 1994 in Houston, USA, and it was thought to be the strongest reply of the West to “Ilizarovians” of the East. The device consists of two aluminum rings connected by six telescopic struts at special universal joints and is connected to bone by half pins and/or tensioned wires (Figure 35). Each strut can be independently lengthened or shortened (Figure 36). The frame’s significant benefit towards all previous CEFs is that the attached bone can be manipulated in six axes (anterior/posterior, varus/valgus, lengthen/shorten) through the adjustable struts.

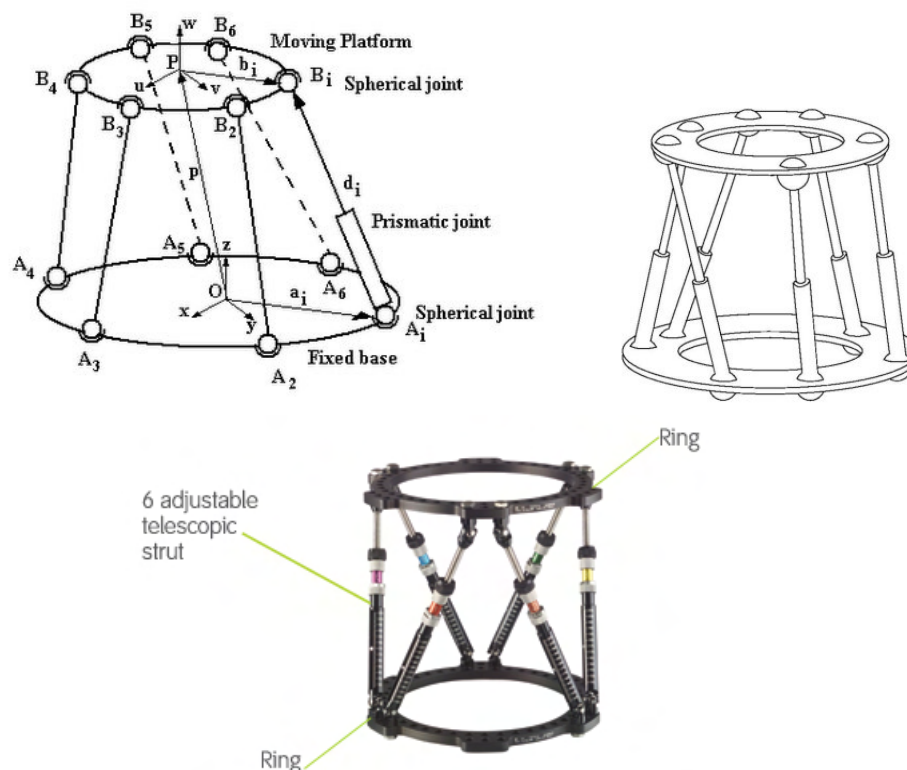


Figure 34: Stewart-Gough platform (SGP) is a parallel manipulator consisting of two rigid bodies: a moving platform and a base, whose position and orientation are fixed. The platform and base are connected with 6 extensible legs (top), The Taylor Spatial Frame by C.Taylor (1994) (bottom)

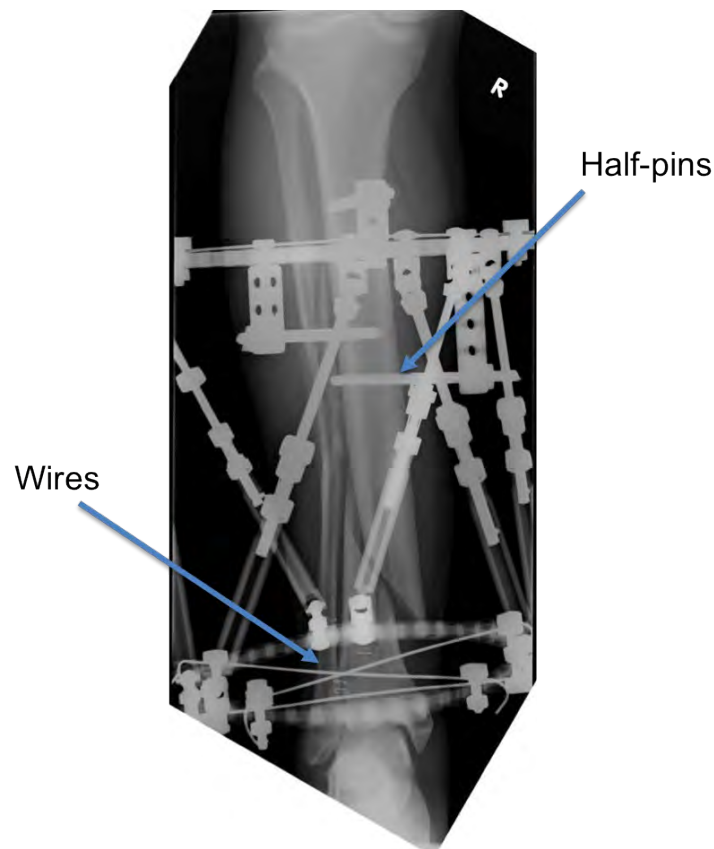


Figure 35: Radiograph of tibia fracture treated with TSF using 3 half-pins, 3 smooth and 1 olive wire (<http://pulseengine.com.au/aboutus.html>)

TSF can correct the simplest to the most complex skeletal deformity utilizing the same frame, using three primary methods of correction :

- Acute fractures may be stabilized with the Spatial Frame using traditional methods
- Rings may be attached to each fragment prior to strut attachments, for fractures or chronic deformities
- A frame may be adjusted to exactly mimic a deformity prior to mounting

In all the above cases, bone segments can be further reduced after frame application, if necessary, only by adjustment of strut lengths, through the TSF software.

In SGP, for a set of given values for the lengths of the six legs, the pose(orientation) of the platform could be generally determined (Gao et al., 2005). Similarly, in the TSF, by adjusting only strut lengths, one ring can be repositioned with respect to the other. Skeletal deformity cases, for example, are characterized by measuring the three projected angles (rotations) and the three projected translations between major fragments.

- STRUTS :

Standard telescopic struts (Figure 36) range in functional length from 75–283mm. They are available in four length groups : x-short (75–96 mm), short (90–125 mm), medium (116–178 mm) and long (169–283mm). For each group, the first number corresponds to its shortest and the second to its longest length while there is a mid-position, too, marked on each strut. They are marked with millimeter graduations with actual strut length printed every 10mm. A newer version of the above groups, FastFX™struts (Smith&Nephew,USA) likewise range in functional length from 91–311mm. Struts are attached to the rings with special shoulder bolts that allow strut rotation around their major axis, since shoulder height is greater than the ring thickness. The holes in the rings for attaching the struts are apparent.



Figure 36: A short strut and a medium strut both set to 120 mm (left), A close-up of the mid-position of a short strut (right) (C.Taylor, *Correction of General Deformity with the Taylor Spatial Frame Fixator™*, 2002)

- RINGS :

The TSF rings are made from aluminum alloy and are only partially radio translucent. For what concerns the rings geometry, proximal and distal ring internal diameters vary, too. The rings come in five different shapes: full, $\frac{2}{3}$, half, foot and 'U' ring (Figure 37). Complete (full) rings range in size from 105–300 mm internal diameter in 25 mm increments. Different size rings may be used in one frame, according to the specific anatomy and the fracture site. Short and long foot plates are available in 155-mm and 180-mm internal diameter.



Figure 37: A $\frac{2}{3}$ ring permits more proximal fixation of the femur and humerus. Accessory rings and partial rings may be attached to extent the levels (ring-blocks) of fixation (www.bonefixator.com)

- FRAME PARAMETERS :

The surgeon as well as the TSF software that accompanies the mounting and helps him, need three parameters to fully describe a particular TSF configuration: proximal ring internal diameter, distal ring internal diameter and neutral frame height or neutral strut length.

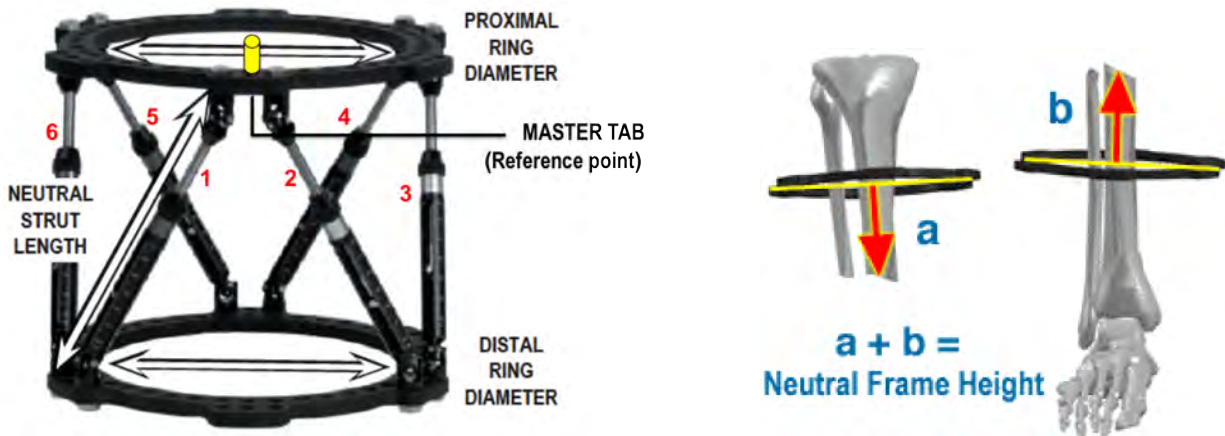


Figure 38: The three parameters that fully describe a configuration are proximal and distal internal diameter and neutral strut length or frame height (C.Taylor, *Correction of General Deformity with the Taylor Spatial Frame Fixator™*, 2002)

The neutral frame height is the distance from the center of one ring to the center of the other ring will all struts at their neutral length and is chosen by the surgeon preoperatively in cases of chronic deformity correction. From this neutral position the frame will subsequently be adjusted to compensate for residual deformity. But, when the frame is used for fractures or malunion/nonunions, the neutral frame height is measured by radiograph or image intensifier. With a is denoted the distance from one ring to the interior end of its bone segment, with b the distance from the other ring to the interior end of its bone fragment and the sum is the neutral frame height, which becomes the target for the surgeon and the program.

In tibia fractures, the mount of the frame is initiated by placing the proximal free ring at the proximal(upper) bone segment. It is important to center the master tab to the knee and, in tibia shaft fractures close to the plateau, place the proximal ring with the master tab under the tibial tuberosity. This way, struts 1 and 2 are located exactly anterior on the proximal fragment. The master tab is the reference point (Figure 38). Then the distal ring is placed in the other bone segment in a position that the surgeon selects and the frame is fixed to the bone fragments with the struts in their sliding mode. It is the moment when the fracture is closed reduced under direct vision or C-arm control and the strut slides are locked, according to an alternative technique of reduction. The traditional technique starts with placing longitudinal traction across the limb to obtain a closed reduction and mounting then the fixator while maintaining the reduction. After the fracture reduction in TSF, the

struts are locked to hold this position. In case the reduction is not anatomic, then through the TSF software acutely or gradually is fine-tuned the movement of the rings reaching the anatomic reduction. Translation between fragments is measured from an Origin on the reference fragment to its Corresponding Point on the moving fragment. Either fragment could be the Reference one. Ideally the one selected should have its anatomic planes the closest possible to the planes of the AP and Lateral radiographs and the latter must include the actual or anticipated level of attachment of a ring to this fragment. The best choices for Origin and Corresponding Point are points that are coincident in the anatomic state (Figure 39).

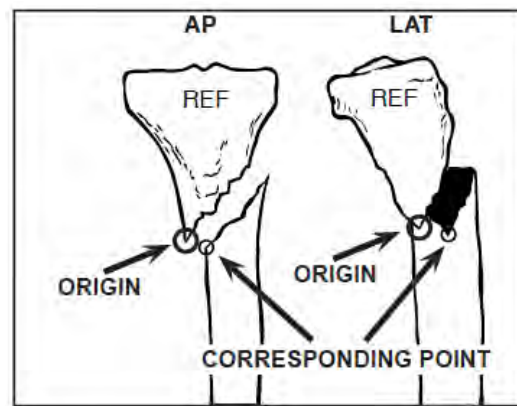


Figure 39: In anatomical reduction, the O and CP are coincident and there is no angulation or rotation between the fragments (C.Taylor, 1997)

The appropriate configuration, including the number of half-pins and wires, is selected following the same principles with the Ilizarov apparatus for the wire crossing angles and pretensioning limits. The fracture site specifies the safe zones, in order to avoid major neurovascular structures and injuries and mainly the orientations of the proximal ring's components, in tibia shaft fractures.

- **HALF-PINS :**

The half-pins used in TSF or hybrid Ilizarov frames are made of stainless steel or titanium. They come in three available section diameters: 4-mm, 5-mm and 6-mm and they are threaded, often called as Schantz screws. 4-mm and 5-mm diameter pins are used for adolescents and small adults while 6-mm diameter pins are preferred in adults or overweight children. Selecting a pin should take into account that the diameter of the pin must be less than $\frac{1}{3}$ of the bone diameter, to minimize the risk of fractures at the pins site. Half-pins are fixed onto the rings using one, two or three-hole Rancho Cubes (Figure 40 right). As the diameter of the pins increases, so does the rigidity (Fragomen et al. (2006). Long fragments are fixed with at least two and often three pins in different planes. In these types of fractures, half-pins should be spread longitudinally along a significant portion of each fragment but always out of the zone of soft-tissue injury.

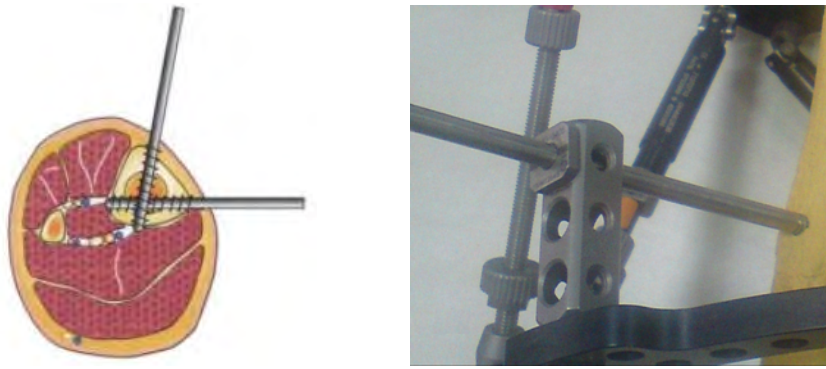


Figure 40: Half-pins are placed with 90° divergence at the mid tibia (left), Three-hole Rancho cube (right) (D.Wiss, *Master techniques in orthopaedic surgery–Fractures*, 2006)

A 90° crossing angle of half-pin is desirable for improved control in multiple planes (Figure 40). Shorter per-articular fragments can be fixed with at least two multiplanar half-pins at approximately 70° to each other. Knowledge of the safe zones is necessary and is explained in the following paragraphs.

Half-pin insertion is realized by hand after careful drilling. The principle of low-speed power and low heat generation during the insertion is of paramount importance. All half-pins should be bicortical and predrilled using a sharp drill bit with a tissue protection sleeve. Frequent pauses to cool the drill bit in cold saline is recommended to avoid thermal damage, because thermal necrosis may be the initiating event of pin loosening and infection.

An alternative choice that becomes more and more popular are hydroxyapatite (HA) coated pins, especially in operations where frames will stay on for several months (e.g. deformity surgery). HA coated pins (Figure 41) have been shown to have lower rates of loosening, increased extraction torque, decreased infection rates and even a lower incidence of secondary deformity during lengthening (Fragomen et al., 2006).



Figure 41: HA is a naturally occurring mineral form of calcium apatite, which makes up to 50% of bone in its inorganic phase. It is commonly used to coat implants (e.g. hip replacements) since it has been suggested that it promotes osseointegration. (Fragomen et al., 2006)

The safe zones of wires and pin placement vary depending on the fracture site and are reported separately:

Proximal to the Tibial Tuberosity:

The safe zone extends from posteromedial border of tibial plateau to the tibiofibular joint, excluding the patellar tendon. Pins can safely be inserted within an arc of 220° and at the oblique lateral or medial aspect of proximal tibia. Transfibular half-pins provide additional fixator stability but first, a guide wire must be inserted through the fibular head and then driven out of the proximal tibia. At this position, later, a cannulated drill is inserted from the tibia into the fibula and when it is removed the selected half-pin is inserted through the tibia. Transfixation wires can be inserted through the anterior portion of fibular head, aiming 30° anterior across proximal tibia. Attention must be paid to place the wire at least 1cm below joint line, to avoid potential septic arthritis.

Distal to the Tibial Tuberosity:

Safe arc of insertion is decreased to 140°. Half-pins are placed at the oblique medial aspect of the tibia while transfixation wires are inserted at the oblique lateral aspect of tibia, just distal to the tibial tubercle, and exits along the postero-medial aspect of tibia.

Mid-Tibia and Distal Tibia:

Transfixation wire is inserted 1 cm lateral to the tibial crest and is aimed posteromedially at an angle of 40-50° so that it passes just anterior to the posterior compartment musculature. If needed, a second wire can be inserted transversely from lateral to medial, through the anterior compartment musculature and out the medial side of the tibia.

Distal Tibia (above the ankle):

The safe arc remains at 120–140°, but the anterior tibial vessels and deep peroneal nerves become vulnerable as they cross the lateral tibial cortex. Transfibular half-pins follow the same trends with the first case. Transverse fixation wire may be inserted from lateral to medial starting at a point 1 cm anterior to the fibula or at a point just lateral to the tibialis anterior and aiming posteromedially to exit the tibia just in front of the tibialis posterior.

When deciding whether to use half-pins or wires for fixation, the clinical scenario may call for one over the other. It is generally preferred to use hybrid frames, consisting of both wires and pins. Transverse wires are useful in the metaphysis, where they avoid muscle compartments. In cases with small bone segments, stable fixation is succeeded by using multiple wires. They allow for axial motion at the fracture/osteotomy site, producing a so-called “trampoline effect” with weight bearing, which is promoting osteogenesis. Because of their easy clinical extraction, wires are preferred in deformities where there is the need for temporary fixation only. Half-pins, on the other hand, share a lot of advantages, such as familiarity in application, patient comfort, rigid fixation and a low infection rate. Maybe these characteristics are responsible for being so famous in USA, unlike wires. Pins are significantly better than wires when placed in the diaphysis, where large crossing angles can be achieved without muscle injury of the leg.

The role of weight bearing in frame stability is very important in TSF, as in all CEFs. The key for successful bone healing is a combination of early weight bearing and functional activity. Weight bearing provides axial loading to the fracture, nonunion or osteotomy site that stimulates osteogenesis and improves the strength of the fracture callus. Ilizarov taught that only the combination of a sufficient blood supply, bony stability and axial loading will provide the necessary environment for osteogenesis. The stability of the bone fragments and the rigidity and design of the fixator will determine how much weight bearing is possible. Several surgeons do not permit weight bearing until the fracture gap is fully reduced. When reduction is completed, for the first e.g. 1-2 weeks loading of 10–50kg is applied and gradually the patient starts weight bearing until pain feedback e.g. by stepping the fractured foot on a scale, in order to control the weight. Uncontrolled weight bearing, however, according to radiographs, has led to large areas of bone resorption around the half pins, which is an undesirable effect. Likewise, full weight bearing is not recommended in patients with a bone defect even they wear a stable frame that enables ambulation, because the bone ends to be *stress-shielded* and the relative motion at the skin interface is then increased. Stress shielding refers to the reduction in bone density (osteopenia) as a result of the removal of axial loading from the bone to the pins and wires, due to lack of bone contact. This phenomenon is obviously explained by Wolff’s law which says that if the loading on a bone decreases, the bone will become less dense and weaker because there is no stimulus for continued remodeling that is required to maintain bone mass.

Finally, when the frame is about to be removed, the bone needs to be prepared for the upcoming loss of external support. The process of gradually increasing weight bearing, described above, called dynamization, prevents stress shielding, results in greater callus formation and when it is accomplished, the fixator is destabilized and ready for removal. However, if dynamization starts earlier than the appropriate time, according to the callus

quality, can lead to frame instability which means delayed union, refracture or development of secondary deformity. Different types of dynamization, for example active, passive or controlled dynamization, produce different mechanical stimuli that define various bone remodeling processes and callus formation strength (Chao et al., 1990).

The decision of when a fixator is ready to be removed is as much an art as a science. General convention is when three of four cortices demonstrate radiographic healing, the bone has enough intrinsic stability to remove the fixator (Fragomen et al., 2006). Anand et al. (2006) assessed intraobserver and interobserver reliability in determining bone healing, with the above criterion, of osteotomy sites on plain radiographs and reported lack of reliability between surgeons. This conclusion revealed the high level of subjectivity in the timing of removal. Therefore, a more objective method was suggested. While patients were still in the Ilizarov frame, the load passing through the fixator was compared to the load through the extremity at multiple intervals in patients during the consolidation phase, creating a load ratio. This ratio was representing the percentage of the weight-bearing load that was being carried by the fixator. As healing progressed, the amount of load that the bone supported increased and the ratio decreased. Fragomen et al. (2006) refer to the above test performed by Aarnes, Steen, Ludvigsen et al. (2005), who documented that when 10% of load passed through the fixator, the frame was ready to be removed. However, even if more accurate methods are being developed to determine ideal timing for frame removal, surgeons are still concerned about the best timing, which will avoid serious complications, such as bone instability.

3 Computational modeling

3.1 Introduction

The development of numerical models is an accurate way to approach the mechanical behavior of any structure, involving mechanical parts, biological tissues, medical devices, tubes and bridges, and enables the discussion of the correlation between literature and numerical findings. Computational models can be produced using Finite Element Analysis (FEA), a method that solves linear and non-linear systems of equations, minimizing the assumptions made in analytical solutions.

In particular, the mechanics of External Fixators is analyzed producing numerical models mainly with the Finite Element Method (FEM) and some supporting parts with CAD interfaces, for both frames and bone tissues. The developed models are implemented in the general-purpose FE program Abaqus (Hibbit, Karlsson & Sorensen), and the analysis is then performed on different configurations, that enrich the computational approach of the problem.

In this thesis, FE models are developed for cases of closed tibial shaft fractures treated with the Ilizarov apparatus and the Taylor Spatial frame (TSF) in different configurations. Single-ring block configurations are modeled for both frames while a double-ring block model is produced for the Ilizarov apparatus. For a hybrid TSF type of fixation, two different configurations are developed, changing wire crossing angles. Interesting conclusions for the overall axial stiffness come of altering the wires pretension, diameter and crossing angles in the models, while numerical results are correlated with clinical findings, when they are available, verifying desired behaviors and explaining undesired complications. The effect of callus development on axial stiffness is also studied, by interposing materials with different densities in the fracture gap and interesting results are documented.

3.2 Materials and method

3.2.1 Model geometry

TIBIA MODEL

The three-dimensional geometry of the shinbone was, initially, developed using data coming from CT (Computed Tomography) technique. Three-dimensional data sets were acquired and segmented (Figure 42) in *marrow* and *tibia* sets and then this data were reconstructed to calculate three-dimensional surfaces, all steps performed using the Avizo software.



Figure 42: Final segmentation step in Avizo. The tibia set is noted in red and the marrow in green (Georgadakis, *Biomechanical Analysis of Ilizarov apparatus using Finite Element Method*, 2010)

The final surfaces were extracted in two *.stl files (Stereolithography – a simple format for triangular surfaces), one for the tibia and one for the marrow (Figure 43). The three-dimensional FEM model was developed in Abaqus software (Hibbit, Karlsson & Sorensen), importing the converted *.stl to *.iges (Initial Graphics Exchange Specification) files with the SolidWorks software. The volumetric mesh produced for the full model of the bone tissue was a tetrahedral mesh (Abaqus element type=C3D4).

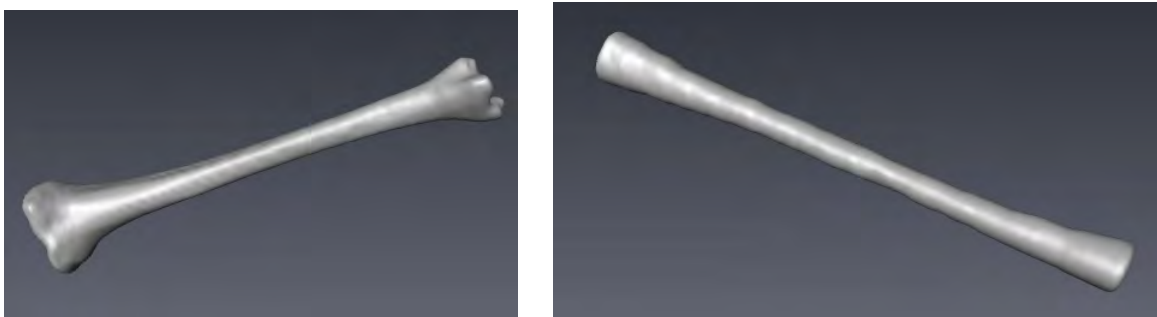


Figure 43: Solid model of tibia (left) and marrow (right) in *.stl form (Georgadakis, *Biomechanical Analysis of Ilizarov apparatus using Finite Element Method*, 2010)

However, in the majority of studies on circular fixators reported in literature, the tibia bone was simulated by solid cylinders. In view of simplicity, we replaced the tibia model from CT scans with a three-dimensional solid cylinder of the same geometry, which was subsequently meshed with tetrahedral or hexahedral elements (Abaqus element type = C3D4 – C3D8, respectively). This method of simulation enables the validation of numerical results with a mechanical testing.

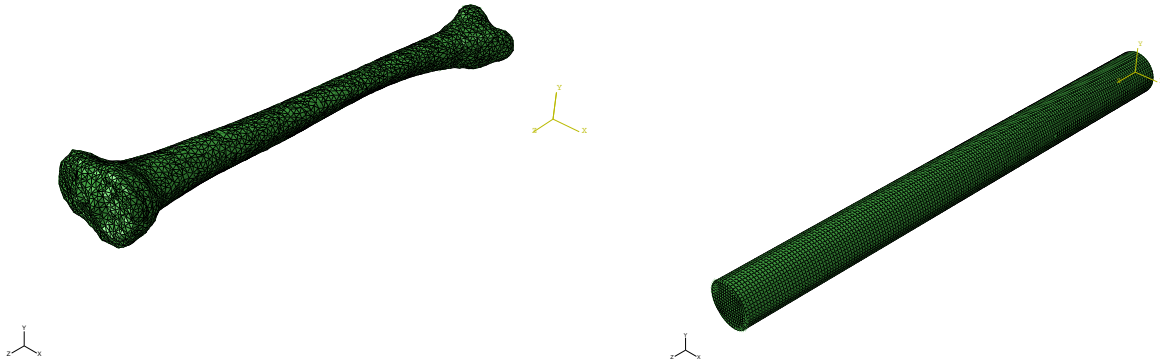


Figure 44: Three-dimensional FE model of tibia from CT images (left) and bone simulation with solid FE cylinder model (right)

According to literature references, bone simulation with polymer cylinders does not have a serious impact on the mechanical response of any configuration of the CEFs. Watson et al. (2007), developed a computational model predicting the mechanical response of different configurations of the Ilizarov apparatus simulating the bone with a nylon cylinder of 30-mm diameter meshed with solid elements and mechanical properties those of Nylon (Young's modulus 2 GPa (1.3–3.7GPa for Nylon 6, www.matweb.com), Poisson's ratio 0.4). Likewise, Galvis et al. (2001), in their article of computational and experimental determination of the stiffness matrix of an Ilizarov fixator used a nylon cylinder to represent the bone fragments giving an elastic modulus of 2.71GPa. Yang et al. (2002), in the mechanical testings they performed on different types of hybrid fixators, used Acrylic rods as bone models and compared the stiffness characteristics of the frames (average Young's modulus value 2.71GPa, www.matweb.com). Antoci et al. (2006) and Roberts et al. (2004), simulated the tibia with a fiberglass cylinder and tested the transfixion wire positioning (Young's Modulus nearly 2.3–2.6GPa, Poisson's ratio 0.33, www.k-mac-plastics.net/data%20sheets/fiberglass_technical_data.htm) while Baidya et al. (2001) used Perspex tubes of 30mm diameter as bone analogues (Young's Modulus 2.7–3.5GPa, www.roymech.co.uk/). Obviously, the selection of a typical polymer, who has a Young's modulus between 2–7GPa, mechanically simulates very well the trabecular bone of tibia, which has lower stiffness than the cortical.

In this thesis, the final configurations of both Ilizarov and TSF fixators are used to treat a transversely fractured tibia simulated by a 30-mm diameter and 350-mm length cylinder (Figure 45) with a 2–4mm metaphyseal fracture gap. The mechanical properties of the cylinder match those of typical cortical bone values (detailed reference in section 3.2.2).

For the hybrid TSF configuration, where the fixation was performed using both wires and half-pins, we created a new solid cylinder, with the necessary holes at the zones where the pins were placed. The development of the new bone as well as the half-pins models were performed using Rhinoceros v5 CAD software, which produced solid parts in *.iges format. The parts were, subsequently, imported to Abaqus and were assembled to the rest of the frame. The volumetric mesh for the imported parts could only be tetrahedral and therefore we used C3D4 continuum elements for the half-pins and the bone.

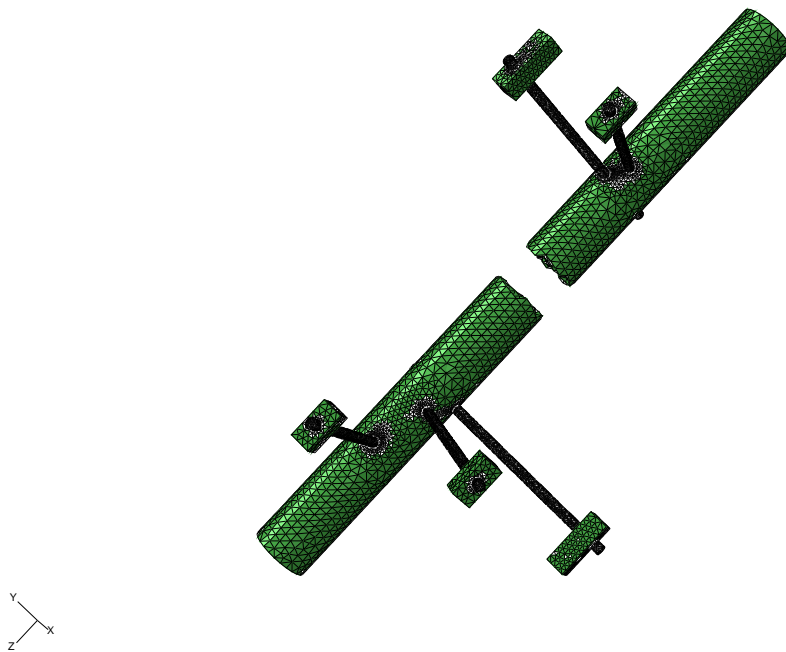


Figure 45: Tetrahedral mesh of bone and half-pins in a hybrid TSF configuration using 2HP at the proximal ring and 3HP at the distal ring

Both Ilizarov and TSF are circular external which they share some same components, such as rings and wires. However, the rings used in the Spatial Frames have a 30-mm increment substituted at the internal diameter at six areas for attaching the struts with bolts that does not exist at the Ilizarov rings.

- **Ilizarov apparatus :**

The rings had internal diameter 180 mm and external diameter 204 mm. Its thickness was 5-mm and 48 holes were symmetrically placed at the ring's perimeter (Figure 46). Rings were meshed with solid hexahedral elements (Abaqus element type = C3D8).

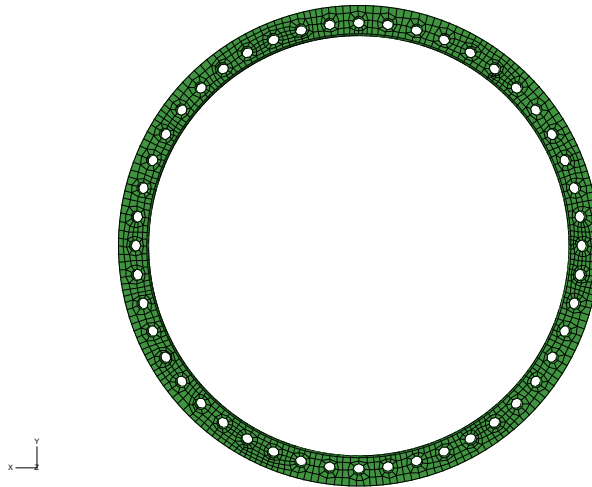


Figure 46: The rings consisting the Ilizarov fixators have internal diameter 180 mm, a typically used size in tibia fractures

The threaded rods, in the single-ring block configuration (Figure 47), were cylindrical beams with a diameter of 5-mm and 175 mm length, as the distance between the proximal and distal ring. In the double-ring configuration (Figure 48), where 2 rings are used per bone fragment, threaded rods had still 5-mm core diameter but their length was 220 mm (like the distance between the first and the fourth ring). The adjacent to the fracture rings had 130 mm distance and consequently the distal ring of each level was placed 40-mm lower than the proximal one. Rods were modeled with quadratic (three-node) beam elements (Abaqus element type = B32).

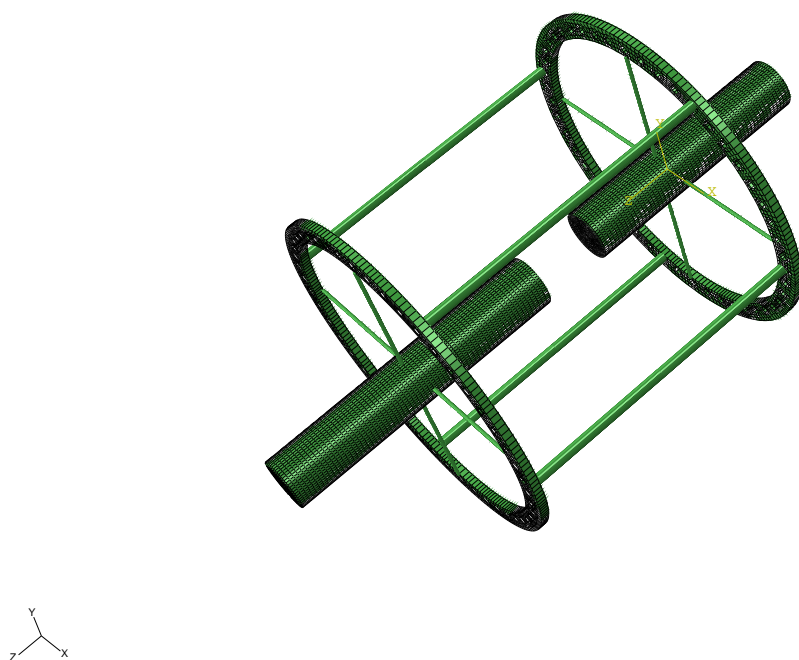


Figure 47: Single-ring block configuration with one ring at each bone fragment

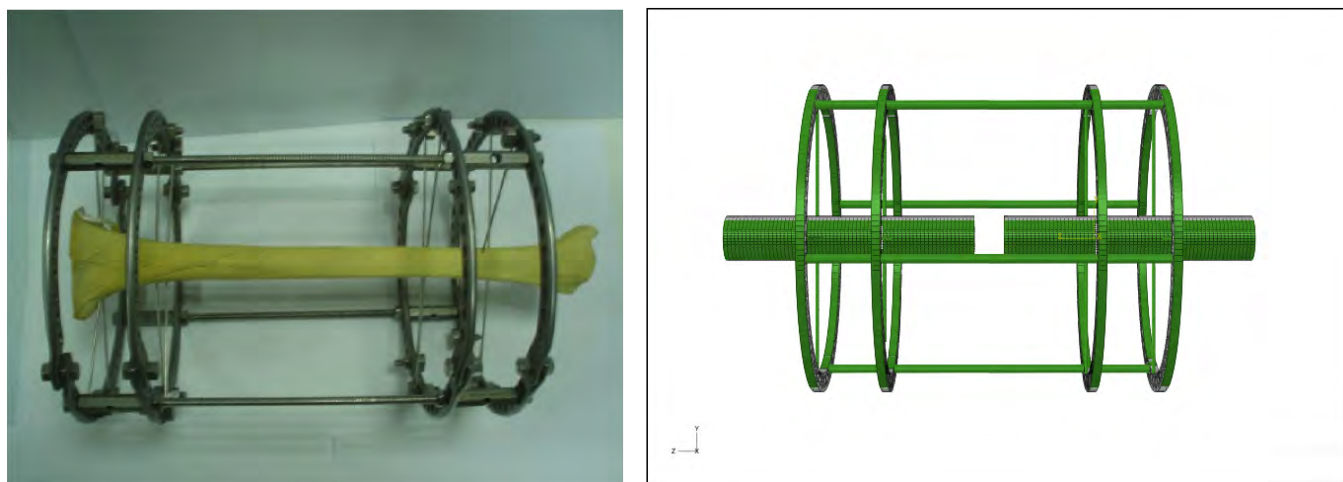


Figure 48: Double-ring block with two levels of fixation at each bone fragment; The prototype configuration assembled from the University Hospital of Larisa (left) and the corresponding numerical model (right)

The Kirschner wires were placed with 90° crossing angles at both Ilizarov configurations and thus, their length is 180mm. The wire core diameter was 1.5-mm or 1.8-mm, in order to test its impact on axial stability. They were meshed with quadratic (three-node) beam elements (Abaqus element type = B32), similarly with the rods.

- **Taylor Spatial Frame :**

The rings had internal diameter 180mm and external diameter 210mm with a 30-mm increment in six areas to attach the struts (Figure 49 right). Its thickness was 8mm and 48 holes were symmetrically placed at the ring's perimeter, while the increments had three holes of 7mm diameter as strut positions. Rings were meshed with solid hexahedral elements (Abaqus element type = C3D8). The rings were placed with 172 mm distance between them.

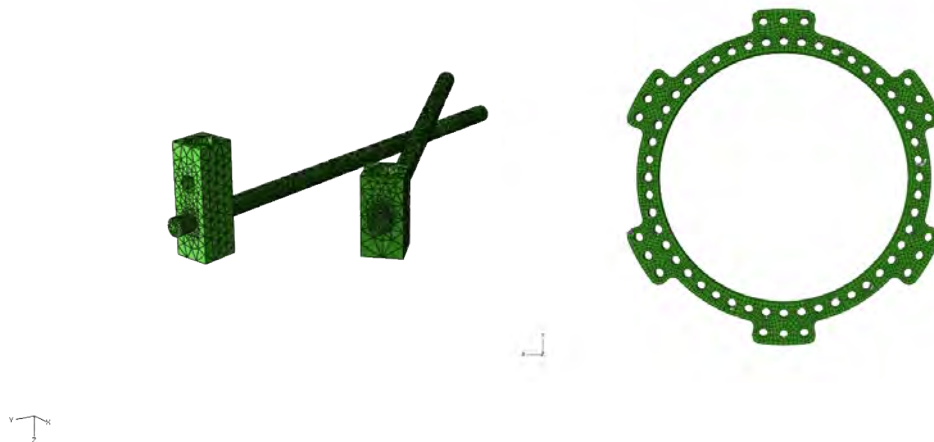


Figure 49: Half-pins are clamped with one or two-hole rancho cubes (left) The TSF ring geometry (right)

The half-pins had a 5-mm core diameter and their length was 130 mm, in order to protrude 3–5mm from the rancho cube and nearly 2 mm from the bone (Figure 49 left). Half-pins were modeled with tetrahedral mesh (Abaqus element type = C3D4). At the hybrid TSF fixator, two half-pins were placed at the proximal ring with 30° crossing angles and almost 90° angle between the second wire and the second half-pin, and three half-pins to the distal ring with almost 40° angle between each two. It is noted that the current configuration of the hybrid TSF is used among others clinically in the Orthopaedics Department of University Hospital of Larisa.

The rancho cubes were of 20 mm and 30 mm height with one or two holes of 5-mm diameter, respectively, to attach the pins. The cubes were modeled with tetrahedral mesh and connected to the rings using constraints that represented the connection with bolts (Fig.49).

In TSF configurations, the K-wires were modeled in the same way as in the Ilizarov configurations using quadratic (three-node) beam elements. In the first configuration with 4 wires (2 wires per ring- bone segment), the wire crossing angles were at the optimum position, 90°, whereas at the hybrid configuration, the two wires in the proximal ring had almost 30° angle of intersection. 1.5-mm diameter wires were used with 100kg pretension,

according to clinical reports.

The struts connecting the rings (Figure 51) consisted of two joint segments of 12 mm length and an inclined main part connecting the joints with 60° ring-strut angle. The length of the sloppy part, that is the size of the strut, depends on the distance in which the rings are placed in relation to the fracture site. In the configurations we modeled, both frames in neutral position, the strut length was 170 mm (medium struts). The hollow part had a 10-mm diameter whereas the circular threaded part 5 mm.



Figure 50: The divergence angle between ring and strut was 60°

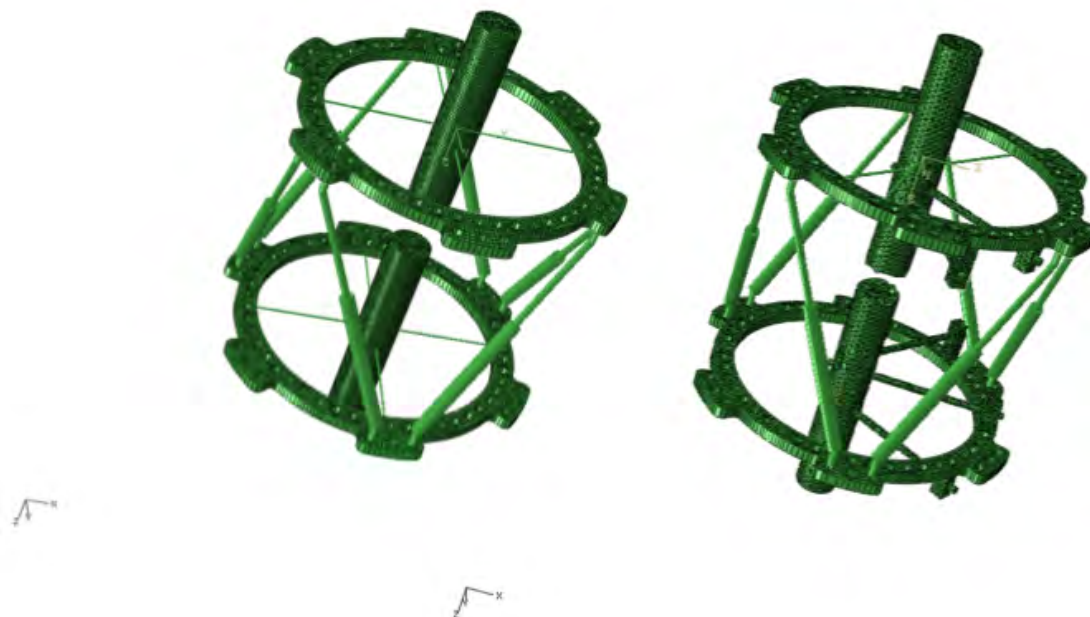


Figure 51: TSF Configuration with 2W per bone segment (left), hybrid fixator with 2W and 5HP (right)

3.2.2 Material assignment

After taking into account the geometrical characteristics of the system, the next basic step in developing FE models is the appropriate material assignment to the corresponding constructs.

BONE

As it was reported in the corresponding part of section 3.2.1, the mechanical properties given to the bone model vary in documented simulations of tibia bones depending on the model used. In cases where the model produced from CT scanning images is used, it is better to assign the Young's modulus of the cortical than of the trabecular bone. Abendschein et al. (1970) testing tibia and fibula cortical bones under ultrasonic loading reported Young's modulus equal to 24.5 GPa. Likewise, Simkin et al. (1973) applied tensile loading to tibia cortical bone and documented 23.8 ± 2.21 modulus of elasticity. With similar techniques of loading, Bovine (1970) and McElhaney (1965) reported 0.482 and 0.28, respectively, for the Poisson's ratio. Consequently, in the tibia solid model the material properties assigned would be of 20GPa for the Young's modulus and $\nu = 0.4$ for the Poisson's ratio. Since the material is considered as isotropic and elastic and the applied load applied is axial, there is no other modulus of elasticity. In the numerical models reported in this thesis, we used typical cortical bone values: $E = 20$ GPa and $\nu = 0.4$.

ILIZAROV FRAME

According to Baidya, Ramakrishna, Rahman and Ritchie (2001), the recommended material for the Ilizarov frame components is stainless steel and sometimes aluminum. Watson (2007) proposed a Young's modulus of 197GPa and $\nu = 0.29$. To the Kirschner wires, rings and threaded rods of both configurations the material assigned was stainless steel, and the mechanical properties given were the values of a typical steel of this group: $E = 200$ GPa and $\nu = 0.3$.

HALF-PINS AND RANCHO CUBES

For the hybrid TSF model, the half-pins and the attached rancho cubes, are both made of stainless steel, as the wires, too. The mechanical properties assigned were the same with the Ilizarov frame, $E = 200$ GPa and $\nu = 0.3$.

TSF RINGS

Although the particular material alloy is not yet known, it is reported that TSF rings are made of aluminum. In the numerical models developed, the mechanical properties of a typical aluminum alloy are used : $E = 70$ GPa and $\nu = 0.35$.

TSF STRUTS

According to the TSF Ilizarov Pocket Reference (Smith&Nephew), graduated telescopic rods are made of aluminum (hollow part) and stainless steel (circular part). However, for the Fast FX™ struts, there is no material information given. Consequently, in both TSF models, struts were considered to be made of aluminum ($E = 70$ GPa and $\nu = 0.35$) and stainless steel ($E = 200$ GPa and $\nu = 0.3$), in the hollow and circular part, respectively.

3.2.3 Assembly and constraints

The Assembly module of modeling the Ilizarov apparatus involved only the assembling of the frame components with the tibia, in both configurations simulated, whereas the TSF models needed extra constraints and connection assignments.

The struts in TSF models required, at first, the definition of local Coordinate Systems (x, y, z) to create the universal joints that enable 6 dof motion of the frame. At the nodes connecting the vertical and the inclined part (top and bottom) of each of the six struts (Figure 52), we created two local CSYS with common x -axis, y -axis at the axial direction of each part and z -axis of the inclined part normal to x -axis of the vertical part ($e_1^v \cdot e_3^{\text{in}} = 0$). We defined 24 local CSYS in total and then we created the connector assignments of the joints.

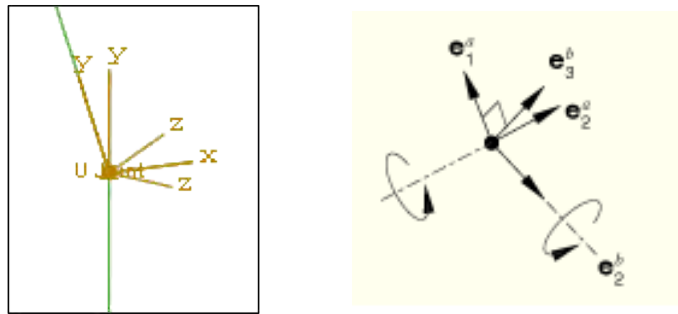


Figure 52: Local CSYS (left), Universal Joints (right)

At each joint, we created a three-dimension connector element (Abaqus element type = CONN3D2) between the two coincident nodes with different numbering and chose the Ujoint type of connection. This connection constrained kinematically the two nodes to have the same displacements and fixed their rotations about y local axis (defined by the local CSYS).

In any configuration using wires for fixation, an important step was the constraint of the wire displacement in the cross-sections of the tibia during loading. At any cross-section of the bone that wires are placed, we edited both wire and tibia meshes so that the nodes of each part coincide: they have the same coordinates and different numbering in order to retain the separate meshes. The desired wire slippage is parallel to the bone, in the same straight line with the related tibia cross-section, disabling node displacement on other directions. Thus, we used the command :

```
* MPC
SLIDER, 2,1,3
```

to keep e.g. the wire-node 2 on a straight line defined by the tibia-nodes 1 (on the left) and 3 (on the right) during loading (Figure 53). We used this constraint for all the nodes meshing the corresponding bone cross-sections in the wire directions in each model. In both Ilizarov configurations and in TSF fixation model with wires, the positioning directions coincide with x and y -axis, since their crossing angles are of 90° .

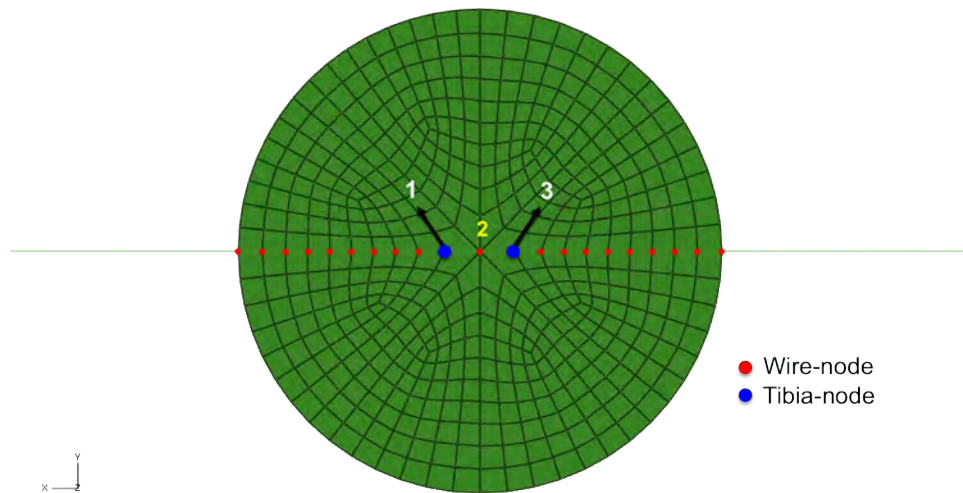


Figure 53: Multi-point constraints between wire and tibia nodes at the tibia cross-section

In the hybrid TSF model, the rancho cubes used to attach the half-pins on the rings, were constrained using the surface-based constraint *TIE. We created element-based surfaces for the cubes and the rings regions that had to be tied together (Figure 54).

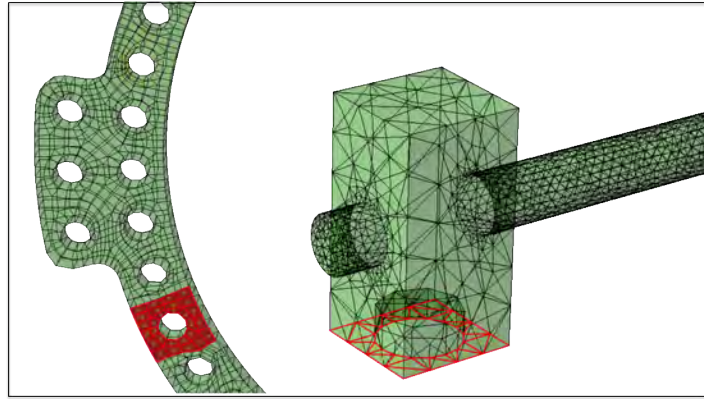


Figure 54: Tie constraints imposed at ring-cube surfaces

The rods in Ilizarov configurations, and the struts in the TSF configuration, were attached to the rings using coupling constraints. The starting and ending node of each rod was considered as a Reference Node and its translational and rotational dofs were coupled with the dofs of the perimetric nodes of the ring holes (Figure 55). Each Reference Node was used to define a point element (type = DCOUP3D) and using the command *DISTRIBUTING COUPLING, the motion of the point element was constrained to the translations of the ring solid elements.

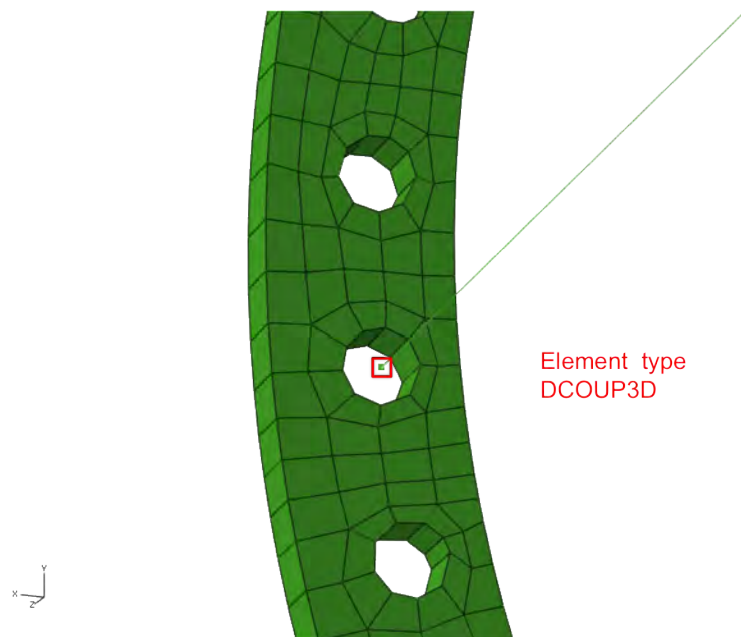


Figure 55: Coupling constraints imposed between rings and rods

3.2.4 Load and Boundary Conditions

In all the configurations, we used boundary conditions to rigidly attach the wires to the rings, as they were connected in the real models with cannulated bolts. To represent weight bearing of the bone, the distal tibia fragment was immobilized and different axial compression loads were applied on the upper surface of the proximal fragment (Figure 56).

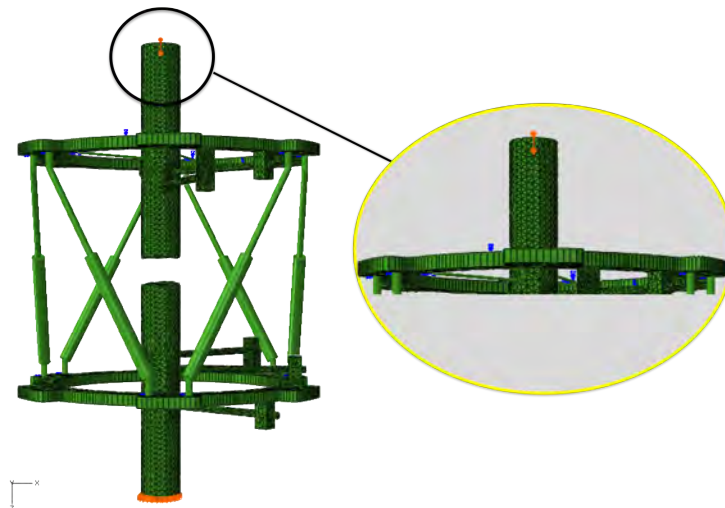


Figure 56: Compressive load is applied on the upper bound of the tibia

Therefore, the lower bound of the tibia was immobilized throughout the analysis, as shown in Figure 57, and the wires were attached to the rings at nodes with fixed rotational degrees of freedom.

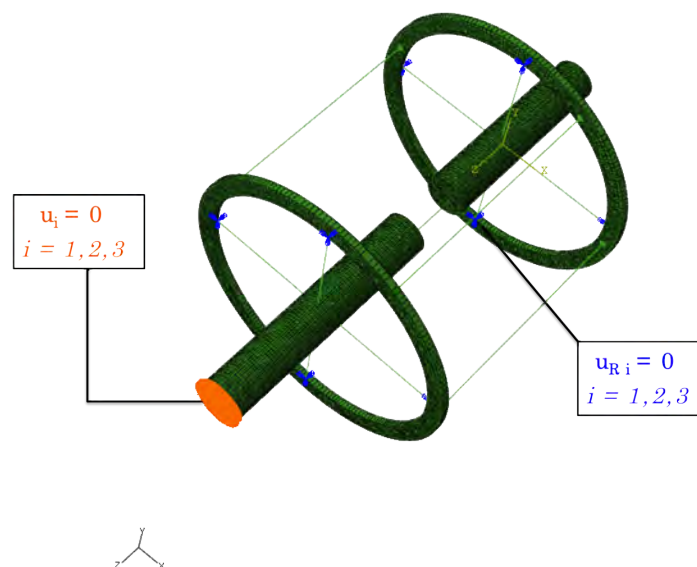


Figure 57: Boundary conditions

The pretension of the wires was imported as an initial step, using the command :

***INITIAL CONDITIONS, TYPE = STRESS**

For the Ilizarov configurations, the pretension of 1.5-mm wires varied between 50kg–100kg (490.5–981N), whereas the 1.8-mm wires had a pretension of 100kg (981 N). For the wires (1.5-mm) of the TSF models, both in typical and hybrid configurations, the pretension was set to 90kg (499.62 N).

Finally, due to the presence of pretensioned wires in the fixator models, geometric non-linearity is used in any of the model analyses.

3.3 FE Models

A fracture gap of 20mm (Config. 2 and 4) and 40mm (Config. 1 and 3) simulated a transverse closed fracture localized at the mid-metaphyseal compartment of the tibia that was maintained throughout the analysis to ensure the entire load transfer through the fixator. A configuration using a tibia with a partial callus consolidation at the fracture gap supported by a hybrid TSF was modeled to test the stability of the frame in different stages of healing procedure. In all the configurations tested, the tibia bone was centered to the frame.

The first configuration (Ilizarov apparatus) tested was the single-ring block Ilizarov frame (Figure 47) consisting of one 180-mm ring per bone segment fixing with two 1.5-mm/1.8-mm wires at each ring, with the angle between them at 90°. The total number of elements and nodes was equal to 64,033 and 73,133, respectively.

The second configuration (Ilizarov apparatus) simulated was the double-ring block Ilizarov frame (Figure 48 right) consisting of two 180-mm rings per fragment and two wires (1.5-mm) in 90° divergence angle per ring, that is a total number of 8 wires. The total number of elements and nodes was equal to 65,490 and 77,881, respectively.

The third configuration (TSF) modeled was the single-ring block TSF construct (Figure 51 left) with one level of fixation per bone segment, as in Configuration 1. One 180-mm ring per fragment was used and two fixation points with two 1.5-mm wires per ring, intersecting at 90°. The total number of elements and nodes was equal to 81,018 and 93,451, respectively.

The fourth configuration (hybrid TSF) simulated was the single-ring block TSF construct (Figure 51 right) using 2 wires and 2 half-pins at the proximal ring and 3 half-pins at

the distal ring for fixation. The rings, wires and half-pins diameter were 180-mm, 1.5-mm and 5-mm. All the fixing components, starting from the wire fixed proximally, were inserted at a zone out of a nearly 200° arc, posterior to anterior direction of the tibia, according to clinical and theoretical indications (see Section 2.4.7). The model was considered to simulate a right-leg fractured tibia bone (regarded as left leg when examined by the surgeon), since each leg requires different zones of placing the wires and pins, in order to prevent disabling motion (commanded from the lateral side of the leg).

Therefore, at the proximal ring, the wires were placed with a crossing angle of 45° while the angle between the first wire (W1-fixed at the proximal side of the ring) and the first half-pin (HP1) was 42°. The angulation between the half-pins (HP1 & HP2) was 32° (Figure 58). They were both placed distally to this ring (that is in the region between the two rings) using one-hole and two-hole rancho cubes for clamping, respectively. The clinical indications gave a maximum of 50° angle between fixing components at the proximal ring.

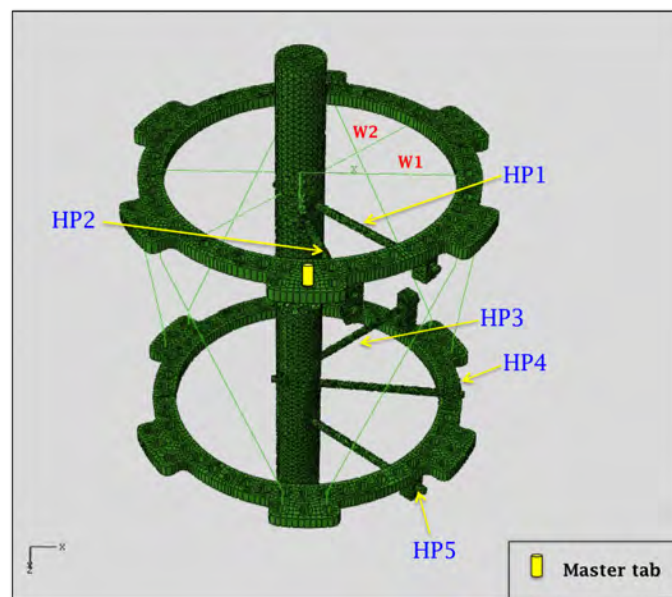


Figure 58: Hybrid TSF treating transversely fractured tibia using 2W and 5HP

At the distal ring, the two half-pins were inserted at the anterior inner quadrant (medial side) of the tibia. Hence, they were placed at the corresponding positions of the wires (proximal ring), with 48° angle between them, and were fixed to the ring proximally with one and two-hole rancho cubes, respectively. The last half-pin (HP5) was inserted in parallel to the second half pin (HP2) of the proximal ring and was fixed distally using a one-hole cube. The angle between the first (HP3) and the third (HP5) half-pin in the distal ring was 85°. The clinical indications gave a maximum of 90° angle (optimum) between the first and last half-pin at the distal ring. In the hybrid TSF, we tested, also, the effect of wires-crossing angles to frame stability by decreasing the angle between W1 & W2 from 45° to 29°. *It is*

noted that the current configuration of the hybrid TSF is used among others clinically in the Orthopaedics Department of University Hospital of Larisa. In either cases, the model has a total number of 261,125 elements and 63,117 nodes.

Finally, the hybrid TSF was used to assess the influence of intrinsic factors, such as the modulus of elasticity of the callus formed on the fracture site, on the rigidity of the frame (Figure 59). For example, the callus that is formed in the first 3-4 weeks, is soft and consists of osteoid and cartilage (Figure 12). Hence, its mechanical properties can be assumed to agree with the literature references for materials simulating cartilage. Charles-Harris & Lacroix et al. (2005) and Benito et al. (2006) reported values for granulated tissue (ground substance) and new bone formation during the early healing stages (partially consolidated fracture): $E = 10$ MPa, $\nu = 0.49$. Juan et al. (1992), in his thorough theoretical and experimental studies on consequences of callus development on the stiffness of different fixators, assumed that there are five types of callus, according to a logarithmic pattern, appearing in the first stages of bone repair. (Stage 1: early callus, few days after the fracture, Stage 5: intact cortical bone). The mechanical properties assigned, in ascending order, were: $E = 1, 10, 100$ & 1000 MPa, $\nu = 0.39$ for all stages.

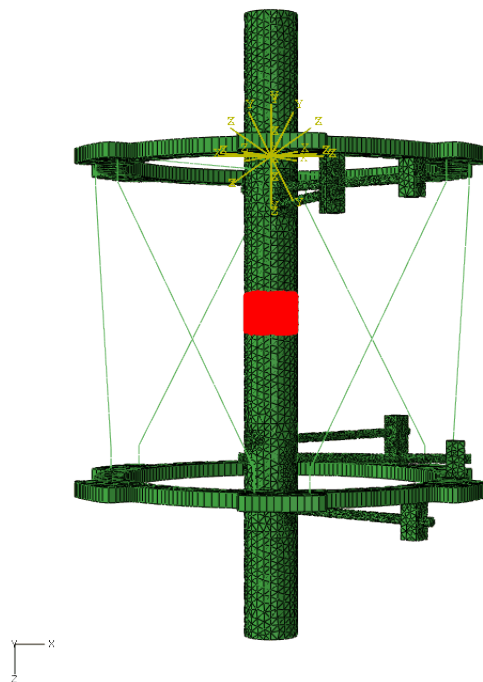


Figure 59: Hybrid TSF supporting a tibia with callus (red region) formed at the fracture site

The tibia bone was modeled with tetrahedral mesh, with the same seeding with the fractured bones used in the previous configurations. The total number of elements and nodes was 263,015 and 63,434, respectively.

3.4 Results

Initially, Ilizarov configurations 1 and 2 were subjected to 300 N and 500 N axial compression loads, respectively, with their wires (1.5-mm) pretensioned to 687 N (70kg). Figure 60 depicts the load–displacement curves of each case.

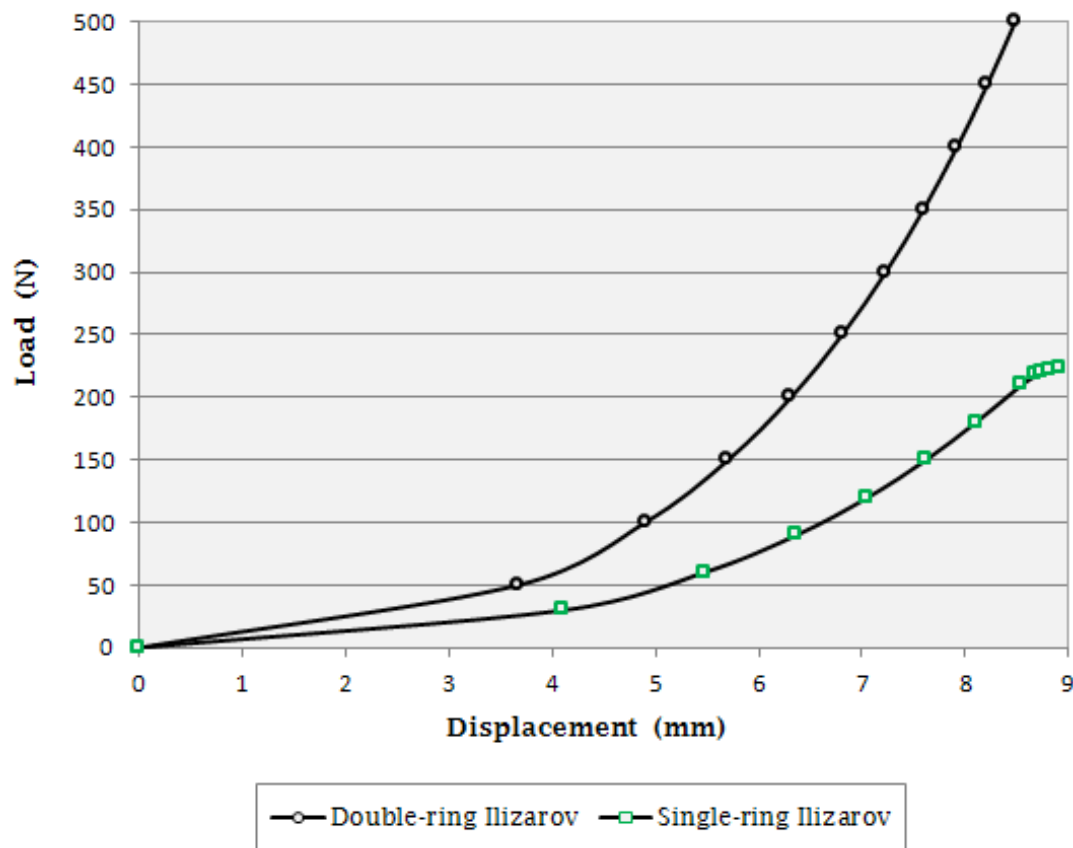


Figure 60: The relationship between load and axial displacement for single and double-ring Ilizarov frames (180-mm rings, 1.5mm wires, 70kg pretension)

Configuration 2, that consists of two levels of fixation per segment, is obviously stiffer than the single-ring frame. It can be seen that at lower loads, the curves show a linear behavior, that is similar for both configurations. Yet, after 100 N loading, the relationship between load and axial displacement becomes non-linear. Since then, the double-ring frame (black) increases its stiffness significantly compared to the single-ring frame (green). At the end of the load cycle, the bone fragment in double-ring construct is axially displaced by 8mm, whereas the single-ring block, when subjected to loads higher than 200 N, shows a gradually increasing unstable behavior. The reduction in stiffness is shown in Figure 61 by the sharp change in the curve's slope. The results of double-ring construct agree with the values reported by Nikonovas & Harisson (2005) in their theoretical approach of wires modeled as chains.

The axial stiffness is calculated as the slope of each load–displacement curve dF/dx (tangent modulus). The initial stiffness value, in all configurations, appears due to the pretension of the wires. For 200 N load, we observe, in Figure 61, that the double-ring frame is nearly 17.7% stiffer than the single-ring frame, that later on shows an unstable behavior at the medial plane. The axial stiffness for the stable configuration (2) ranges between 13.6 and 186.25 N/mm, calculated as tangent modulus, while the corresponding secant modulus is 38.1 ± 14.27 N/mm (mean \pm standard deviation).

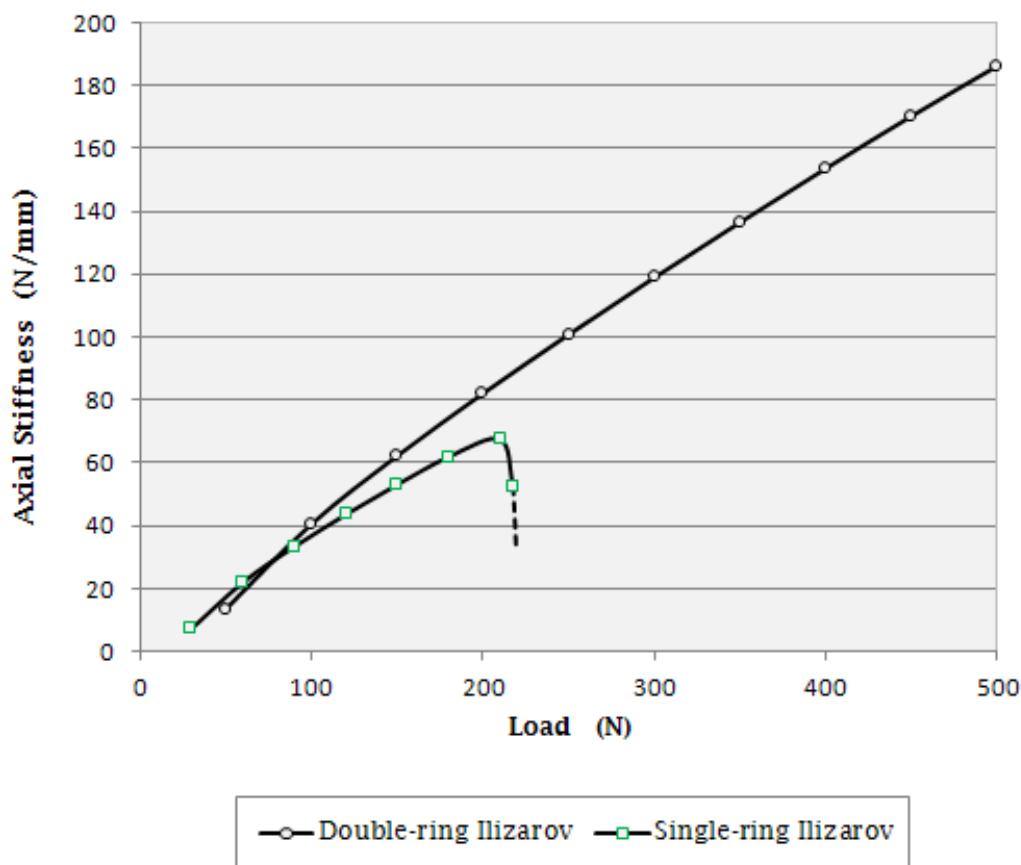


Figure 61: The non-linear effect of load on axial stiffness for single and double-ring Ilizarov frames (tangent modulus) (180-mm rings, 1.5-mm wires, 70kg pretension)

A further study was developed on the stable Ilizarov configuration, i.e. double-ring block, to test the effect of wire pretension in axial stiffness. The 1.5-mm wires were pretensioned to 277.7 MPa, 388.79 MPa and 499.87 MPa (50kg, 70kg and 90kg, respectively) and their load-displacement curves are depicted in Figure 62, for a load cycle of 500 N.

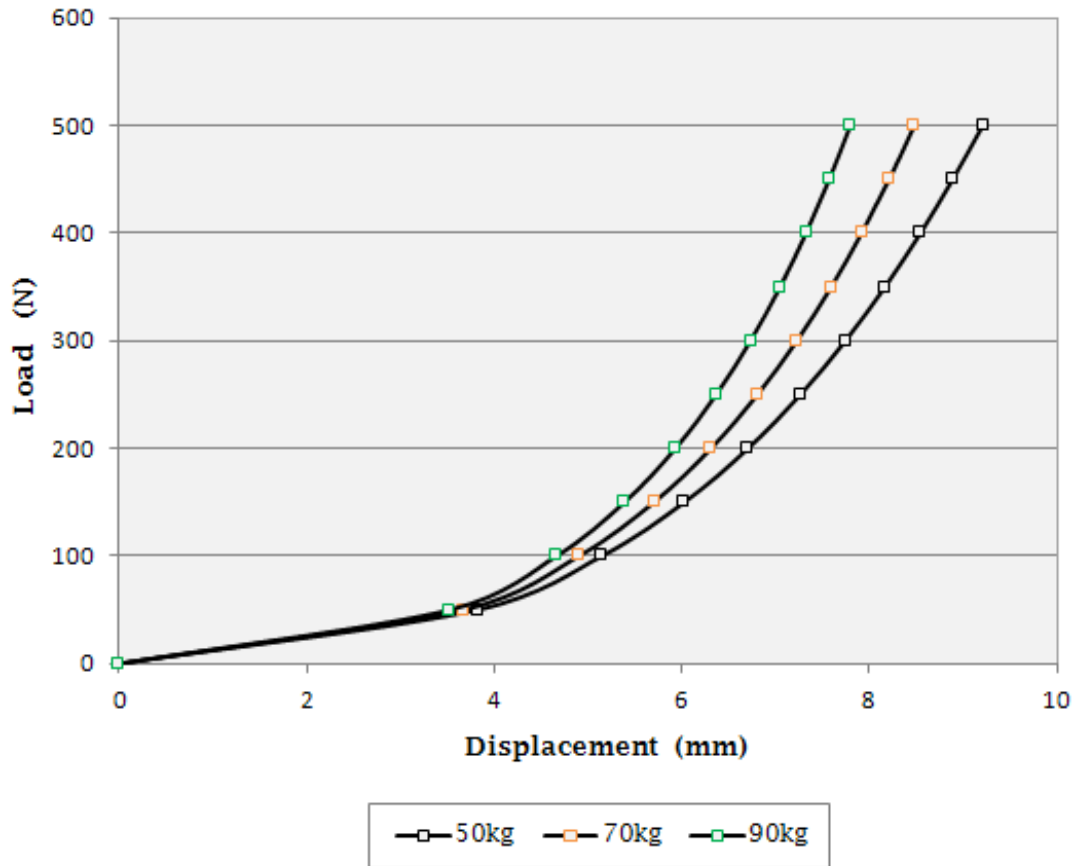


Figure 62: The effect of wire pretension on axial stiffness
(Ilizarov config. 2 , 180-mm rings, 1.5mm wires)

Increasing the pretension from 50kg to 90kg leads obviously to a higher axial stiffness. As it can be seen from the graph, the linear region is slightly wider for the lowest pretension (50kg), but the slope is sharper for the highest pretension (90kg) throughout the whole load cycle. The stiffer case is the configuration with 90kg of wire pretension, as expected. A high axial stiffness represents a high resistance to motion along this axis; hence, the final displacement for 50kg of pretension was the greatest (15% greater than the displacement for 90kg). Studying more carefully the graph, we observe, also, that as the pretension level grows, the displacement versus load curve tends to become more linear; thus, the non-linearity decreases with the increase of pretension. The same trend was also reported in the computational results of Hillard et al. (1998) and Zhang (2004b) and in the theoretical approach of Zamani & Oyadiji (2009).

Figure 63 shows the deformed and undeformed states of Configuration 2, for a load cycle of 500 N. Figure 64 reveals that due to high stress concentration in the wire-bone interface, bone resorption is observed on the tibia cross-section in the areas where wires are bended.

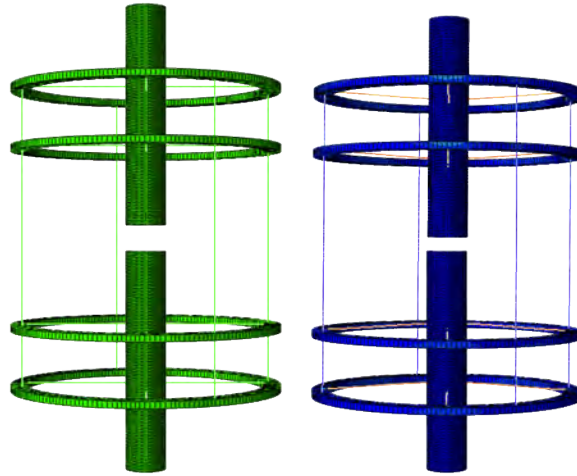


Figure 63: Deformed (contour plot) and undeformed (green) shapes of Configuration 2 (Ilizarov config. 2, 180-mm rings, 490.5 N pretension, load 500 N)

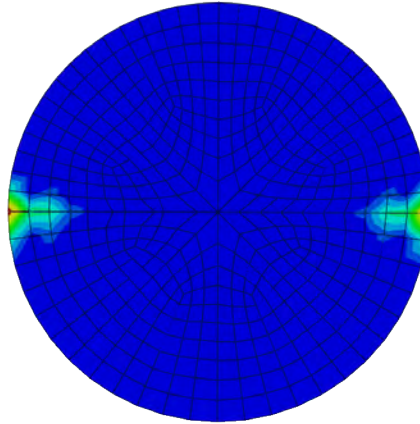


Figure 64: Bone resorption on the tibia cross-section in the areas where wires are bended (wire - bone interface) (Ilizarov config. 2, 180-mm rings, 883 N pretension, load 500 N)

Another study performed was the impact of wire diameter to the overall stiffness of the Ilizarov device. Configuration 1, (single-ring block of 180-mm rings), using 1.5-mm and 1.8-mm wires pretensioned to 981 N, was subjected to a load cycle with a magnitude of 200 N. The effect of wire-diameter in load-displacement curve is shown in Figure 65.

Figure 66 shows that increasing the wire diameter from 1.5-mm to 1.8-mm improves the axial stiffness of the frame. In particular, increasing the diameter by 16.7% produces a 7% lower axial displacement. The linear region of the red curve (1.8-mm wires) is sharper than the corresponding of the black curve (1.5-mm wires). In terms of stiffness, in the case with 1.5-mm wires, the secant modulus is 19.4 ± 7.6 N/mm, while in the 1.8-mm case, the secant modulus ranges within 21.6 ± 7.6 N/mm (Figure 66). The FE results of this model agree with the values documented on the theoretical studies of Hillard et al.(1998), for both load-displacement and stiffness-load profiles.

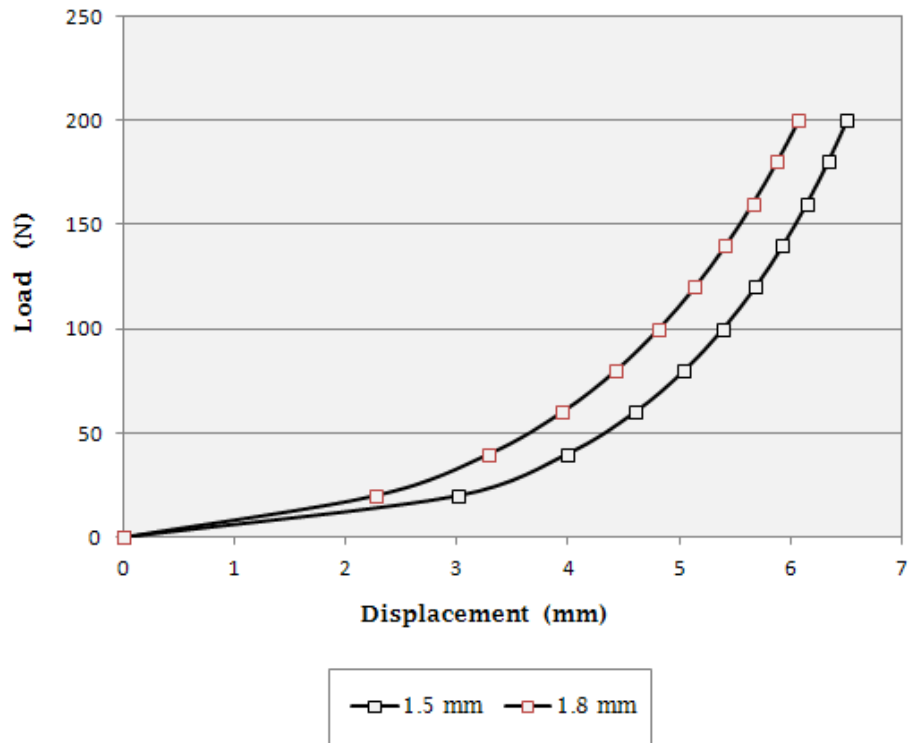


Figure 65: The effect of wire diameter on load-displacement profile (Ilizarov config. 1, 180-mm rings, 981 N pretension)

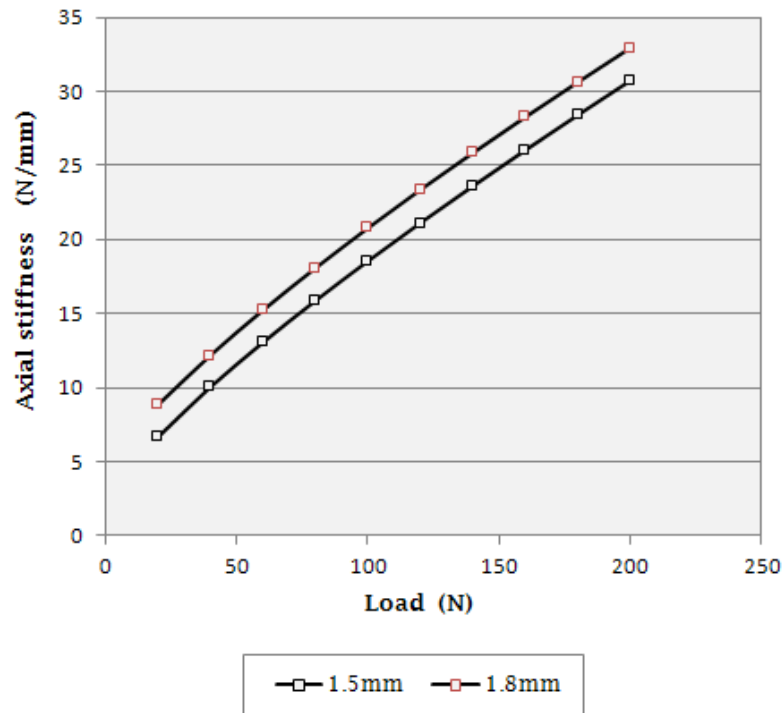


Figure 66: The effect of wire diameter on axial stiffness (Ilizarov Config. 1, 180-mm rings, 981 N pretension)

Since the single-ring Ilizarov (Configuration 1) and TSF (Configuration 3) models share the same fixing components (180-mm rings, four 1.5-mm wires with 90° angle of intersection), a comparison of the load-displacement curves would give interesting conclusions. Hence, we studied the correlation between the two profiles, giving an axial compression loading of 300 N, to both configurations, and a pretension of 883 N (90kg) to their wires.

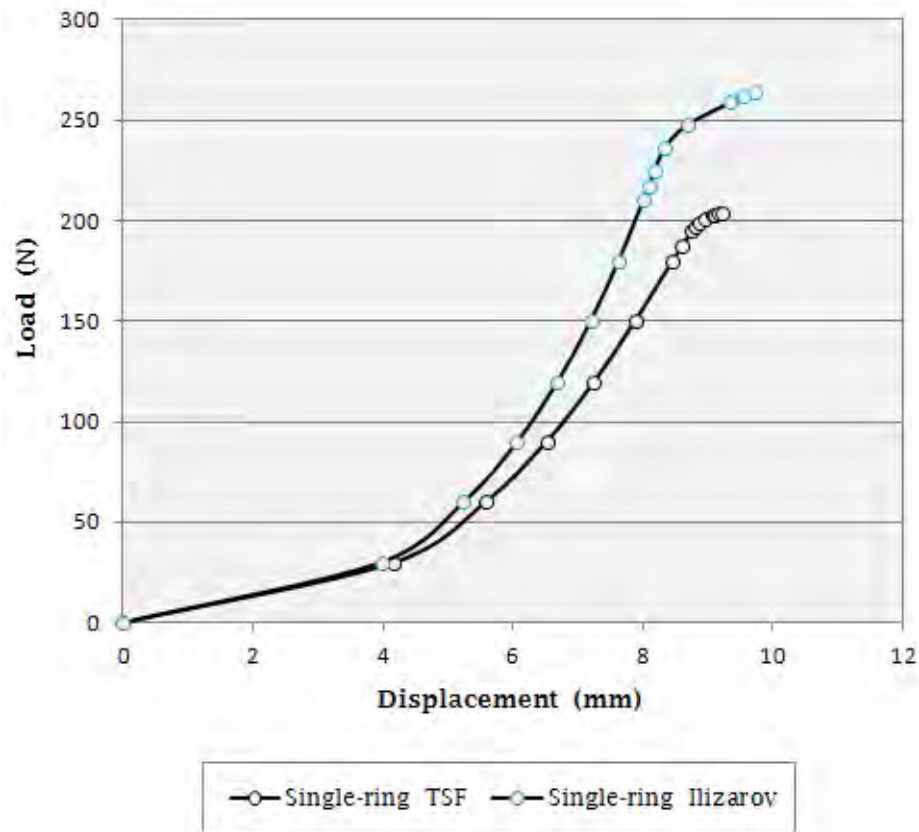


Figure 67: Load-displacement curves of single-ring Ilizarov and TSF (180-mm rings, 1.5-mm wires with 883 N pretension)

According to Figure 67, when loading does not exceed a magnitude of 50 N, the two models have exactly the similar linear behavior. In higher loading, however, Ilizarov frame (noted in blue) shows a stiffer profile, that is enhanced in a non-linear way. Both frames, over a magnitude of 200 N, indicate an unstable trend that is depicted with an increasing bending behavior to the anterior-medial plane (Figure 68 right). The different results of the two configurations are explained from parameters, especially concerning the rings. In the Ilizarov configuration, the rings were made of stainless steel (5-mm thick), whereas the rings in the TSF model were made of aluminum (8-mm thick). Kummer (1992) tested the relative stiffness of 150-mm rings made of these materials in compression and reported that rings made of steel were 24% stiffer than aluminum rings (stiffness values: 1 and 0.76 N/mm, respectively). In the same paper, Kummer referred to the effect of the unsupported length between the rings to the frame rigidity. The overall stability of the frame is increased when

the adjacent to the osteotomy site rings are placed in closer proximity to the gap in a double-ring block (Gasser, 1990). Bronson & Lewis (1998) referred that the increase of the distance between rings has a significant improvement in bending stiffness. Since the corresponding distance between the rings in these models slightly differs by 2.5mm, this might likely be a factor that influences the different profile of the curves. It is also possible that, the type of longitudinal components connecting the rings, with simple cylindrical rods and telescopic struts in Ilizarov and TSF configuration, respectively, affects the load distribution during the analysis and in conjunction with different deformation values, influence the axial stability of the frame. Kristiansen et al. (2010) documented that the substitution of an extra distal ring on TSF and Ilizarov models treating limb lengthening cases with half-pins, produced two configurations with no difference regarding axial correction, on an average of 47 cases. However, they observed a higher number of segments with reduced callus formation, that required bone transplant, in the TSF group, a fact that indicates lower stability, and higher pin track infections in the Ilizarov group.

Configuration 3 of TSF model verifies, like the Ilizarov configuration 1, the effect of wire pretension to the axial stiffness. The models using 1.5-mm wires for fixation were tested to 687 N (70kg) and 883 N (90kg) pretension, under compression loading of a magnitude of 200 N. Figure 68 left shows the non-linear relationship between loading and axial stiffness for the two values of pretension. The tangent modulus is 35.94 ± 15.5 N/mm for 90kg and 30.64 ± 13.6 N/mm for 70kg.

Figure 69 (left) shows the “bending trend” (instability) of the TSF Configuration with wires, in conditions of 90kg pretension and 300 N loading. According to Lewis & Bronson (1998), a possible translation of proximal bone segment along the wire, is partially responsible for the reduction in axial and bending (Kummer, 1992) stiffness. Indeed, the data obtained by the model analysis at the tibia cross-section, where the first wire was positioned, showed that, in the unstable cases the “bending trend” was accompanied by a translation of the bone along the wire.

Figure 69 (right) shows the Free Body Diagram of the latter configuration for a load cycle of 300 N. We observe that there is a kind of “load symmetry” to the struts, in relation to the coronal (zx) plane, between Struts 1 & 6 and 2 & 5 (see Fig. 38). The greatest portion of the load is tracked on Strut 5 (28%) and is almost 93 N, whereas the minimum load flow appears on Struts 1 (2.7%) and 6 (2.8%) (9 N on average). Struts 3 & 4 show high load transmission (18.6 and 23%, respectively) because they are located close to the connection of the first wire on the ring, in the side of the “bending trend”. The percentages refer to the axial z component of the total force vector and were derived after vector addition of section forces SF1 (axial force), SF2 and SF3 (transverse shear forces in the local 2- and 1-direction, respectively) on the beam elements of the struts. Obviously, the whole load is carried by the frame, since there is no bony contact yet.

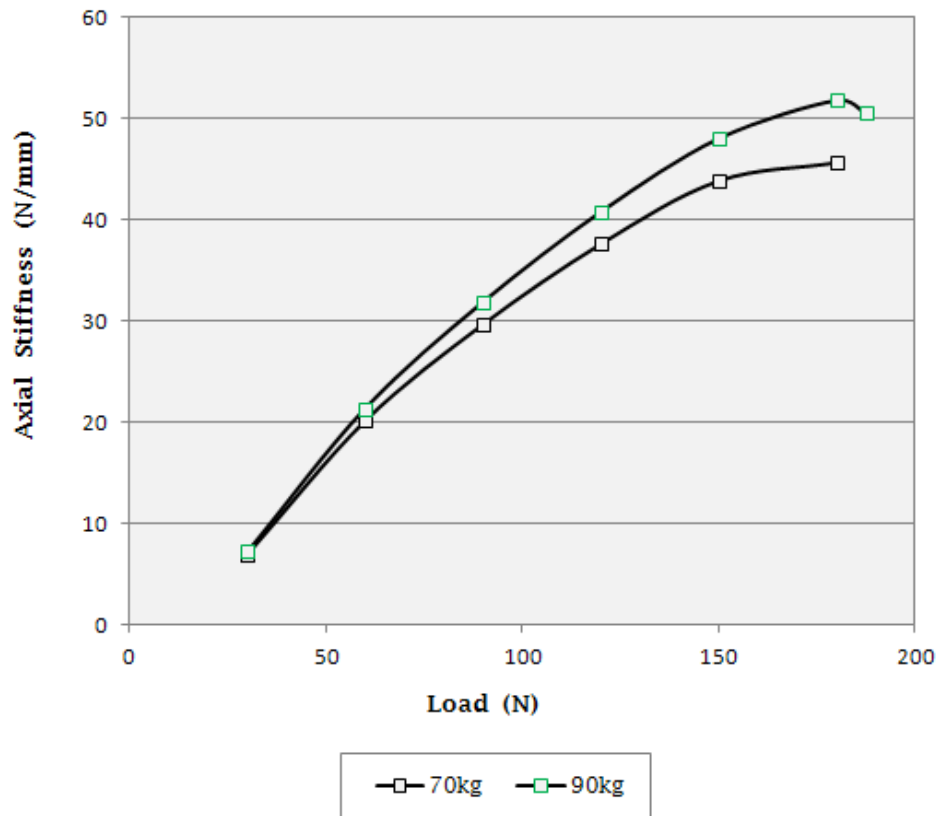


Figure 68: The effect of wire pretension on axial stiffness
(TSF Config. 3 , 180-mm rings, 1.5mm wires)

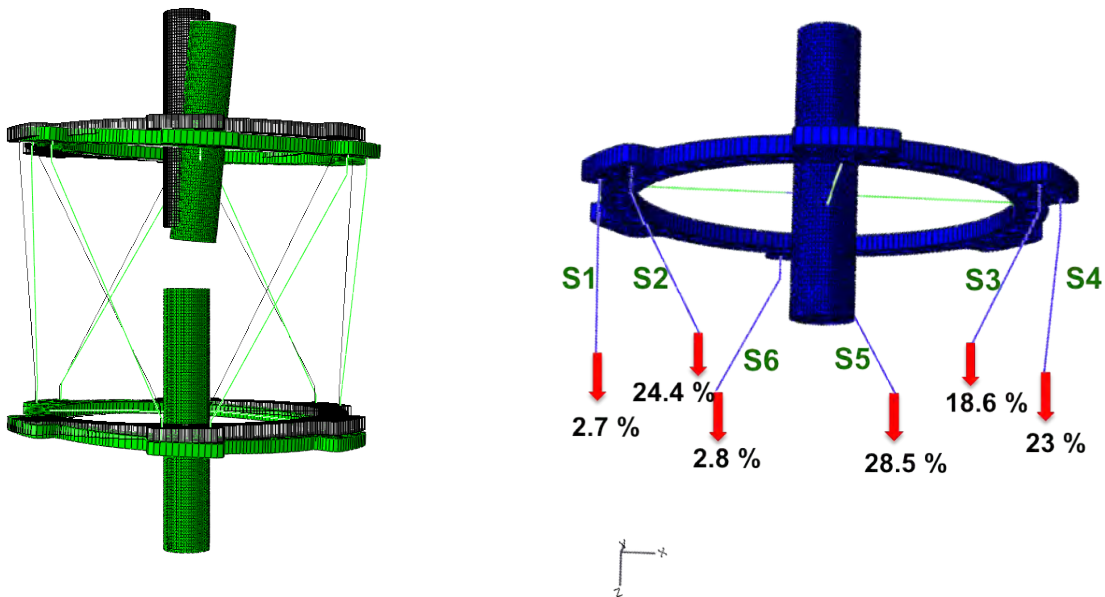


Figure 69: Deformed (green) and undeformed (grey) shapes (left), Free Body Diagram (right) (180-mm rings, 1.5-mm wires with 883 N pretension, 300 N)

The analysis of hybrid TSF model (Configuration 4) indicates a relatively different behavior in compression loading. The load-displacement curve, for 883 N (90kg) wire pretension and 45° crossing angle, shows a far wider linear region compared to the TSF Configuration 3, depicted in Figure 70. The model is subjected to a load cycle of 500 N. The elastic range for the hybrid configuration is nearly 350 N, and only these load ranges are correlated with the simple TSF model. Unlike configurations 1 & 3, the bending trend starts at low loading steps of the load cycle.

Figure 70 shows that, for axial loading until a magnitude of 180 N, the hybrid fixator model is on average 48% stiffer than the TSF with wires, initiating with 19.6 N/mm and 7.19 N/mm values of axial stiffness, respectively. In higher loads, the TSF (in red circles) exhibits a gradually decreasing stiffness to compression loading while the hybrid TSF (in blue circles) loses its rigidity in an almost linear rate.

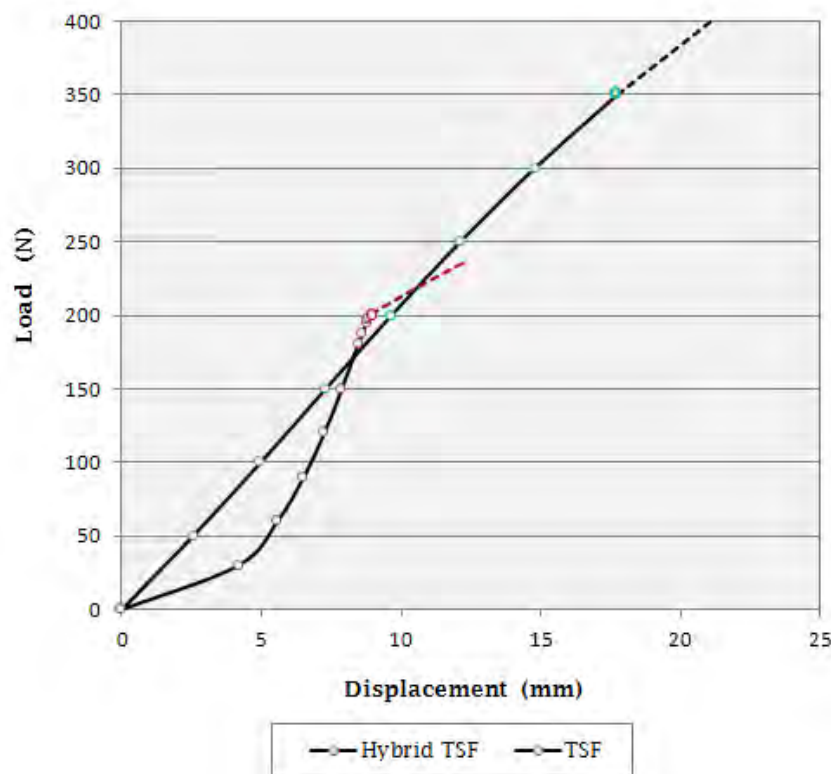


Figure 70: Load-displacement curves of TSF and hybrid TSF Configurations (180-mm rings, 1.5-mm wires with 883 N pretension)

Although this configuration uses 2 wires for fixation (at the proximal ring), that evidently allow pure axial motion and are affecting in a non-linear manner the axial frame stiffness, the insertion of 5 half-pins (in the positions described before) seem to contribute, undesirably, to the shear motion of fragments, diminishing the axial stiffness. According to the mechanics of hybrid fixators, transfixion wires are loaded in a four-point bending manner, whereas half-pins are subjected to cantilever bending when loaded axially (Lewis & Bronson, 1998). Since their mechanics differs, the combination of half-pins with tensioned

wires in a hybrid TSF frame, does not necessarily encompass the benefits of both types of fixation in any configuration tested.

In the same report, Bronson (1998) noted that the axial motion allowed by the tensioned wires can place excessive stress on constructs using an inadequate number of half-pins. Studying this indication in relation to our model, we observe the Von Mises stress distribution on the half-pins pins of Configuration 4 (Figure 71). Excessive stresses, in a range of 145–1737 MPa (see legend), are applied especially to the distal half-pins, which are articulated to the distal bone segment, subjected to immobilization. The maximum value was tracked in the location where the third half-pin (HP3) is rigidly connected to the cube, due to stress concentration.

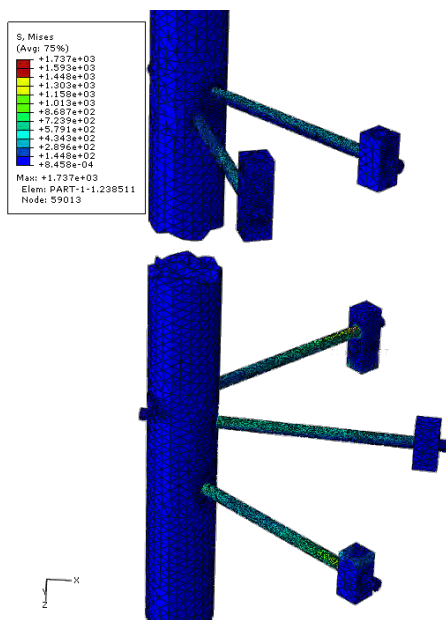


Figure 71: Von-Mises stress distribution on half-pins (Hybrid TSF, load 500 N)

Kummer (1992) noted that the angulation between crossing wires affects bending stiffness and stability. Therefore, in the hybrid TSF model, we tested a smaller wire intersection angle, at 29°, and studied its influence on stiffness (see Figure 72). The 1.5-mm wires were pretensioned to 883 N (90kg) in both models.

As we can see in Figure 72, decreasing the angle of wire intersection, has a negative contribution to the frame stiffness. Literature reports refer that, by changing the crossing angle from 90° to 45°, the axial stiffness was diminished, since the maximum stability with the minimum shear is achieved by crossing the wires as close to 90° as the regional anatomy safely permits. Podolsky and Chao, 1993 noted a decrease of 14-20% in double-ring Ilizarov frames with 150-mm rings. Consequently, a further decrease, to angles lower than 45°, produces a less stiff configuration. In crossing angles less than 45°, Podolsky and Chao (1993), in the same study, note that the tensile force on the rings becomes effectively unidirectional and the resulted ring deformation reduces the frame axial stiffness.

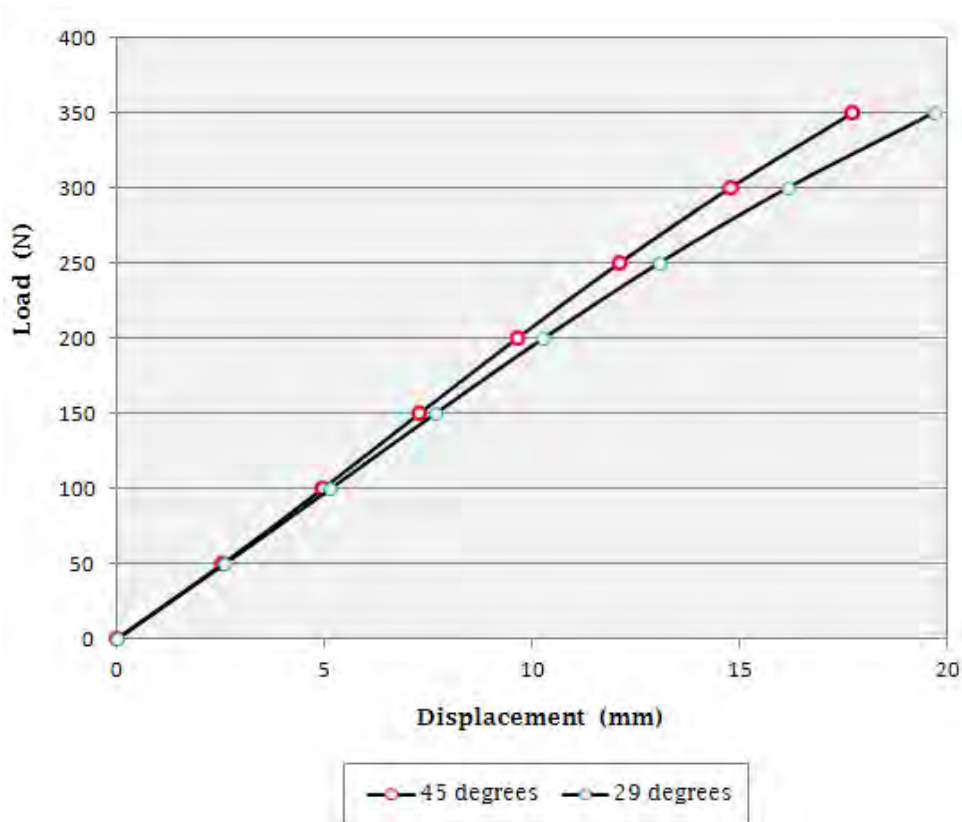


Figure 72: Wire-crossing angle effect on axial stiffness of hybrid TSF Configurations (180-mm rings, 1.5-mm wires, 883 N pretension, load 500 N)

Observing the stress distribution in the rings for the two cases (45° – 29°), for a load cycle of 500 N, we note that the regions around the wires and the distal half-pins are highly stressed (Figure 73). In particular, the configuration with more acute angle of wire intersection, presents a maximum stress value of 672 MPa in the region around the fifth half-pin (inserted distally), that is 11% higher as opposed to the corresponding maximum value of 601 MPa (in the region around the third half-pin, placed proximally) in the other configuration. Taking into account a mean value of yield point of a typical stainless steel (603 MPa, *www.matweb.com*), reveals a close to plastic deformation of the rings that, in conjunction with the sliding of the proximal bone fragment along the wire, are partially responsible for the reduction in axial (see Figure 72) and bending (according to Kummer, 1992) stiffness.

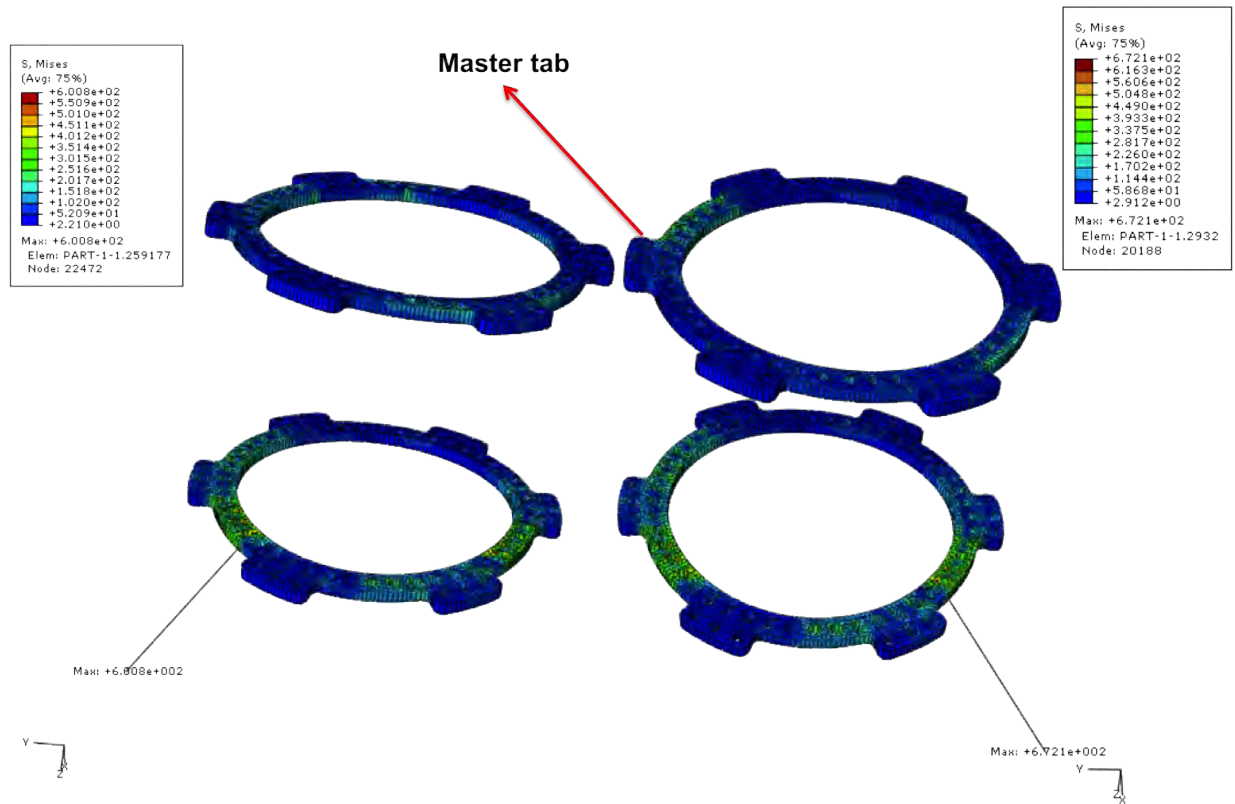


Figure 73: Stress distribution on rings for 45° (left) and 29° (right) wire angle (Hybrid TSF, 180-mm rings, 1.5-mm wires, 883 N pretension, load 500 N)

Finally, we used the hybrid TSF Configuration 4 to assess the differences in the rigidity of the bone-callus-fixator system when small variations of callus mechanical characteristics appear in the first stages of bone repair. At the fracture site, we considered three different stages of callus consolidation (type I, II and III), by interposing materials of different densities, such as reported in the study of Juan et al. (1992) (Section 3.3). The model was subjected to a cycle load of 500 N and the wires were pretensioned to 883 N (90 kg).

The analysis indicated that an increase on the callus elastic characteristics causes an evident increase of load transmission at the callus site. Figure 74 shows the Von Mises stress distribution on the tibia for the four cases (fracture gap & 3 types of callus). Obviously, the stress concentration to the bone around half-pins was higher in the case of fracture gap and for this reason, these areas showed intense bone resorption. As the callus elasticity increased (Type II and III), the stress distribution along the bone became more uniform and thus, the resorption was diminished. Lewis & Bronson (1998) refer to large areas of bone resorption around pins in cases of fracture gap as a result of uncontrolled weight bearing.

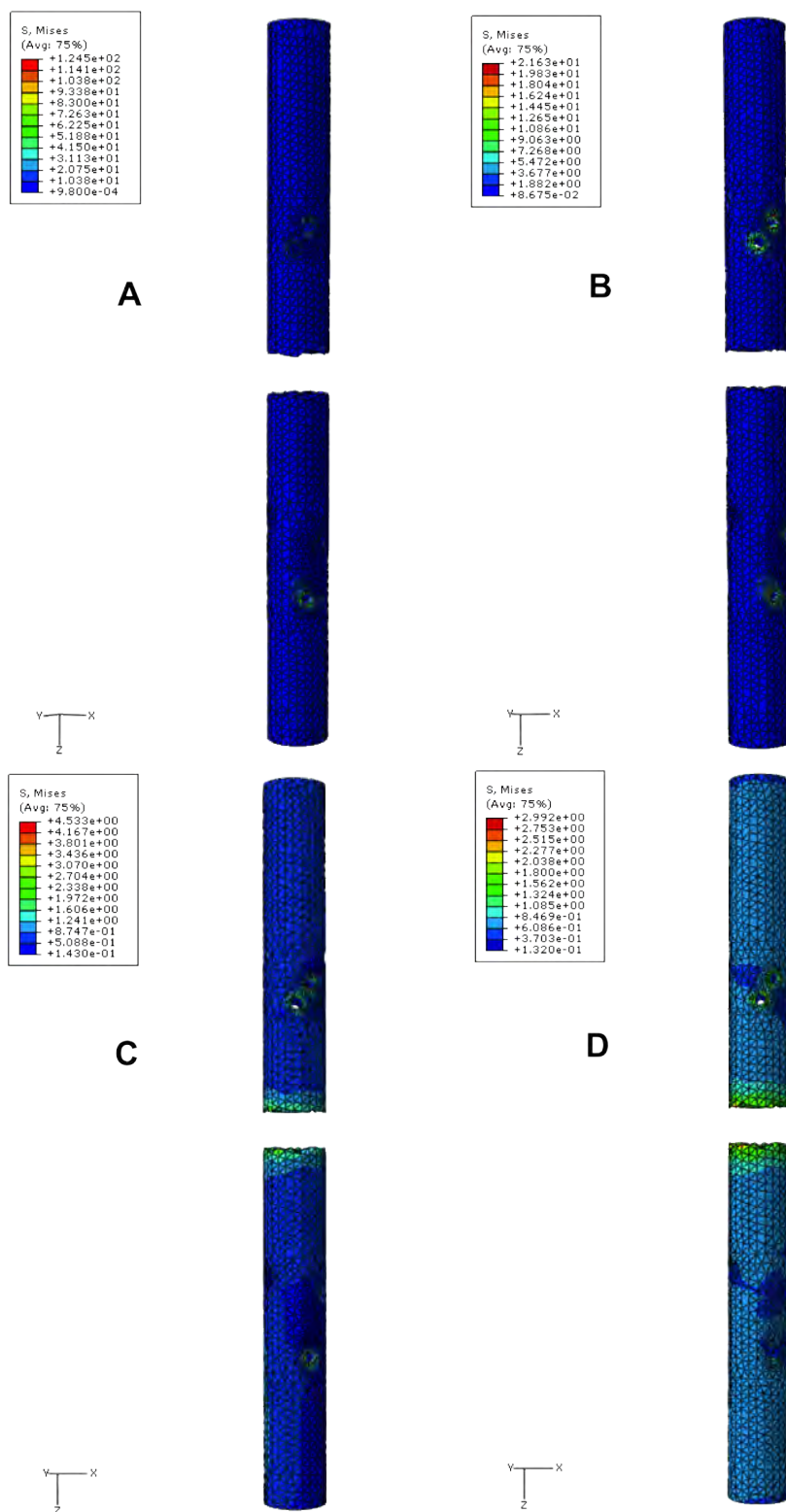


Figure 74: Stress distribution on tibiae with (A) fracture gap, (B) Callus Type I, (C) II and (D) III (Hybrid TSF, 180-mm rings, 1.5-mm wires, 883 N pretension, 500N)

The increase of surface area contact between the bone fragments resulted in higher load transmission in the region around the callus which indicates improved internal stability. The effect of callus density on axial stiffness throughout the load cycle is presented in Figure 75. The results are given in logarithmic scale, due to the order of magnitude difference in values between stages I, II and III.

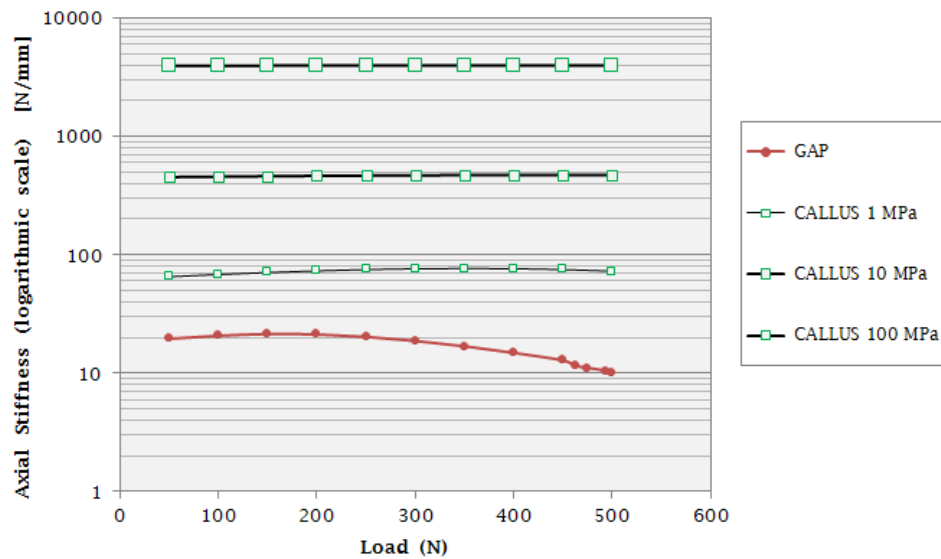


Figure 75: Effect of callus elastic characteristics on axial stability (Hybrid TSF, 180-mm rings, 1.5-mm wires, 883 N pretension, 500N)

The graph depicts the influence of loading on the axial stiffness for different stages of bone repair. Lower axial stiffness by 98% is observed on callus stage I, compared to the stiffness on stage III.

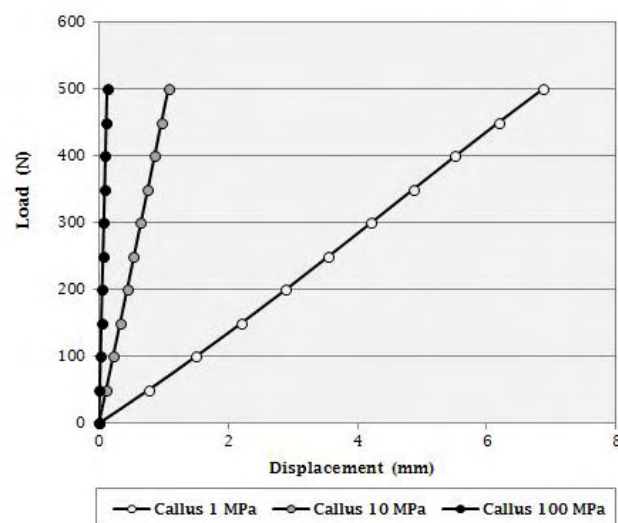


Figure 76: Load-displacement curves for different stages of fracture healing (Hybrid TSF, 180-mm rings, 1.5-mm wires, 883 N pretension, 500N)

Load-displacement curves (Figure 76) become steeper, with an elastic range of 500 N for all three stages, as the healing procedure continues. Evidently, there is a negligible rigidity of the fixator during early consolidation stages (type I) to control the linear displacement in axial direction. The lower frame rigidity seen at lesser loads allows more axial micromotion; for 500 N load, the displacement for case A (*fracture gap*) was approximately 38% higher in relation to case B (*Callus I*), whereas in case D (*Callus III*) the bone was displaced 88% less than in case C (*Callus II*). The simulation results for the hybrid TSF are in good agreement, in terms of behavior, with the findings documented by Juan et al. (1992) for single-ring Ilizarov. The analysis concluded to the statement that callus is a substantial parameter of the total rigidity.

CLINICAL APPLICATIONS AND RESULTS :

The Orthopaedics Department of University Hospital of Larisa collected radiographs of postoperatively management of hundreds of cases they have treated the last years and provided us with clinical results of fixations performed with the Ilizarov and the TSF devices. Studying different cases of tibia fractures with the help of X-Ray images can be very helpful to approach, especially the TSF post operative technique followed by the surgeons, since it is a second generation CEF.

Figure 77 shows the application of a hybrid fixator on a closed proximal tibia fracture of left leg. It is a single-ring block frame with one level of fixation per bone segment. Each ring has 3 fixation points; in the proximal ring 3 smooth wires are placed in the anterior compartment of tibia, leaving the safe arc zone of 200°, posterior to anterior, free. In the distal ring, three half-pins are inserted to stabilize the segment; one pin is placed proximally to the ring, in a vertical distance of 1cm, while the other two are inserted at the distal side, attached with one and three-hole rancho cubes, respectively. The pictures are taken after the reduction of the bone fragments and the Spatial frame is placed in neutral position.



Figure 77: Hybrid TSF configuration with 3 wires and 3 half-pins
(Case from the Orthopaedics Department of University Hospital of Larisa, granted by Dr. N.Karamanis)

The following radiographs present the case of a 31-year-old male who fell from height and suffered a proximal tibia fracture. It was an oblique and closed fracture that was treated with a hybrid Taylor Spatial Frame mounted and was post operatively managed by the surgeons of the University Hospital of Larisa.



Figure 78: Anterior and medial view of proximal tibia fracture (X-ray image) – 31-year-old male
(Case from the Orthopaedics Department of University Hospital of Larisa, 2011)

The configuration used was a single-ring block (one ring per bone fragment) with 3 wires fixed at the proximal ring and 2 half-pins and 1 wire at the distal ring. The X-Ray images in Figure 79 & 80 show the post operative management of the fracture 1, 3 and 5 months after the surgery. The first image was taken immediately after the anatomic reduction of the fracture at the operation. After the reduction, the rings were fixed to the bone fragments and the struts were adjusted and locked to the initial position, shown on the left.

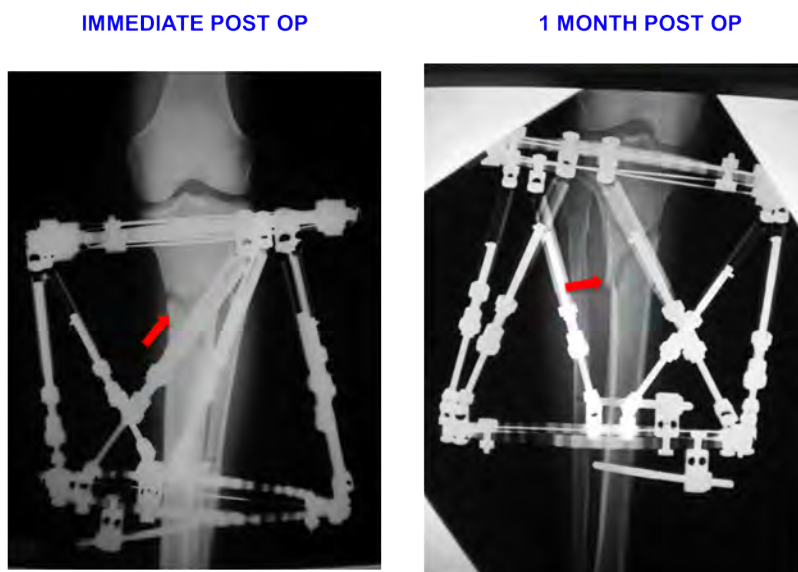


Figure 79: Front and lateral view of the fracture – Immediate and 1 Month after Post. Op. (X-ray image)
(Case from the Orthopaedics Department of University Hospital of Larisa, 2011)

One month later, the bone fragments were still aligned, certifying the successful reduc-

tion that preserved bony contact, which generally augments frame stability and the ability to bear-weight, despite any motion of the frame. During this month, the struts were adjusted according to the prescription of the Taylor software in order to correct the deformity before tissue formation. The patient kept the fixator for 3 months, until the process of callus consolidation began at the fracture site.

Figure 80 depicts the fracture condition when the frame was removed. Three months after the mounting, a great portion of callus has been formed at the fracture gap (noted in red circle). However, a closer look gives another important information: The ossification along the fracture site was not realized in a uniform manner, since evidently the bone has remodeled itself mostly at the medial part of the tibia. Because axial compression allows micromotion along the fragments and enhances callus formation, we assume that the bone was subjected to higher loads on the medial side. This can be a usual complication due to uncontrolled weight bearing or a kind of mechanical failure of the frame (i.e. inadequate fixation points) that had low axial stiffness and followed a bending trend at the sagittal plane. In either cases, higher mechanical stimuli was applied to the medial compartment and, following Wolff's law, the bone growth resisted to high loading by strengthening.

Five months after the operation, the ossification has almost been completed and the fracture gap is filled with bone tissue in the greater portion.

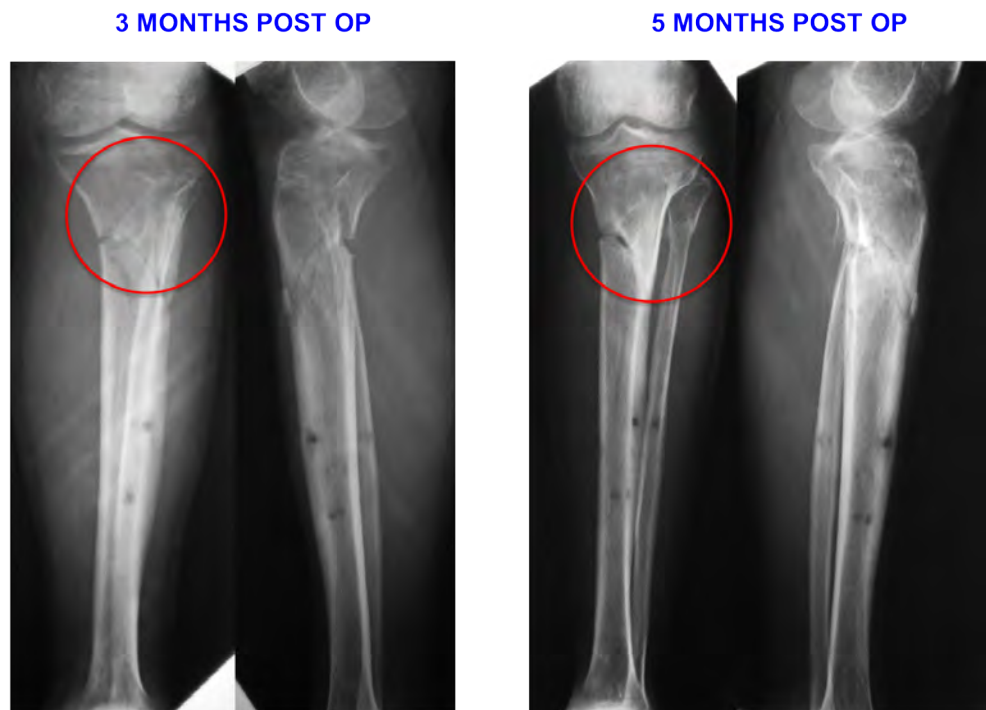


Figure 80: Front and lateral view of the tibia – 3 and 5 Months Post. Op. (X-ray image)
(Case from the Orthopaedics Department of University Hospital of Larisa, 2011)

The post operative management of a case with multiple open fractures is presented in steps in the next images (Figure 81–85). The fixation used was a hybrid Ilizarov frame, consisting mostly of wires, smooth & olive, and half-pins. It refers to a 25-year-old male who suffered open bipolar tibia fractures due to heavy object drop on his right foot.

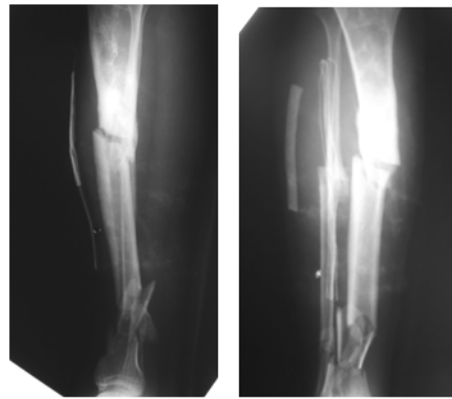


Figure 81: Open bipolar tibia fractures (X-ray image) – 25-year-old male
(Case from the Orthopaedics Department of University Hospital of Larisa, 2006)

We observe that there were one severe open fracture at the distal part of the shaft, close to ankle joint, and two open fractures at proximal tibia (mid-metaphyseal compartment) and fibula that needed immediate fixation. The Ilizarov configuration used consisted of 6 rings, in order to stabilize all fractured segments. Two rings were placed adjacent to the lower fracture distally and on its proximal part a third ring, that was connected with rods with another three rings, one distal and two proximal to the upper fracture of tibia. The medial two rings close to the fractures were used to minimize the unsupported length between the fractures and increased the frame's stability (see Figure 82). The percutaneous wires were not inserted into the fibula bone.

IMMEDIATE POST OP

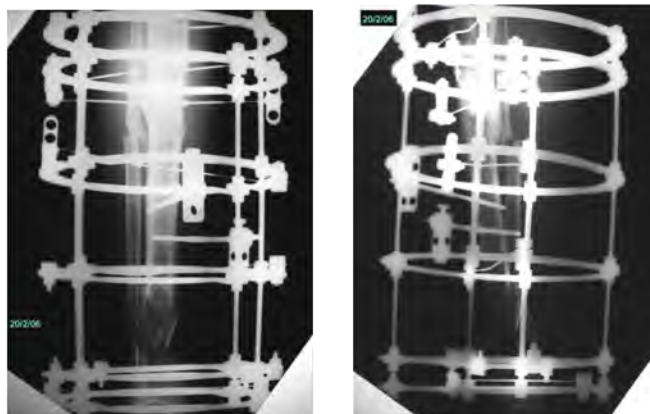


Figure 82: Open bipolar tibia fracture (X-ray image) – Immediate Post. Op.
(Case from the Orthopaedics Department of University Hospital of Larisa, 2006)

Bone fragments were aligned and the immediate post operative condition is figured in the above image. Reduction was realized also to the fibula fragments. The proximal two rings used two smooth wires to stabilize the proximal part of the upper fracture and two olive wires to improve bending stiffness. The accessory ring placed distally to this fracture had two points of fixations: one half-pin and one olive wire, inserted in anterior-medial with opposite direction, to minimize bone translation along the wire. Two olive wires and another half-pin were placed on the fourth ring, with the half-pin attached to the distal side, in an acute angle of divergence with the previous one and the olive wires crossed in a narrow angle of intersection. The adjacent to the lower fracture (close to ankle joint) rings used four smooth wires, two per ring for fixation, eccentrically positioned (medially and laterally from the center, respectively) to enhance axial and bending stiffness.

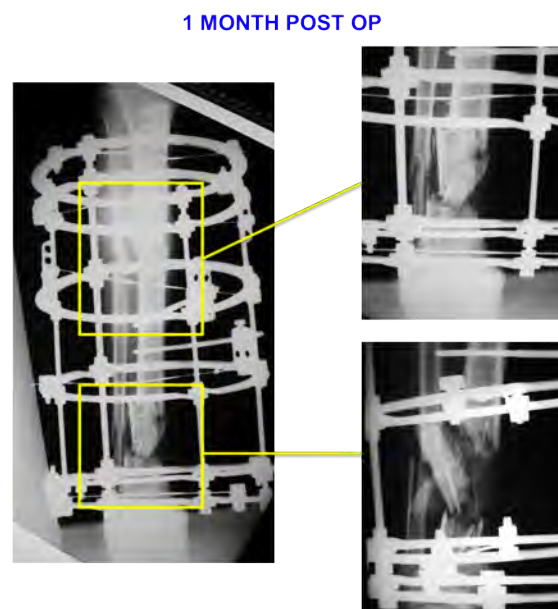


Figure 83: Open bipolar tibia fracture (X-ray image) – 1 Month Post. Op.
(Case from the Orthopaedics Department of University Hospital of Larisa, 2006)

Nine months later, the proximal tibia metaphyseal fracture has been partially consolidated, with a callus region formed mostly at the lateral side of the bone. The fixator has been dynamized and one half-pin (third ring) supporting distally the upper fracture was removed. The distal fracture, however, presented delayed union (or non-union) and surgeons enhanced the fixation using alternative techniques (such as iliac graft placement), in order to support the ossification process (Figure 84).

Nineteen months after the operation, when the patient was still in the frame, assessment of the solidity of the bone regenerate (or callus) indicated that the fixator should not be removed yet, because the rate of healing procedure of the distal fracture was still slow. The patient remained under medical supervision for approximately another 4 years. The remodeled bone is presented 23 months and 4,5 years after the operation (Fig.85).

9 MONTHS POST OP

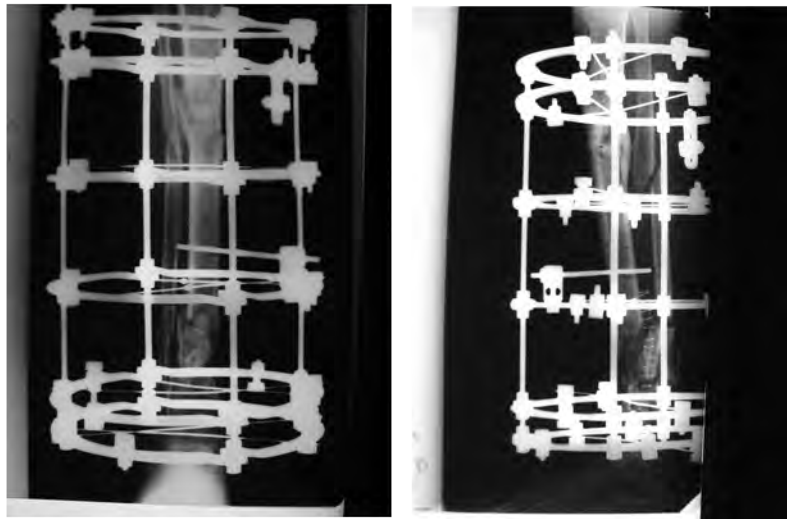
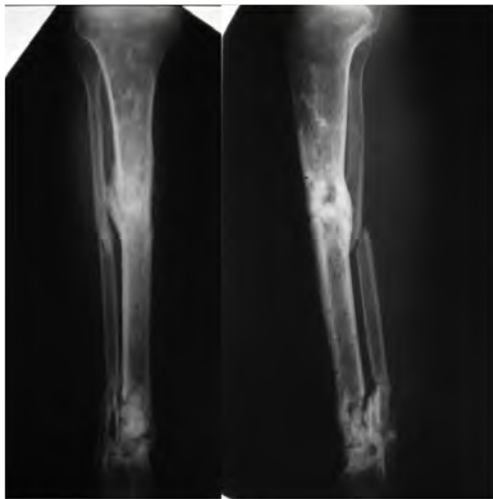


Figure 84: Open bipolar tibia fracture (X-ray image) – 9 Month Post. Op.
(Case from the Orthopaedics Department of University Hospital of Larisa, 2006)

23 MONTHS POST OP



4,5 YEARS POST OP



Figure 85: X-ray image of healed tibia – 23 Months & 4,5 Years Post. Op.
(Case from the Orthopaedics Department of University Hospital of Larisa, 2006)

3.5 Discussion

The correlation between the numerical results presented with similar findings in clinical applications and literature references, is a proximate method of validation that can be considered as a general guideline for the research of external fixators.

The axial stiffness of Ilizarov Configuration 2 loaded with axial load of 500 N, ranges among 13.6 – 64.12 N/mm, when using 1.5-wires pretensioned between 50–90 kg for fixation. The range of stiffness values is in good agreement with the results reported by Zamani et al. (2009) (27 – 73 N/mm), since they tested a similar construction with 1.8-mm wires and 220-mm rings subjected to 250 N axial loading and wire pretension between 50–130kg. Kummer (1992) documented axial stiffness equal to 110 N/mm, for 1.8 diameter wires with 150-mm span pretensioned between 50–90 kg, which is very close to the tangent modulus calculated for Configuration 2 (mean value 106.3 N/mm). Roberts et al. (2005) noted 117.5 ± 4.41 N/mm for a configuration with 160-mm rings and 1.8-mm wires loaded to 100 N. The secant modulus reported by Podolsky and Chao (1990) was between 45.54 – 124 N/mm for 1.5-mm wires and 58.7 – 145.5 N/mm for 1.8-mm wires (150-mm rings).

The load-displacement curve of the same configuration for 90kg pretension showed an elastic range for approximately 4-mm, which is in good relation to the experimental finding of almost 3-mm reported by Watson et al. (2007) for 130kg pretension and same load. Galvis et al. (2006), in their experimental and numerical study of a similar configuration with 160-mm rings, supported the corresponding elastic range for nearly 6mm.

Hillard et al. (1998) reported an axial stiffness between 10 – 100 N/mm, for a single-ring Ilizarov block (180-mm rings, 1.8-mm wires, 100kg pretension) under axial loading of 200 N magnitude, which is in good agreement with the corresponding value of 8.83 – 101.8 N/mm derived for the same compression load in this thesis (Configuration 2). The load-displacement profiles showing the effect of wire diameter on axial stiffness also agree with the findings in the same study by Hillard and co-workers.

Gasser et al. (1990) presented axial stiffness between 60 – 125 N/mm (4-ring Ilizarov construct, 1.8-mm wires tested under axial load of 900 N) while Paley et al. (1990) reported 40 – 60 N/mm in a simulation of a similar fixator. Antoci et al. (2006), testing the influence of wire positioning within the bone, concluded to a mean of 120 N/mm axial stiffness for a ring with two 1.8-mm wires positioned at the center subjected to 100 N, and 170 N/mm for the configuration with three wires placed in the same position and under the same conditions (110 kg pretension).

The linear relationship between load and displacement in hybrid TSF model (Configuration 4), for almost 400 N of a load cycle of 500 N, is related to the use of 5 half-pins, that act as cantilevers when loaded axially and do not substitute non-linear trend on the curve, opposed to wires. This behavior was supported by the experimental study performed

by Khurana et al. (2010), in which the comparison between transfixing wires and half-pins in 180-mm rings of TSF models documented a linear relationship between load and displacement in rings using 6.5-mm half-pins (elastic range of 400 N), unlike transfixion wires (non-linear behavior for the same load). The axial stiffness for a 180-mm ring with half-pins was 98.04 ± 2.03 N/mm and 62.39 N/mm, for divergence angle of 90° and 45° , respectively.

The simulation of partially consolidated tibiae fixed with a hybrid TSF (Configuration 4) produced linear behavior in the load displacement curves, that became steeper as the callus increased its elastic characteristics. Walke et al. (2008), reported linear relationship between load and displacement in the case of fractured tibia (oblique fracture at distal metaphysis part) fixed with 6-mm threaded screw and subjected to axial compression load 600 N. The same behavior was documented by Juan et al. (1992), in their numerical (FEA) and experimental study on various Ilizarov configurations – including 180-mm rings and 1.5-mm wires with 45° angle of intersection – fixing fractured tibiae in different stages of callus development. The results were compared mostly in terms of behavior, since we tested larger callus sizes and used extra half-pins for fixation and so a quantitative correlation would not be right.

4 Closure

In this thesis, a biomechanical analysis of circular external fixators was performed in terms of the parameters affecting the axial frame stiffness under compression loading. The fixators were used in the treatment of closed tibia fractures and in partially consolidated tissues. The method of assessment was simulation of different configurations of Ilizarov and Taylor Spatial Frame, in particular, with three-dimensional Finite Element Models. The numerical results were correlated with experimental, theoretical and numerical findings of other studies, reported in literature the last 25 years.

In general, the stiffness of the fixator and, accordingly, the stability of the fracture are sensitive to every part of the fixation system, including rings, Kirschner wires, half-pins, threaded rods, telescopic struts as well as the fracture zone itself. Since it is practically impossible to test all probable combinations of the referred parts, our calculations were restricted to a wide range of cases of the most sensitive configuration parameters: wires, half-pins, rings and fracture zone. The goal of this mechanical investigation was to determine their influence on the stiffness of each fixator.

Ilizarov and TSF configurations using only wires for fixation showed a non-linear relationship between load and displacement, under typical ranges of loading, corresponding to axial weight bearing during ambulation when the frame is on. Load-displacement curves of hybrid TSF configurations, on the other hand, when subjected to similar load cycles, presented an almost linear profile, particularly in a range of 350 N.

The axial stiffness was proved to be load-dependent, as reported in the literature. This means that, reporting the particular stiffness of a particular configuration should always be accompanied by the load range for which this is valid. It is interesting to note that the relationship between stiffness and load was non-linear, in all the configurations tested. The low frame rigidity seen at lesser loads allows more axial motion and is presumed to be useful for stimulation of fracture callus formation. The higher frame rigidity seen at increased loads is thought to protect the healing fracture tissues from excessive motion preventing pain and fibrous nonunion.

The addition of two rings and two wires (Configuration 1 \rightarrow Configuration 2) substantially increased the stiffness of the frame. The load-displacement curve became steeper and a significant decrease was observed in the displacement of the bone segment, under the same load. This fact indicated that, by using more rings and wires to support the bone fragments, stiffens the fixation device.

The wire diameter was proved to be the most sensitive of the parameters tested in terms of its impact on the axial stiffness. Indeed, increasing the wire diameter from 1.5 to 1.8-mm (pretensioned to 981 N) in the single-ring Ilizarov block (Configuration 1) resulted in 10% stiffer frame, opposed to an increase of almost 7% produced by the change in the pretension from 491 to 883 N in the same configuration.

Assessing the influence of wire pretension in double-ring Ilizarov blocks (Configuration 2), the increase in axial stiffness was verified when the pretension was risen from 50kg to 70 and 90kg. The latter corresponded to the sharpest slope in the load-displacement curve and, obviously, to the smallest axial displacement value. The same trend was supported by the TSF Configuration 3, where the stiffness was increased by 11%, on average, when the pretension was augmented from 70 to 90kg. A careful study of the load-displacement graph in double-ring Ilizarov block has shown a linearization effect of the increasing wire pretension on the curve; as the pretension level was growing, the curved tended to become more linear. However, it should be mentioned that pretension is limited by the yielding point of the stainless steel-wires, since some plastic deformation would occur and the tension in the wires would be reduced. As the stiffness of the frame is a function of the tension in the wires, a drop in wire tension will definitely compromise the fixator's ability to resist the shear and high-amplitude axial motions, which would be deleterious to the healing outcome (Hillard et al., 1998).

The comparison between a TSF configuration with transfixing wires only and a hybrid TSF (Configuration 4) with 5 half-pins and wires in a narrower, by half, crossing angle indicated that the latter had a wider and steeper elastic range in the load versus displacement graph, when subjected to the same load. For axial loading up to 180 N, the hybrid configuration was almost 50% stiffer than the TSF wire-configuration.

Narrowing the crossing angle of the wires led to a decrease in the axial stiffness of the hybrid TSF fixator. In particular, decreasing the angle between the wires from 45 to 29° lowered the frame's stiffness on average by 13.8%, when both configurations were loaded to 500 N. Apart from negatively influencing the axial stiffness, more acute wire-crossing angles were proved to increase the maximum stress values close to yielding points on to the rings. In addition to the fact that the crossing angles between half-pins (calculated by two) were also narrow and all less than 60°, this configuration permitted unwanted sliding of the bone segment along the wires. The phenomenon was more evident in the configuration with the 29° angle of wires, as expected. In a load cycle of 500 N, the displacement (as magnitude) of the tibia nodes in relation to the wire nodes at the cross-section of the bone where the first wire was positioned, reached a maximum percentage of 5%!

Finally, the influence of the callus development in the healing process turned out to be a substantial factor of the frame's rigidity. In the fracture gap model used in Configuration 4, we interposed materials of logarithmically increasing elastic properties to resemble different stages of bone repair. The analysis revealed that when there was no interposition

material between bone fragments, there was no load sharing by the bone model and high bone resorption was observed around half-pins as a result of uncontrolled weight bearing. As the material of the callus was approaching the elastic characteristics of cortical bone, we observed higher load transmission to the bone and particularly in the last tested stage (type III), when the majority of the load was carried by the bone rather than by the fixator. The differences between the values of axial stiffness in the cases of the three callus types were almost logarithmic.

After the analysis performed in the two systems of fixation, it is obvious that there is no ideal configuration that can treat any type of fracture with the maximum stiffness and the minimum of complications. A general convention is that a recommended fixator would be one with a non-linear axial stiffness and a high shear stiffness, that is a configuration which allows low-amplitude cyclical axial motion, but inhibits high-amplitude axial motion and shear motion between fragments.

In general terms, this mechanical investigation concluded that the addition of extra wires and rings (to minimize the unsupported lengths of the tibia), the selection of wires with bigger diameter than 1.5-mm pretensioned to higher levels than 70 kg (limited to 105 kg for 1.5-mm and 150 kg for 1.8-mm wires to prevent yielding) and crossing angles of at least 60° for both half-pins and wires, have a significant effect on achieving a high axial frame stiffness. The combination of half-pins with tensioned wires in hybrid frames can have an additive effect on construct's stiffness if, in addition to the above, they are placed in a configuration that performs multiplanar fixation and the pins used have an increased diameter, compared to typical 4-mm half-pins. The insertion of olive wires from opposite directions in configurations with inadequate components, i.e. TSF configuration 3, or low stability in medial or high loads due to acute crossing angles, i.e. hybrid TSF, can prevent bone translation along the wire and substantially improve bending stiffness and stability.

It was concluded, also, that a reconsideration of the modeling of the bone-wire interface is required, since the wires are not placed to the bone as parallel components to the tibia fiber, as it was considered, but are inserted in predrilled areas. Cylindrical holes must be created to the tibia model to simulate the holes where the wires pass through in clinical application. In this configuration, the wires will be meshed with solid elements and special contact elements will be defined for the area of the holes in the bone.

The mechanical testing planned to assess the configurations simulated with Finite Element Analysis, will provide us with results that are likely to relate to the numerical findings. A correlation between experimental and numerical results with the corresponding found in literature will certainly validate this research and will lead to interesting conclusions on the study of circular external fixators.

References

- [1] ABAQUS, Analysis User's Manual, Version 6.7, ABAQUS Inc., 2007.
- [2] V.Antoci, E.Raney, V.Antoci Jr., M.Voor, C.Roberts, Transfixion Wire Positioning Within the Bone: An Option to Control Proximal Tibia External Fixation Stiffness, *J Pediatr Orthop* **26** (4) (2006) 466–470.
- [3] A.S.Banks, E.Dalton McGlamry, McGlamry's comprehensive textbook of foot and ankle surgery, *Lippincott Williams & Wilkins* (2001)
- [4] A.T.Fragomen, S.R.Rozbruch, The Mechanics of External Fixation, *HSSJ* **3** (2007) 13–29.
- [5] E.Galvis, P.Lasso, A.Machado, J.J.Garcia, Computational Determination of the 3-D Stiffness Matrix of an Ilizarov Fixator, *Advances in Bioengineering* **51** (2001) 1–2
- [6] X.S.Gao, D.Lei, Q.Liao, G.F.Zhang, Generalized Stewart–Gough Platforms and Their Direct Kinematics, *IEEE Transactions on Robotics* **21** (2) (2005), 141–143
- [7] B.Gasser, B.Boman, D.Wyder, E.Schneider, Stiffness Characteristics of the Circular Ilizarov Device as Opposed to Conventional External Fixators, *Journal of Biomechanical Engineering* **112** (1990), 15–20
- [8] A.Georgiadakis, Biomechanical Analysis of the Ilizarov external bone-fracture fixation system, Diploma Thesis, University of Thessaly, Department of Mechanical Engineering (2010)
- [9] S.Green, Taylor Spatial Frame Disorients Ilizarovians, *Distraction, The Newsletter of Asami* **5** (1) (1997), 1–9
- [10] M.Charles-Harris, D.Lacroix, I.Proubasta, J.A.Planell, Intramedullary nails vs osteosynthesis plates for femoral fracture stabilization: A finite element analysis, *Journal of Applied Biomaterials & Biomechanics* **3** (3) (2005), 157–167
- [11] P.J.Hillard, A.J.L.Harrison, R.M.Atkins, The yielding of tensioned fine wires in the Ilizarov frame, *Proc Instn Mech Engrs* **212** (H) (1998), 37–46
- [12] R.Huston, Principles of Biomechanics, *CRC Press* (2009)
- [13] J.A.Juan, J.Prat, P.Vera, J.V.Hoyos, J.Sanchez-Lacuesta, J.L.Peris, R.Dejoz, R.Alepuz, Biomechanical Consequences of Callus Development in Hoffmann,Wagner,Orthofix and Ilizarov External Fixators, *J Biomechanics* **25** (9) (1992), 995–1006
- [14] A.Khurana, C.Byrne, S.Evans, H.Tanaka, K.Harasharan, Comparison of transverse wires and half pins in Taylor Spatial Frame: A biomechanical study, *Journal of Orthopaedic Surgery and Research* **5** (23) (2010), 1–7

- [15] L.P.Kristiansen, H.Steen, O.Reikeras, No difference in tibial lengthening index by use of Taylor Spatial Frame or Ilizarov external fixator, *Acta Orthopaedica* **77** (5) (2006), 772–777
- [16] F.J.Kummer, Biomechanics of the Ilizarov External Fixator, *Clinical Orthopaedics and Related Rresearch* **280** (1992), 11–14
- [17] D.Lacroix, P.J. Prendergast, A mechano-regulation model for tissue differentiation during fracture healing: analysis of gap size and loading, *Journal of Biomechanics* **35** (2002), 1161–1171
- [18] D.Lewis, D.Bronson, M.Samchukov, R.Welch, J.Stallings, Biomechanics of Circular Skeletal Fixation, *Veterinary Surgery* **27** (1998), 454–464
- [19] D.P.Moss, N.C.Tejwani, Biomechanics of External Fixation: A Review of the Literature, *Bulletin of the NYU Hospital for Joint Diseases* **65** (4) (2007), 294–299
- [20] G.E.Nelson,Jr., P.J.Kelly, L.F.A.Peterson, J.M.Janes, Blood supply of Human Tibia, *J Bone Joint Surg Am.* **42** (1960), 625–636
- [21] D.L.Nelson, External Fixation for Distal Radius Fractures. Presentation at the American Society for Surgery of the Hand course, San Francisco (2001)
- [22] B.M.Nigg, W.Herzog, Biomechanics of the musculo-skeletal system, *Wiley* (1999)
- [23] A.Nikonovas, A.J.L.Harisson, A simple way to model wires used in ring fixators: analysis of the wire stiffness effect on overall fixator stiffness, *J Engineering in Medicine* **219** (H) (2005), 31–42
- [24] M.Nordin, V.H.Frankel, Basic Biomechanics of the musculoskeletal system, *Lippincott Williams & Wilkins* (2001)
- [25] G.Pathak, R.Atkinson, Military external fixation of fractures, *ADF Health* **2** (2001), 24–28
- [26] A.Podolsky, E.Chao, Mechanical Performance of Ilizarov Circular External Fixators in Comparison With Other External Fixators, *Clinical Orthopaedics and Related Research* **293** (1993), 61–70
- [27] W.R.Pontarelli, External Fixation of Tibial Fractures, *The Iowa Orthopaedic Journal* **2** (1982), 80–86
- [28] D.T.Reilly, A.H.Burstein, The Mechanical Propertied of Cortical Bone, *J Bone Joint Surg Am.* **56** (1974), 1001–1022
- [29] C.S.Roberts, V.Antoci, V.Antoci Jr., M.Voor, The effect of transfixion wire crossing angle on the stiffness of fine wire external fixation: A biomechanical study, *Injury, Int. J. Care Injured* **36** (2005), 1107–1112

- [30] D.C.Schoen, Adult Orthopaedic Nursing, *Lippincott Williams & Wilkins* (1999)
- [31] L.A.Spyrou, Muscle and tendon tissues: constitutive modeling, numerical implementation and applications, PhD Thesis, University of Thessaly, Department of Mechanical Engineering (2009)
- [32] J.C.Taylor, Correction of General Deformity with the Taylor Spatial Frame Fixator™, Memphis, Tennessee (2002)
- [33] W.Walke, J.Marciniak, Z.Paszenda, M.Kaczmarek, Biomechanical analysis of tibia-double threaded screw fixation, *Archives of Materials Science and Engineering* **30** (1) (2008), 41–44
- [34] M.A.Watson, K.J.Mathias, N.Maffulli, External ring fixators: an overview, *Proc Instn Mech Engrs* **214** (H) (2000), 459–468
- [35] M.A.Watson, K.J.Mathias, N.Maffulli, D.W.L.Hukins, Yielding of the clamped-wire system in the Ilizarov external fixator, *Proc Instn Mech Engrs* **217** (H) (2003b), 367–374
- [36] M.A.Watson, K.J.Mathias, N.Maffulli, D.W.L.Hukins, D.E.T.Shepherd, Finite element modeling of the Ilizarov external fixation system, *Proc Instn Mech Engrs* **221** (H) (2007), 863–871
- [37] D.A.Wiss, Master Techniques in Orthopaedic Surgery Fractures, *Lippincott Williams & Wilkins* (2006)
- [38] A.R.Zamani, S.O.Oyadiji, Analytical modeling of Kirschner wires in Ilizarov circular external fixator as pretensioned slender beams, *J. R. Soc. Interface* **6** (2009), 243–256
- [39] G.Zhang, Avoiding material nonlinearity in an external fixation device, *Clinical Biomechanics* **19** (2004), 746–750
- [40] <http://orthopedics.about.com/od/brokenbones/a/tibia.htm>
- [41] <http://www-personal.une.edu.au/~pbrown3/skeleton.pdf>
- [42] http://www.wheelsonline.com/ortho/menu_for_the_tibia_tibia_frx
- [43] <http://www.engin.umich.edu/class/bme456/bonefracture/bonefracture.htm>
- [44] www.matweb.com

